SYNTHESES, CHARACTERIZATION, AND APPLICATIONS OF INJECTABLE CITRATE-BASED MUSSEL-INSPIRED BIODEGRADABLE ADHESIVE (iCMBA) POLYMERS AND HYDROGELS

by

MOHAMMADREZA MEHDIZADEH

Presented to the Faculty of the Graduate School of

The University of Texas at Arlington in Partial Fulfillment

of the Requirements

for the Degree of

DOCTOR OF PHILOSOPHY

THE UNIVERSITY OF TEXAS AT ARLINGTON

December 2012

Copyright © by Mohammadreza Mehdizadeh 2012

All Rights Reserved

ACKNOWLEDGEMENTS

I would like to take this opportunity to acknowledge all the people who helped me to accomplish this work. First, I would like to express my sincere appreciation to Dr. Jian Yang for providing me with the opportunity to work in his lab, and for his supports, guidance, patience, and encouragement. Without his persistent help, this dissertation would have not been possible. I would like to thank my committee members, Prof. Liping Tang, Prof. Pranesh B. Aswath, Dr. Yaowu Hao, and Dr. Fuqiang Liu for their time, interest, and helpful comments, which have helped me to successfully complete this work. My special thanks to Prof. Liping Tang, for all his supports and guidance to make parts of my dissertation possible.

To the faculty and staff of Materials Science and Engineering, and Bioengineering departments, thank you for all your assistance to make my PhD experience productive. I also would like to thank the members of Dr. Yang's research group.

My deepest gratitude to my parents, Gholamhassan Mehdizadeh and Kokab Haghgoo, for their unconditional love, supports and sacrifices throughout my life, and for paving my path to success.

Last but not least, to my lovely wife, Leila Sadegh, I cannot thank you enough for all you have done for me to make this journey possible and productive. My deepest gratitude to you for always believing in me, supporting me, and for standing by me when situation pushed me to the limits. It was your love, supports and encouragement that gave me the strength to make this work possible. Thank you.

November 26, 2012

ABSTRACT

SYNTHESES, CHARACTERIZATION, AND APPLICATIONS

OF INJECTABLE CITRATE-BASED MUSSEL-INSPIRED

BIODEGRADABLE ADHESIVE (iCMBA)

POLYMERS AND HYDROGELS

Mohammadreza Mehdizadeh, PhD

The University of Texas at Arlington, 2012

Supervising Professor: Jian Yang

Tissue adhesives are increasingly gaining more popularity in various areas of biomedical applications. They are utilized as surgical adhesives, as a replacement or adjunct to conventional wound closure and bleeding control techniques such as suturing, as well as in other applications such as tissue engineering and drug delivery.

Unfortunately, the existing surgical adhesives are not ideal for wet tissue adhesion required in many surgeries such as those for internal organs. Developing surgical adhesives with strong wet tissue adhesion, controlled degradability and mechanical properties, and excellent biocompatibility has been a significant challenge. Herein, learning from nature, we report a one-step synthesis of a novel family of injectable citrate-based mussel-inspired bioadhesives (iCMBAs) for surgical use. Within the formulations investigated, iCMBAs showed 2.5-8.0 folds stronger wet tissue adhesion strength over the clinically used fibrin glue (39 to 123 kPa for iCMBAs vs. 15 kPa for fibrin glue), demonstrated controlled degradability and tissue-like elastomeric mechanical properties, and exhibited excellent cyto/tissue-compatibility both in vitro and in vivo. iCMBAs were able to stop bleeding instantly and suturelessly, and close wounds (2

cm long × 0.5 cm deep) created on the back of Sprague-Dawley rats. Equally important, the new bioadhesives facilitated wound healing, and were completely degraded and absorbed without eliciting significant inflammatory response. Our results support that iCMBA technology is highly translational and could have broad impact on surgeries where surgical tissue adhesives, sealants, and hemostatic agents are used.

In the second part of this work, iCMBAs application in tissue engineering was also investigated by developing a new injectable in-situ crosslinkable bone composite based on iCMBA-hydroxyapatite (HA) with tunable set time, biodegradability, and excellent in vitro cyto-compatibility. The iCMBA-HA composites induced in vitro mineralization and differentiation of preosteoblast cells to osteobalsts. In vivo test showed that iCMBA-HA composite accelerated the bone repair and new bone tissue formation when injected to the region of a comminuted fracture in a New Zealand rabbit model.

iCMBAs were also found to be pH sensitive polymers, from which we developed a new pH-responsive hydrogel for application in stimuli-responsive controlled drug delivery systems (CDDS). The controllable swelling ratio and degradation of pH-sensitive iCMBA hydrogels render them suitable for applications such as delivery of drugs and biological molecules to lower gastrointestinal tract through oral administration. In addition, iCMBA can be used to not only close wounds, but also prepare drug-eluting hydrogels, which can sense and release drugs, e.g. anti-infectives, upon an increase in local pH due to worsening wound condition. iCMBA's tunable swelling and degradation, and cyto/tissue-compatibility make them a suitable candidate for this type of applications. In addition, we successfully fabricated iCMBA nanoparticles through a facile and safe technique, which can earn additional advantage for iCMBA nanogels as a novel pH-responsive drug delivery system.

TABLE OF CONTENTS

LIST OF ILLUSTRATIONS

LIST OF TABLES

Table Page

CHAPTER 1

INTRODUCTION TO BIOADHESIVES

1.1 Adhesive Biomaterials

Biomaterials have become an essential element of the modern medicine in a broad range of applications from regenerative medicine, tissue engineering, and prosthetic applications to targeted drug delivery, bioadhesives, and treatment of injuries. As an important member of biomaterials family, tissue adhesives, sealants, and bioadhesive hydrogels have many existing and potential applications in medicine and dentistry and are increasingly gaining more popularity in various areas of clinical applications. These applications include, for example, surgical adhesives and sealants for hemostasis and wound management, preparing targeted drug delivery vehicles, tissue engineering and regeneration, implantation of medical devices, and dental and bone applications [1-3].

In wound management and bleeding control, tissue adhesives and sealants are particularly important in situations that other techniques such as suturing are either impractical or ineffective. In addition, adhesives have demonstrated high efficacy in preventing massive blood loss, caused by traumatic injuries or might occur during surgical operations, where rapid bleeding control is vital to minimize probable damages to patient's organs, which can otherwise happen due to hemorrhage-induced hypotension. Additionally, bleeding control during a surgery has many advantages, such as preventing unstable hemodynamics, decreasing the need for blood transfusions, lowering operative time, minimizing the risk of infection, lowering overall morbidity and mortality rate, and reducing cost. In general several techniques and mechanism are used to control bleeding, including mechanical hemostasis, active hemostasis, and tissue adhesives and sealants. Various types of these wound management tools and their functioning mechanisms are listed in Table 1.1. In general, hemostasis is generally referred to the stoppage

of bleeding. During the biological hemostasis in the body three steps can be considered, including formation of platelets plug, creation of fibrin clot through a complex coagulation cascade, and the final step, break-down of fibrin clot by plasmin enzyme (fibrinolysis). Thisphysiological bleeding control system is usually sufficient to control blood loss for minor injuries and wounds. However, during a surgical operation or in severe trauma injuries, and in order to reduce preoperative and postoperative massive bleeding, utilization of hemostatic agents, or simply hemostats, might be necessary to contain massive blood loss [4]. While suturing has conventionally been the primary choice to close wounds and stop bleeding, it is not always as effective and practical as it is required to be, in order to satisfy clinical requirements, particularly when it comes to rapid bleeding control and blood oozing restrain [5]. To provide and maintain a rapid and effective bleeding control, especially during surgeries or traumatic injuries, hemostats are utilized [3].

Table 1.1 Various types of major hemostats, sealants, and adhesives, available for clinical use in the Unites States

Type and major components	Functioning mechanism
Mechanical hemostats Bovine collagen Porcine gelatin Oxidized regenerated cellulose Polysaccharide spheres	-Available in various forms of powder, sponge, microfibrillar, sheets and flowable products, these hemostats swell upon contact with blood and mechanically impede bleeding.
Active hemostats Human pooled thrombin Bovine thrombin Recombinant thrombin Bovine gelatin with human thrombin Porcine gelatin with thrombin	-Comprise thrombin as an active ingredient, which converts fibrinogen available in patient's blood to fibrin clot, accelerating cessation of bleeding.
Sealants Fibrin sealant and hemostat PEG based sealants	-Typically consist of two or more components that undergo chemical reaction upon mixing, forming a solid body or hydrogel that seals the wound area.
Adhesives Cyanoacrylates Albumin and glutaraldehyde	- Create covalent/secondary bonds with biological surfaces, which result in adhesion to tissue and/or approximating wound edges to close wounds and control bleeding.

Hemostatic materials may be categorized into mechanical agents and active agents [6]. The ‘mechanical hemostats’ usually do not contain active biological materials such as thrombin. Gauze, sponges or any surgical packing, and adhesives acting as sealant or embolic agents are a few examples of mechanical hemostatic agents [6, 7]. Mechanical hemostats prevent bleeding by forming a mechanical barrier to the flow of the blood from an injured site. They can be in the form of powder, sponges, sheets or micro particles, which are used alone or in combination with active hemostats such as thrombin to enhance their hemostatic efficacy [8]. Porcine gelatin, bovine collagen, and oxidized regenerated cellulose are some of the commercially available hemostats [8, 9]. Hemostats are also available in the form of viscose and paste-like flowable matrix, which can be injected to wound area [8]. The main concerns over using these mechanical hemostats are possible allergic reaction of patients to bovine- or porcine-originated products, swelling of these products upon contact with blood and other body fluids resulting in compressive pressure on neighboring tissue, and probable foreign body reactions to these agents [8]. Hemostatic agents containing active biological components, particularly thrombin, are referred to as ‘active agents’. These agents actively participate in the process of fibrin clot formation, when applied to a bleeding wound site. For instance, thrombin available in an active hemostat interacts with patient’s blood fibrinogen to accelerate fibrin clot formation. Thrombin is an enzyme, which can be of bovine, human, or recombinant origin, and is available both as a stand-alone product and in combination with gelatin matrix. In the latter case when the matrix contacts the blood the gelatin swells and assists to block bleeding while thrombin accelerates the clot formation [10]. The major concern of using thrombin-containing hemostats is interfering with blood stream [8]. Moreover, bovine thrombin antigenic property and bovine Factor V impurities can stimulate human antibody formation and subsequently cause serious complications. Possible allergic reactions to bovine- and porcine-originated products and foreign body response are other issues to be watched when using this type of hemostats [8]. In addition, hemostats are temporary bleeding control tools, which typically have short-lived effect and are not effective in larger wounds. Obviously, they are not helpful in wound closure

practice, which is required to permanently stop bleeding and help cure the wound. To address the described shortcomings and achieve effective wound closure, tissue adhesives and sealants have attracted researchers' attention. Bioadhesives have demonstrated numerous existing and promising applications in not only in preventing blood loss and wound management, but also in drug delivery and tissue engineering. Tissue adhesive and sealants are further discussed in details in the following sections.

1.2 Tissue Adhesives and Sealants

Tissue adhesives and sealants in the current context represent liquid or semi-liquid compounds that can be applied to a tissue incision or wound for the purpose of closing wounds, adhering to soft tissues and hemostasis. They comprise natural substances and/or synthetic chemicals, typically in the form of monomers, pre-polymers, or non-crosslinked polymers, which undergo polymerization and/or crosslinking reactions within a limited period of time to form an insoluble adhesive matrix, when delivered to a tissue [3]. Before reviewing the existing tissue adhesives and sealants, the mechanisms of adhesion and the supporting theories are briefly discussed in the next section.

1.3 Adhesive and Adhesion; Theory and Mechanisms

An adhesive is a material, usually in the form of liquid or semi-liquid, that can join articles together when applied to their surfaces and withstand separation by transferring applied loads from one adherent to another across the joint area. The terms adhesive and glue are used interchangeably. However, there is a slight difference between them. Glues are usually obtained from natural sources while adhesives are synthetic materials. There are many advantages of using adhesives over traditional joints such as ability to join materials with different geometry and dimensions (e.g. thin or thick bodies), better distribution of any applied stress over the joint area, which is specially crucial in dynamic loadings, ability of attaching similar and dissimilar adherents, sealing the joint area, and convenience of use [11, 12]. Disadvantages of using adhesives in comparison with mechanical bonding techniques can be lower service life, negative effect of harsh service environment on adhesives and adhesion

strength, and inferior strength and toughness to some mechanical joints [11]. If at least one of the substrates involved in an adhesion process is a biological body, the phenomenon is called “bioadhesion” [13].

Several mechanisms for adhesion and bioadhesion have been described in literatures, which can be categorized into four main mechanisms including mechanical interlocking, chemical bonding, diffusion theory, and electrostatic theory [11]. Although adhesion in a system might arise predominantly from one of these mechanisms, often a combination of various mechanisms is accountable in most adhesion systems. These adhesion mechanisms are briefly discussed in this section.

1.3.1 Mechanical interlocking

In the mechanical interlocking concept, adhesive material infiltrates into the pores and irregularities of adherends’ surfaces and mechanically locks into the microscopic surface roughness of the substrates that leads to binding to the surface. A well known example of this mechanism is the traditional tooth cavity filling method by means of amalgam, where adhesion between amalgam and the pretreated tooth surface is facilitated by mechanical interlocking. In order to achieve the required surface topography for good mechanical interlocking the surface pretreatment is essential. However, there are some doubts uncertainties about how significant role this mechanism plays in adhesion, as some studies show that good adherence can occur between smooth surfaces as well. Although mechanical interlocking plays an important role in the adhesion between roughened surfaces, other factors such as elimination of weak surface layers during surface treatment and consequent enhancement in interfacial contact area are believed to have more contribution to adhesion strength than mechanical interlocking [11, 12].

1.3.2 Intermolecular Bonding

This theory, which is the major mechanism of adhesion between adhesive materials and substrates, particularly in bioadhesion, arises from interatomic/intermolecular forces and bonds between atoms/molecules of adhesives on one side and atoms/molecules present on the surface of substrates on the other. These forces include primary interactions or chemical bonds

as well as secondary forces. Various types of primary forces or chemical bonds (also referred to as “Chemisorptions”) can be formed across the interface including covalent, ionic and metallic bonds. Since the primary bonds are of high energy, they will usually form a strong adhesion. However, formation of strong primary bonds across interface in most cases needs special preparation techniques such as chemical modification of adhesive molecules by incorporating specific groups into the chemical structure of adhesive or pretreatment of adherents’ surfaces by means of primers, adhesion promoters and coupling agents [11].

Secondary forces such as hydrogen bonds, dipole-dipole interactions, London dispersion, and van der Waals forces can be of significant importance in adhesion. Although the energy of primary bonds is much higher than that of the secondary forces, but in many cases only the secondary forces are accountable for bonding strength, particularly when a large number of sites for secondary forces is available in the interface of adhesive and substrates. In some studies a different approach has been taken to explain the adhesion between adhesive and substrate. They have considered electron donor-acceptor interaction to be involved in intrinsic adhesion. Lewis acid and base can be considered as electron acceptor and donor, respectively. In this manner hydrogen bond can also be classified as donor-acceptor interaction. Molecules with donor and acceptor properties are also able to form molecular complex that helps the bonding between these types of molecules and forming stronger adhesion [11, 12]. Adsorption theory is the major adhesion mechanism in most soft tissue adhesives, where the bonding between adhesive materials and tissue surface arises from primary chemical bonds or secondary forces or a combination of both.

1.3.3 Chain Entanglement

Diffusion theory has been proposed to explain, in particular, the adhesion of two similar polymers (also known as 'Autoadhesion') as well as to other polymers. In this mechanism polymer macromolecules diffuse mutually over the polymer-polymer contact interface, which typically has a thickness of 1-100 nm, and forms a layer of interpenetrated polymer chains. For this diffusion to happen, the giant polymer molecules must have enough mobility. Thus,

diffusion does not occur in highly crystalline and crosslinked polymers, neither in amorphous polymers below their glass transition temperature, due to lack of large scale molecule mobility. Additionally, the two interdiffusing polymers must be mutually soluble. One example, where this kind of interdiffusion takes place, is when two plastics with similar solubility parameters are welded to one another. In such welding, mobility of polymer molecules is commonly facilitated by applying heat or solvent to the interface areas [11, 12]. In bioadhesive systems, diffusion mechanism has also been employed to explain some bioadhesion phenomena [13]. For example, in mucoadhesive drug delivery systems, interpenetration and entanglement of bioadhesive polymer chains and glycoproteininc network of mucus is believed to be accountable for the adhesion of polymer carrier to the mucus. The diffusion of polymer chains into the network of glycoproteins (bioadhesion) occurs when they are brought in intimate contact and is a function of interface topological characteristics, diffusion coefficient of the macromolecule through the mucus network, chemical potential coefficient, and the difference between solubility parameters of bioadhesive medium and glycoproteins [13].

1.3.4 Electrostatic Absorption

When the surface of two materials with different electronic band structures are brought to a close proximity, the possible transfer of some electrons, which occurs to equalize the Fermi levels, might form a double layer of electron charge in the interface area. These charges are believed to induce electrostatic forces, which may play a significant role in the intrinsic adhesion of the two contacting surfaces. However, in the case of insulator substrates the charge build-up would be very slow and the number of available electrons might be limited, hence it would require a long time to build up charge concentration. Although the presence of electrostatic forces arisen from the charge double layer have been observed in some metals and semi-conductors, this mechanism does not play a significant role in adhesion of nonmetallic systems [11, 12]. However, this mechanism is believed to have a possible role in bioadhesion. For example, electron transfer in the contact area between a bioadhesive material and glycoprotein of mucus is thought to be one of the plausible mechanisms of mucoadhesion [13, 14].

1.4 Existing Tissue Adhesives and Sealants

In the past two decades, clinical surgical practices have significantly benefited from using bioadhesives, tissue sealants, and hemostatic agents to control blood loss and promote tissue healing [8]. Despite enormous amount of efforts and researches, only a few tissue adhesives have been approved by FDA for specifically indicated applications. A list of FDA approved tissue adhesives and sealants, together with their indicated applications, advantages and limitations are summarized in Table 1.2 [3]. The existing tissue adhesives and sealants, their structure, functioning mechanisms, indicated applications, and limitations are briefly reviewed in this section.

1.4.1 Fibrin Glue

Fibrin-based glues are one of the most widely used tissue adhesives in clinical applications. The use of fibrin as a scaffold for tissue regeneration and local hemostatic agent was first reported as early as 1910's [15, 16]. During the First World War Fibrin patches were used to control bleeding and then during 1940's the combination of fibrinogen and thrombin were used as biological glue for human skin grafting [17, 18].

The use of fibrin glue took momentum when the ability of producing high concentrated fibrinogen was developed, which led to making fibrin glue with stronger adhesion properties [17]. Fibrin glues had been in broad clinical use in Europe many years before it was approved by FDA in the United States in 1998.

Fibrin glues mimic the last stage of blood clotting during which fibrinogen is converted to fibrin clot through a complex coagulation cascade. The fibrin glue typically consists of two major components including concentrated human-derived fibrinogen (together with factor XIII and some other blood plasma proteins) and human or bovine thrombin in combination with calcium chloride solution as the second component [17, 19].

Table 1.2 FDA-approved tissue adhesives, sealants and hemostats available in the US market

Bioadhesives/Sealants family	Product Brands (Chemical name)	Manufacturer	Indicated Applications	Pros	Cons	Reference
Cyanoacrylates	Dermabond (2-Octyl cyanoacrylate)	Ethicon Inc. (Johnson & Johnson Co)	• Topical applications to hold closed easily approximated skin edges from surgical incisions • Dermabond may be used in conjunction with but not in place of subcuticular sutures	• Fast polymerization • Strong adhesion • Ease of use • Relatively inexpensive	• Exothermic polymerization • Work best on dry surfaces • Prolonged degradation • Safety concern over degradation products • Limited to topical uses	[20-24]
	Indermil (n-Butyl-2-cyanoacrylate)	Covidien Inc.	• Closure of topical skin incisions that are simple, thoroughly cleansed, and have easily approximated skin edges • In conjunction with but no in place of deep dermal stitches • Microbial barrier			
	Histoacryl and Histoacryl Blue (n-Butyl-2-cyanoacrylate)	B. Braun Medical Inc.	• Closure of smooth and fresh skin wounds • Closure of skin in endoscopic incisions • Sclerosation therapy of large esophageal and fundal varices			
Albumin and Glutaraldehyde	BioGlue (Bovine serum albumin and 10%glutaraldehyde)	Cryolife Inc.	• As adjunct to standard methods of achieving hemostasis (such as suture and staple) in open surgical repair of large vessels (such as aorta, femoral and carotid arteries)	• Fast Polymerization, begins in 20-30 sec and reaches full strength in 2 min • Good adhesion to tissue	• Safety concerns over risk of glutaraldehyde toxicity • Relatively	[8, 25]

Table 1.2-Continued

Fibrin glue	Tisseel (Human pooled plasma fibrinogen and thrombin)	Baxter Inc.	• As an adjunct to hemostasis in surgeries involving cardiopulmonary bypass and treatment of splenic injuries when control of bleeding by conventional surgical techniques, including suture, ligature, and cautery, is ineffective or impractical • As an adjunct for the closure of colostomies • Vitagel is used during surgical procedures (except neurosurgery and eye surgery) as an adjunct to clotting when control of bleeding using suture or other conventional procedures is not effective, or seems impractical • The autologous Cryoseal system fibrin sealant is indicated for use as an adjunct to hemostasis on the incised liver surface in patients undergoing liver resection	• Fast curing • Biocompatibility • Biodegradability	• Risk of transferring blood-borne disease • Risk of allergic reaction Risk of infection transmission • Long preparation time • Ancillary equipment required • Poor tissue adhesion • Relatively expensive	[17-19, 26-28]
	Evicel (Human pooled plasma fibrinogen and thrombin)	Ethicon Inc. (Johnson & Johnson Co)				
	Vitagel (Autologous plasma fibrinogen and thrombin)	Orthovita Inc.				
	Cryoseal system (Autologous plasma fibrinogen and thrombin)	ThermoGenesis Corp.				
Poly(ethylene glycol) (PEG) based sealants	Coseal (2 four-armed PEGs: one capped with glutaryl-succinimidyl ester and the other with thiols, and dilute solution of hydrogen chloride and sodium phosphate-sodium carbonate)	Baxter Inc.	• Sealing suture lines and vascular graft	• Rapid gel formation • Fast hemostasis • Biocompatibility • Adhesion to tissue	• Risk of swelling • Possible allergic reaction • Relatively expensive	[8, 29, 30]
	Duraseal (PEG ester powder and trilysine amine solution with FD&C blue No.1 dye)	Covidien Inc.	• Sealing of cerebrospinal fluid (CSF)			

Upon mixing the two components, fibrinogen is converted to fibrin monomers by thrombin which consequently forms a polymer. In the meantime thrombin activates factor XIII (in presence of calcium chloride) into XIIIa, which stabilizes the network through crosslinking of fibrin molecules by creating amide bonds and forming an insoluble clot (Figure 1.1) [3, 17, 19]. In order to prevent fibrinolysis (disassociation of fibrin clot, which happens by plasmin enzyme), an antifibrinolytic agent (such as aportinin) is used in some formulations. Depending on the amount of thrombin the rate of clot formation can be adjusted to be reached within seconds with higher concentration of thrombin or after a couple of minutes as the thrombin concentration is lowered. The maximum adhesion strength is usually achieved within 3 to 5 minutes and is directly proportional to the concentration of fibrinogen [27].

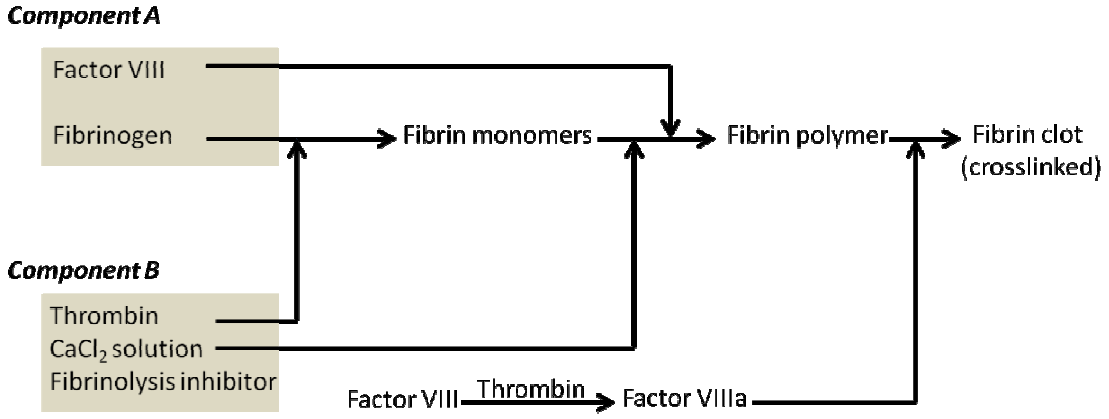

Figure 1.1 Schematic diagram of functioning mechanism of fibrin glue, resembling the last stage of physiological coagulation cascade in the body.

Family of fibrin glues has been broadly utilized in clinical applications. The majority of reported applications were in surgical procedures, to control bleeding and leaking during and, particularly, after surgeries [9, 31]. There are numerous reports on using fibrin glue as hemostatic agent and sealant in cardiovascular surgery, particularly to prevent bleeding from suture line and graft area, which is a common issue in this type of operations [9, 31-37]. Fibrin sealants are also utilized in neurosurgery to seal cerebrospinal fluid after operation on the central nervous system and peripheral nerve repair and grafting [31, 38, 39]. The application of fibrin glues in treatment of gastrointestinal tract diseases such as in patients suffering from

bleeding peptic ulcers has also been investigated with the aim of replacing surgical procedure by noninvasive endoscopic injection of fibrin sealant. This application demands sealants with specific flow and crosslinking characteristics to make them suitable for injection through lumen catheters and allow enough time for handling and injection [31]. There are also numerous reports on the applications and performances of fibrin sealants in a variety of medical disciplines such as plastic surgery and skin grafts [40], ENT (ear, nose and throat) and head and neck surgery [41], trauma surgery [42], urology [9, 31], and ophthalmology [43].

Despite of having many advantages, such as fast curing, biocompatibility, and biodegradability, using fibrin glue might be associated with some risks and safety concerns. The thrombin from bovine source can trigger allergic reactions in some patients. Additionally, in reaction to bovine factor V or thrombin some antibodies are produced that might cross-react with human clotting factor can cause serious hemorrhage. There is also a risk of transmission of infectious agents to human when bovine-source thrombin is used [28]. Thrombin of human can be used in order to overcome these safety concerns [28]. Another concern in using fibrin sealant- despite the extensive efforts to minimize it, is the risk of blood-borne disease transmission, such as HIV and hepatitis A, B and C, as the result of using pooled human plasma as the source for extracting fibrinogen and thrombin [18, 44]. To eliminate this concern some fibrin sealants make use of fibrinogen and/or thrombin derived from patient's own blood plasma. The side effects of using antifibrinolytic agents, which are used to prevent untimely fibrinolysis (breakdown of fibrin clot), are another possible area for concern associated with using fibrin glue [18]. Additionally, direct injection of the glue into large blood vessels can result in thromboembolic event and interfere with blood stream [45]. Another weakness of fibrin glues is their poor adhesion to tissue when compared to other adhesives such as cyanoacrylates and gelatin-resorcinol-formaldehyde/glutaraldehyde (GRF/GRFG) [46]. Other disadvantages of fibrin glues are their long preparation time, which takes approximately 20 minutes [26], and their inefficacy in high pressure bleeding [17]. Finally, fibrin sealants perform best when applied to dry surfaces, which is a limiting factor when wet tissue adhesion is required.

1.4.2 Cyanoacrylates

Invented by H. Coover in mid 20th century, cyanoacrylate- based adhesives, also known as “Superglue”, have been one the strongest and multipurpose adhesives available. They have broad applications from general household uses to medical applications. The general structure of cyanoacrylates (or alkyl-2-cyanoacrylates) monomer, an alkyl ester of 2-cyanoacrylic acid, is shown in Figure1.2 [3]. It is a liquid monomer that rapidly polymerizes at room temperature through an exothermic- anionic polymerization in the presence of nucleophile species, particularly hydroxyl ion, including water [21].

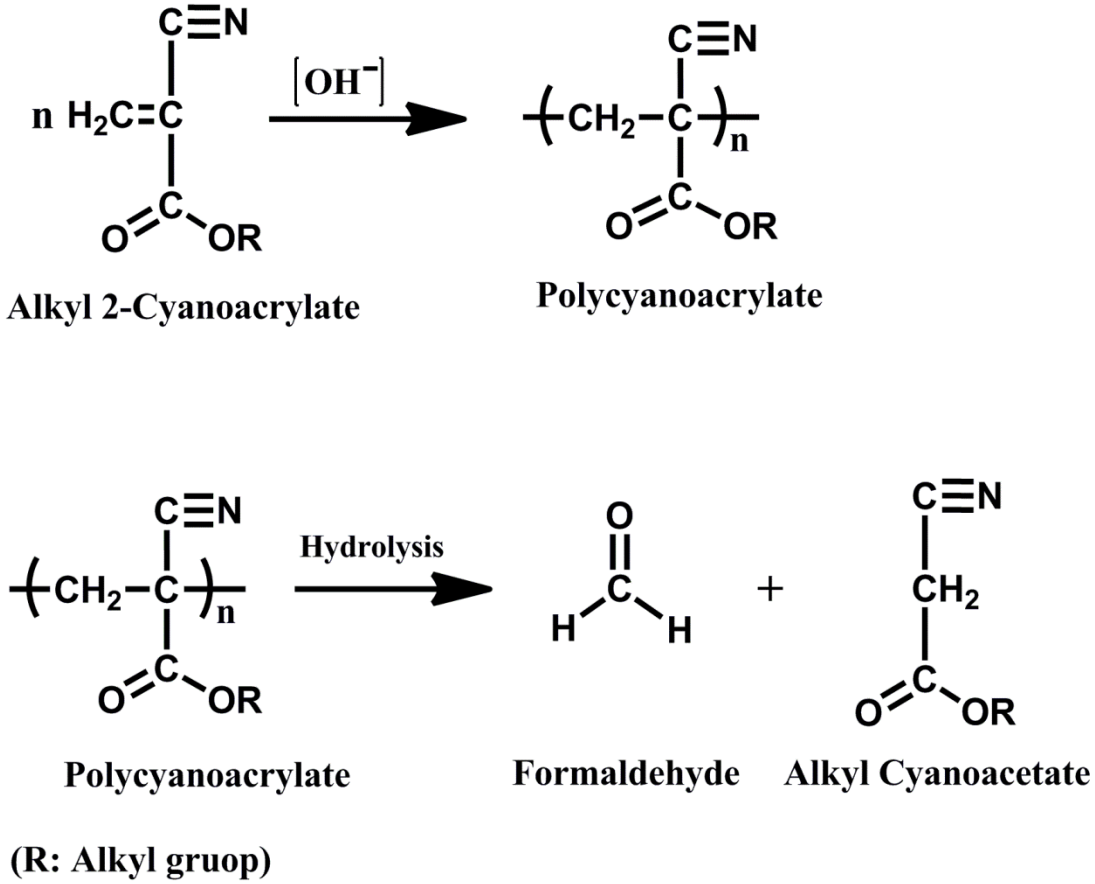

Figure 1.2 Polymerization (A) and degradation (B) of cyanoacrylate adhesives.

The first cyanoacrylates adhesive used in clinical application for skin incision closure in Europe and Canada, was n-butyl-2-cyanoacrylates in 1980’s. In the United States FDA approved the first cyanoacrylate adhesive with indicated application of topical skin

approximation in 1998, an adhesive based on 2-octyl-2-cyanoacrylate, which also contains plasticizer, radical and anionic stabilizers and colorant [21]. Another available medical adhesive from cyanoacrylate family is based on n-butyl-2-cyanoacrylate, which was approved by FDA for closure of the topical skin incisions [21].

The pending alkyl groups (-R, Figure 1.2) largely influences the polymerization and properties of final polymer. Increasing the length of side alkyl group lowers polymerization rate and causes formation of polymers with less stiffness and more flexibility. Longer alkyl group also decreases the mechanical properties of polymer, such as tensile strength and modulus, and lowers adhesion strength. It also causes slightly less tissue response but increases the stability against hydrolytic degradation [23].

Cyanoacrylate adhesives properties, such as strong adhesion, rapid setting time, instantaneous adhesion to tissue and their ease of use with simple preparation make them very attractive for clinical uses and are widely used in emergency rooms, dermatology and plastic surgery. There are some other reported applications, such as endoscopic intervention for gastric varices outside the United States.[22] They are also getting more popularity in dentistry applications, as tissue adhesive, bonding orthodontic brackets, repair of dentures, etc [20]. On the other hand exothermic reaction, i.e. heat generation during polymerization, and concerns about toxicity of degradation by products, namely cyanoacetates and formaldehyde, have caused limitations in medical use of cyanoacrylate adhesives. Furthermore, despite of having fast polymerization and strong adhesion, it might lack required flexibility specially when used for soft tissue adhesion. This is particularly observed in cyanoacrylates with short alkyl groups such as methyl-2-cyanoacrylates [21, 24]. Polymers with short alkyl group and lower molecular weight (i.e. shorter polymer chain) degrade faster causing more histotoxicity, while high-molecular-weight polymers with longer side chain degrade slowly, which translates in producing less toxic degradation products [21]. However, this decelerates the rate of hydrolytic degradation of adhesive and even might result in a non-degradable polymer, which can cause medical complications [23]. There are also some other issues associated with cyanoacrylates

adhesives including difficulties in accurate delivery due to its low viscosity, weak shear strength of joint area especially in presence of water, high stiffness that can cause undesired consequence such as adhesion failure and tissue irritation and, infection due existence of non-absorbable polymer [23]. These disadvantages have limited the application of cyanoacrylate adhesives to topical skin approximation in the United States. Nevertheless, researchers are trying to address the problems associated with clinical usage of cyanoacrylate adhesives in order to broaden their medical applications. For example, to address prolonged biodegradability issue, Linden et al developed absorbable adhesive polymers based on using more hydrophilic cyanoacrylates including (for example methoxypropyl cyanoacrylates) instead of using alkyl cyanoacrylates such as n-butyl, isobutyl or n-octyl cyanoacrylates.[23] Plasticizers, stabilizers, accelerators, viscosity- adjustment agents and other additives might also be included in the adhesive formulation to improve the properties of cyanoacrylate adhesives in order to make them more accommodating for broader tissue applications.

1.4.3 Protein-Based Adhesives

Another family of commercially available adhesives and sealants for clinical utilizations is based on proteins or protein-like compounds that undergo crosslinking reaction upon exposure to proper crosslinking agent, while simultaneously form covalent bonds with the tissue surface. Unlike fibrin glue, these adhesives do not mimic the coagulation mechanisms.

One of the adhesives of this type is a gelatin-based glue called Gelatin-Resorcin-Formaldehyde/Glutaraldehyde (GRF or GRFG), which was developed in Europe in 1960's [47]. GRF/GRFG has been clinically utilized in Europe and Japan for the past decades. Gelatin, a naturally occurring protein, is derived from collagen of bovine or porcine skin or bone. Depending on production method gelatin is categorized into type A, prepared by using acid extraction, or type B, which is conditioned by a base which is followed by acid extraction. Gelatin is a biocompatible and bioabsorbable material that can form strong and transparent gels and flexible films, granting it suitable properties for medical application. However, due to its solubility in water and consequently low stability in aqueous environment, gelatin network

requires to be stabilized through crosslinking in order to be used in physiological environments [47, 48]. Gelatin can be crosslinked by reacting with aldehydes, which decreases its solubility and increases the cohesive strength. The combination of gelatin and aldehyde was initially proposed as a tissue adhesive, but due to its poor performance in aqueous environment, a phenolic component (1,3-benzenediol), namely resorcinol or resorcin, was added to improve its strength through reducing the negative effect of water [49].

GRF/GRFG glue (gelatin resorcinol formaldehyde/glutaraldehyde), also known as “French glue”, is a two-component glue consisting of: 1) gelatin and resorcinol mixture; and 2) formaldehyde or formaldehyde/glutaraldehyde combination as polymerizing agent. The gelatin chains are crosslinked by aldehyde through polycondensation reaction with amine groups of gelatin. Simultaneously, reaction of aldehyde groups with amine groups of living tissue forms a strong bond with the tissue (Figure 1.3) [3]. Resorcin molecules are also linked to one another by aldheyde groups [47, 49]. Due to their strong bonding even in the presence of moisture, these type of adhesives have been used in medical applications particularly in Europe for the treatment of aortic dissections [46, 50], liver surgeries [51], gastrointestinal tract surgeries [52], and urinary tract surgeries [53].

Despite of being used for many years, particularly in Europe, the presence of formaldehyde, as a residue of unreacted aldehyde or as a degradation product, is a major point of concern due to its possible mutagenicity and carcinogenicity [54]. Therefore studies about using less toxic glutaraldehyde glyoxal have been done [54]. In addition, developing other crosslinking techniques rather than using chemical agents can eliminate the risk of using aldehydes. Researchers reported synthesis of a tissue sealant that was prepared based on a photo-crosslinkable gelatin [48]. In another attempt a research group reported a hemostatic technology using photo-curable gelatins and a hydrophilic difunctional macromer. They developed hemostatic glue consisted of gelatin, poly(ethylene glycol) diacrylate, and ascorbic acid, all of which were dissolved in a saline solution and produced a swollen gel upon irradiation of the glue by visible light [55].

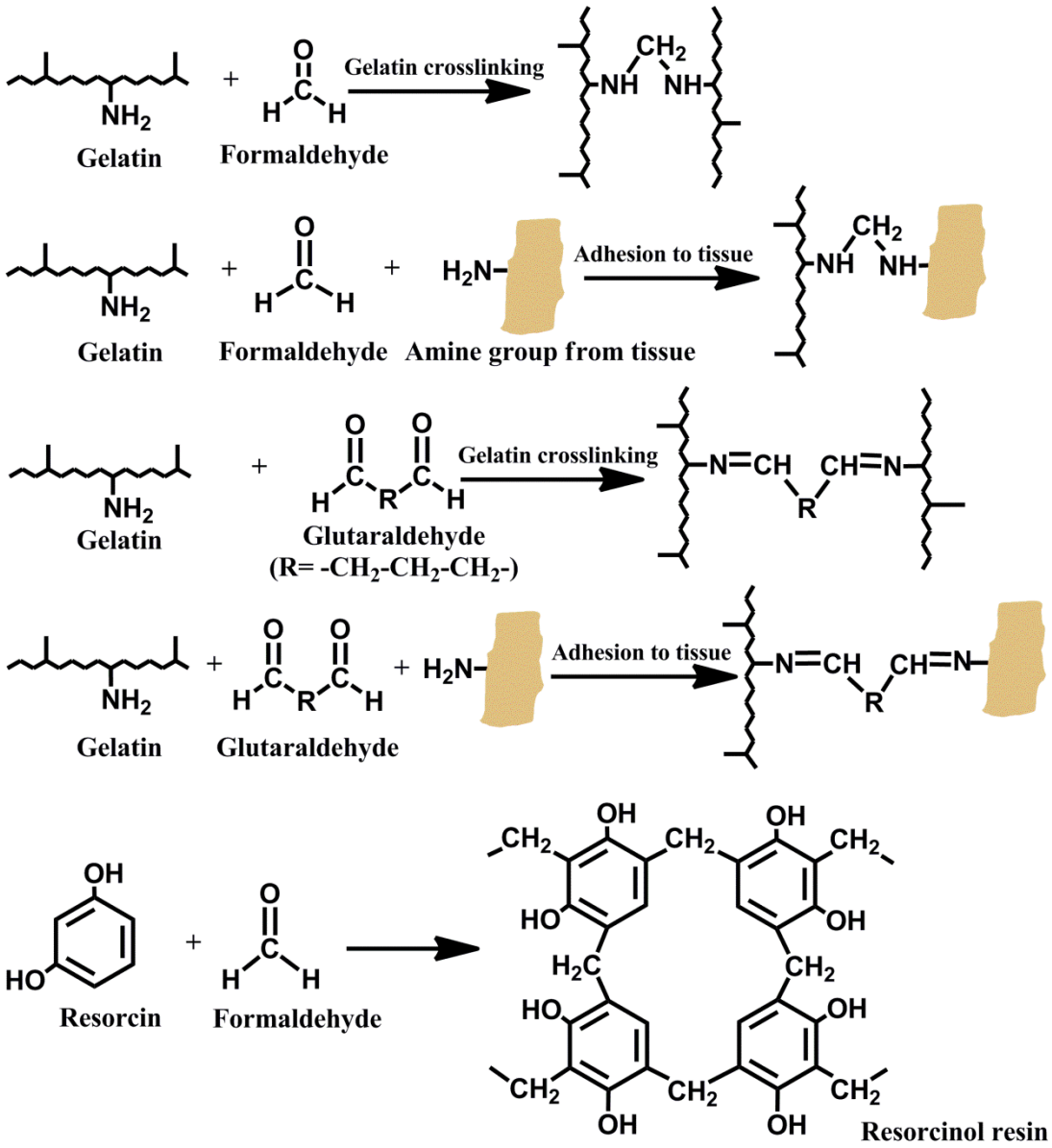

Figure 1.3 Schematic adhesion and crosslinking mechanisms of GRF/GRFG glue (gelatin resorcinol formaldehyde/glutaraldehyde).

There is currently no FDA-approved GRF/GRFG glues in the United States. However, a glue and sealant based on albumin-glutaraldehyde is available in the United States (BioGlue), which has FDA approval for application as adjunct to standard methods of hemostasis (such as suture and staple) in open surgical repair of large vessels (such as aorta, femoral and carotid arteries). This protein-based sealant consists of bovine serum albumin protein that is

crosslinked through linkage formation between amine groups of albumin protein chains by aldehyde groups of glutaraldehyde. The adhesion mechanism to tissue is similar to previously described GRFG glues (Figure 1.3). This kind of product has been approved and used for sealing large blood vessels, vascular prostheses and aortic dissection [8, 25]. However, as for GRFG glues, similar safety concerns of using aldehyde-containing products has limited their wide utilizations [8].

1.4.4 Polyethylene glycol (PEG)-Based Hydrogel Sealants

Another type of synthetic tissue sealants are polymeric hydrogels developed based on PEG. PEG is a well known nontoxic, non-immunogenic, biocompatible and FDA-approved material which has found many applications in modern medicine including surface modification of materials for enhanced biocompatibility and hydrogel for drug delivery [56]. This family of tissue adhesive is typically consists of chemically modified linear or branched PEG molecules. Depending on available chemical groups, these modified PEGs can be crosslinked upon mixing through chemical crosslinking or upon irradiation of light by photo-crosslinking of PEGs capped with a photo-reactive elements such as acrylate groups to form a hydrogel adhesive. For example, one of the FDA-approved PEG-based adhesives is composed of two four-armed PEGs (with pentaerythritol core), one of which has terminal groups of glutaryl-succinimidyl ester and the other is terminated with thiols [29]. When the two PEG solutions are mixed together (with dilute solution of hydrogen chloride and sodium phosphate-sodium carbonate [8]), the polymer begins to crosslink and form a network through the reaction of thiol groups with the carbonyl groups of the succinimidyl ester, resulting in formation of a covalent thio-ester bond between PEG molecules (Figure 1.4) [3, 29]. The main application of this adhesive is for sealing suture lines and vascular grafts [30]. Another FDA-approved PEG sealant, which consists of PEG ester and trilysine amine solutions, is used as an adjunct to dural closure for sealing CSF (cerebrospinal fluid) leakage following a neurosurgery [8]. Although PEG-based tissue adhesives offer many advantages such as rapid gel formation, adhesion to biological surface, good biocompatibility of polymer and degradation products and inducing mild to moderate

inflammatory response, there are some concerns associated with them including a swell ratio of up to 400% of original volume, which requires more caution when using in closed spaces to avoid pressure build up (e.g. nerve compression) [8]. In addition, it requires a relatively dry surface for better adhesion, which is a challenge to achieve in physiological condition of the human body, particularly when dealing with open bleeding wounds [30].

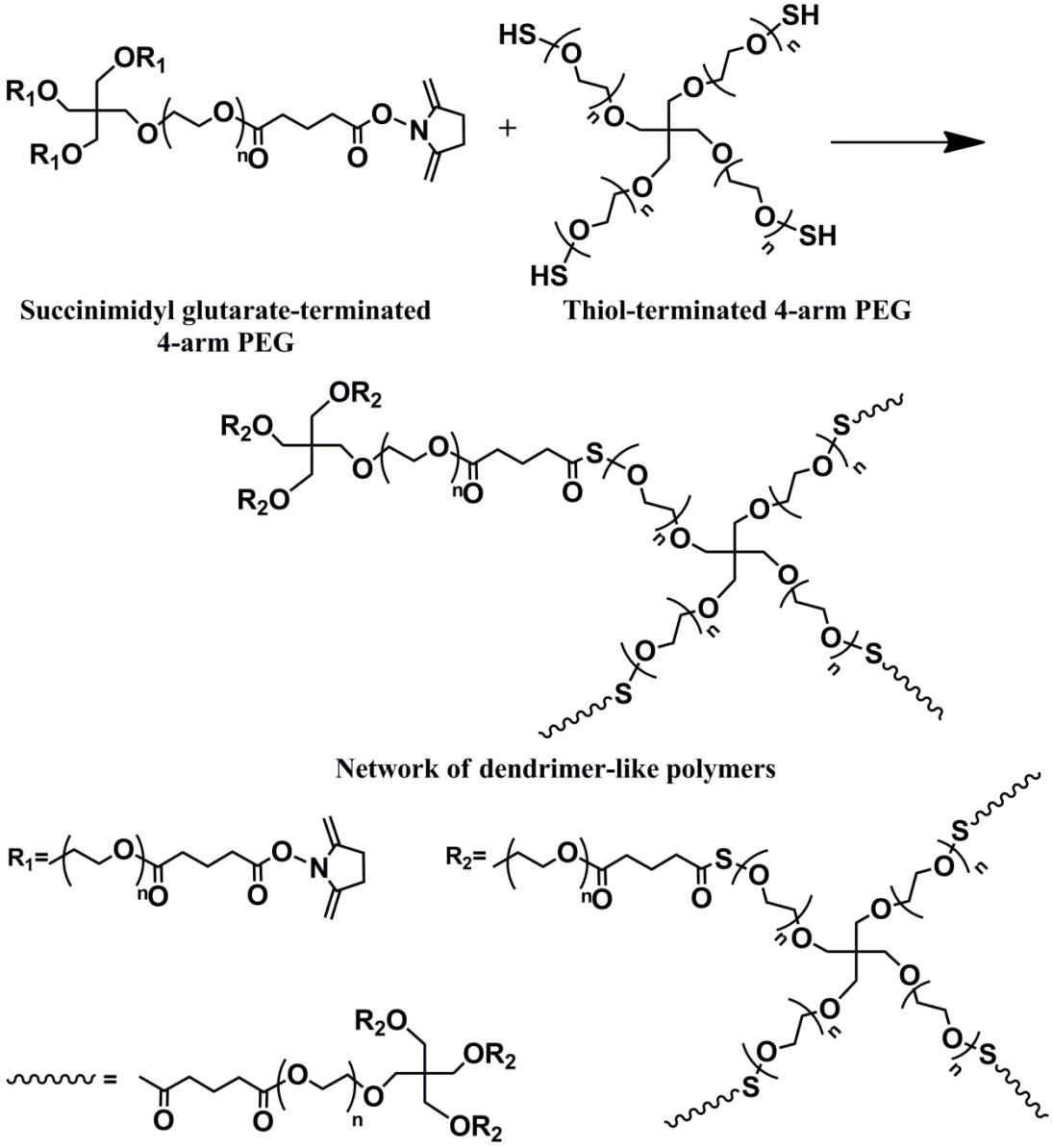

Figure 1.4 Crosslinking and network formation of sealants based on dual-PEG (poly(ethylene glycol)) comprising two 4-arm PEGs capped with succinimidyl glutarate and thiol.

1.5 Recent Developments in Tissue Adhesives

As discussed earlier, a number of tissue adhesive systems have already been approved by FDA for indicated applications and are commercialized. However, the performance inefficacy, safety concerns and limitations associated with the use of each of these adhesive and sealants have driven researchers to address those problems by developing new adhesives, which have better performance in biological environment, broader applications and fewer drawbacks. In this section, some of the recent developments in the field of tissue adhesives are discussed.

1.5.1 Urethane- Based Adhesives

In the recent decades, polyurethanes, a family of polymers synthesized based on polyaddition reaction between diisocyanates and diols, have been utilized in many medical applications such as bladders, catheters, cardiovascular applications, wound dressing and pacemakers [57]. Urethane chemistry is based on high affinity of isocyanate groups to nuclephiles such as hydroxyl- or amine-containing chemicals. Taking advantage of this feature, researchers tried to develop urethane-based adhesive systems. Typically this type of adhesives consists of isocyanate-terminated pre-polymers, which form a polymer network in reaction with water molecules upon contact with wet biological environment. Simultaneously, these pre-polymers will covalently adhere to tissue through formation of urea bond between available isocyanate groups and protein amines available in physiological body (Figure 1.5) [3]. Various aromatic and aliphatic polyisocyanates with different polyether/polyester diols have been used to synthesize tissue adhesives [58-60]. However, there are three major challenges associated with using urethane adhesives: prolonged set time, ether-based polyurethanes are not readily biodegradable, and toxicity and carcinogenicity of degradation products [61]. As mentioned earlier, an ideal tissue adhesive must solidify rapidly. Isocyanate-terminated pre-polymers usually exhibit long set time- in the order of tens of minutes, when no catalyst is used, which makes them unacceptable as tissue adhesives. This problem is more critical when aliphatic isocyanates, such as hexamethylene diisocyanate (HDI) are used. These isocyanates are

employed in the place of more reactive aromatic isocyanates (such as TDI: toluene diisocyanate or MDI: methylene diphenyl diisocyanate), which even though make the urethane formation faster, are more toxic and can result in releasing carcinogenic aromatic diamines, such as 2,4-diaminotoluene upon hydrolytic degradation of urethane bonds. To address the issue of long set time a research group used more reactive fluorinated HDI [59]. In another attempt researchers utilized linear and multi-armed pre-polymers capped with more reactive Isocyanate groups [60, 62]. They synthesized Lysine di- and tri-isocyanates (LDI and LTI) that reacted with glucose and PEG with different molecular weight to yield isocyanate-capped pre-polymers. These pre-polymers are reportedly crosslinked within 30 sec to 2 min upon applying to tissue surface [60]. Using this type of isocyanates also diminished the safety concerns associated with aromatic isocyanates. To tackle the challenge of prolonged in-vivo biodegradability of polyether based polyurethanes, hydrolytically-degradable ester components (such as polylactide/poly-□-caprolactone) were incorporated into the structure of polyurethanes, which resulted in a polymers with accelerated rate of degradation [63]. Despite of all these breakthroughs and other improvements in urethane chemistry and raw materials to address existing safety concerns, there is no FDA-approved tissue adhesive based on polyurethane to date.

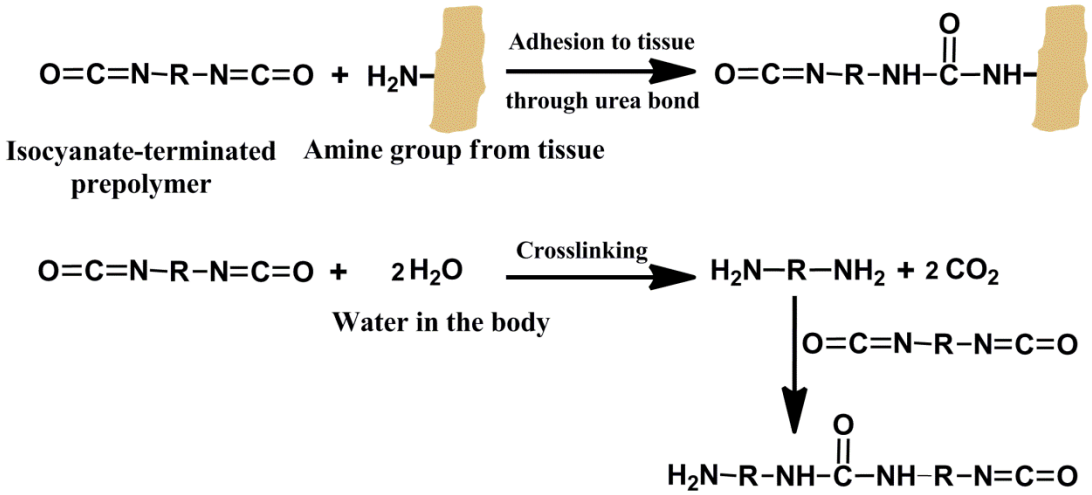

Figure 1.5 Tissue adhesion and crosslinking mechanisms of urethane-based adhesives.

1.5.2 Nature-Inspired Adhesives

Nature and natural phenomena have always been a major source of inspiration for human to develop and invent new materials and applications. Adhesive technology has not been any different. An outstanding example is biologically-derived fibrin glue, discussed earlier in this review. Adhesive materials are widely used by many organisms ranging from biofilm in microscopic bacteria to proteinous adhesives secreted by sea organisms such as mussels and barnacles. One of the most important features of the adhesive polymers produced by sea creatures is their capability to firmly adhere to any substrates (non-specific) in wet condition, where water must be displaced from the adherent surface. Furthermore, these adhesives show strong resistance against destructive effect of water, which often adversely influences the strength of many chemical bonds and, hence, the strength of adhesives [64].

1.5.2.1 Mussel Adhesive Proteins

Tissue adhesives must effectively function in aqueous environment in order to be able to create strong adhesion to wet biological surfaces. Thus, understanding the adhesion mechanism of organisms that stick to wet surfaces can help the development of adhesives with strong wet- tissue adhesion for use in biological environment. One of these creatures that has been extensively studied, mostly through the works of H.J. Waite, is mussel [65]. Mussels, such as Mytilus edulis, secrete adhesive materials (also called Mussel Adhesive Proteins or MAPs) that enable them to firmly adhere to various underwater surfaces such as sea rocks and ship hulls, and resist detachments even in marine's harsh and wavy condition. Studies have shown that this strong wet adhesion is primarily due to the presence of a catechol-containing amino acid called L-3,4-dihydroxyphenylalanine (L-DOPA), a post-translational hydroxylation of tyrosine, in the structure of secreted mussels adhesive proteins [65-67]. Although the adhesion and crosslinking mechanisms of MAPs are not completely known, it has been proposed that hydroxyl groups of DOPA are able to generate chemisorption to polar surfaces such as formation of hydrogen bonds to the hydrophylic surfaces [65]. Furthermore, under oxidizing or alkaline condition DOPA promotes the crosslinking reactions of MAPs through the oxidation of

catechol hydroxyl groups to ortho-quinone, which triggers intermolecular crosslinking between MAPs, rendering cohesion and bulk elastic properties to these proteins. In addition, oxidized DOPA contributes in strong adhesion to biological surfaces, through the formation of covalent bonds with available nucleophile groups on these surfaces such as –NH2, –SH, –OH and –COOH [66, 68-70]. Furthermore, DOPA is also able to undergo crosslinking through formation of a strong complex with multi-valent metals and metal ions, which are present in marine environment [71].

Considering the outstanding and unique properties of mussel adhesives such as fast curing, even in wet condition, and strong adhesion to non-specific surfaces, many researchers have tried to mimic the adhesion strategy of mussels to make bioadhesives that can robustly function in wet/dry condition. Initially researches focused on direct extraction and isolation of adhesive protein from mussels and other organisms as well as on genetically engineering these proteins.[72, 73] In one study adhesive strength of extracted MAPs crosslinked by different curing agent has been measured and compared with some cyanoacrylate-based adhesives [74]. It was concluded that, depending on curing system, the adhesion strength of MAPs could be higher than that of some cyanoacrylates with longer side chain (e.g. butyl and octyl cyanoacrylates) but was inferior to short-side-chain cyanoacrylate such as ethyl cyanoacrylate [74]. Since isolation and purification of MAPs from mussels is a complicated procedure with relatively low yield (10,000 mussels to obtain 1g of MAP) [75], there have been many investigations concerning synthesis of polymer adhesive mimetic of MAPs. In addition to studies about synthesizing DOPA-containing polypeptides [76-80], researchers have also investigated the functionalization of other monomers/polymers with DOPA or compounds analogous to DOPA. A group of researchers reported modification of poly(ethylene glycol) (PEG) by DOPA [81]. They conjugated amine-terminated linear- and branched- PEG with DOPA and studied the crosslinking behavior and hydrogel formation of DOPA-functionalized PEG using different oxidation agent such as horseradish peroxide, hydrogen peroxide, sodium periodate and mushroom tyrosinase [81-83]. The reported gel times varied from seconds to hours depending

on structure of pre-polymer, its spatial architecture, and the oxidation agent used. In a recent study, in-vivo performance of a synthetic glue based on branched-PEG functionalized with 3,4-dihydroxyhydrocinnamic acid (a catechol containing compound), which was crosslinked using sodium periodate solution, was evaluated in extrahepatic islet transplantation of a mice model. Minimal acute or chronic inflammation was reported while the interface with the tissue remained intact for up to one year, according to the reported results [84]. In another attempt, investigators reported synthesis of surgical meshes coated by DOPA-functionalized PEG and polycaprolactone (PCL). The presence of DOPA in the structure of the coating polymer rendered adhesion properties to the coated mesh, hence, reportedly eliminated the need for mechanical fixation of mesh and made it suitable to be utilized as a reinforcement for surgical repair of soft tissues [85].

The non-specific dry/wet surface adhesion of synthetic mussel-inspired adhesives has exposed a new ground for developing a new family of soft tissue adhesives that are not only capable of forming strong adhesion to wet tissues, but safe enough for utilization in human body without any adverse effect during application and degradation. However, there are some limitations such as complicated syntheses routes, expensive starting materials, and most importantly, non-/ prolonged degradability of the described synthetic mussel-inspired adhesives. In some cases complex structural modifications are necessary to make these adhesive biodegradable and bioabsorbable [86].

1.5.2.2 Gecko-Inspired adhesive

Geckos are capable of climbing and strongly attaching to vertical and inverted surfaces. Yet, temporary nature of this adhesion enables geckos to detach and reattach to the surface with high pace, making it possible for them to run fast over vertical and inverted surfaces. This extraordinary adhesion feature of geckos relies on millions of nano-structured hairs, called setae, covering gecko's soles [87, 88]. In sub-microstructure scales, capillary forces and van der Waals interactions are the main mechanisms for adhesion to hydrophilic and hydrophobic materials, respectively [87]. Inspired by geckos, Geim et al reported fabrication of a gecko-

mimetic adhesive, based on micro-patterned pillars that were made of flexible polyimide films using electron-beam lithography and dry etching in oxygen plasma.[87] They reported that the adhesion strength these adhesives is directly proportional to the number of foot-hairs sticking to the surfaces and the flexibility of the pillars, which is required for attaching to rough surfaces [87]. However, the adhesion is adversely affected when the micro-patterned pillars are immersed in water. To address this problem, researchers took advantage of the combination of the sticking mechanisms of gecko and the adhesion power of mussels [88]. They prepared nanoscale pillars, similar to gecko foot hairs, out of poly(dimethylsiloxane)(PDMS) that was then dip-coated by a mussel-mimetic polymer film to create an adhesive with the capability of reversibly adhering to different surfaces in dry and wet condition [88]. By combining these two adhesion strategies, mechanical and chemical, they reported a significant increase in the adhesion strength between an individual pillar and the residing surface in dry and, particularly, in wet environment.

In another attempt a group of investigators reported the preparation of gecko-inspired tissue adhesive by making nano-patterned poly(glycerol-co-sebacate acrylate) (PGSA), which was then coated by oxidized dextran. The presence of dextran reinforces the covalent adhesion of nano-structured PGSA to wet tissue through formation of imine groups, which is the result of reaction between aldehyde functional groups of dextran and amine group of tissue proteins [89]. They have taken advantage of the elasticity and biodegradability of PGSA to prepare this reportedly biocompatible tissue adhesive [89].

1.6 Applications of Bioadhesives in Tissue Engineering and Reconstruction

In addition to being utilized for wound management and hemostasis, bioadhesives are increasingly emerging in other bioapplications such as tissue engineering and regeneration as well as drug delivery systems [3]. One of the biggest challenges of using biomaterials in regeneration of tissue defects is the discontinuity in the interfacial region between biomaterials and tissue, which can cause the failure of the integration between the two. To prevent this separation from occurring, various integration techniques, such as suturing and tissue

adhesives, are employed. However, for different tissues with distinctive functional requirements, tissue adhesive with a specific set of properties might be necessary. Thus, to minimize the risk of failure, customized tissue adhesives are developed to tailor the requirements of a specific tissue. In a recent development, investigators employed adhesive moieties to promote graft integration in cartilage tissue repair/engineering. To enhance cartilage tissue repair, chondroitin sulphate (CS), a polysaccharide found in cartilage, was functionalized with photo-crosslinkable methylacrylate and chemically-crosslinkable aldehyde groups [90]. The modified CS was then used as a biodegradable injectable adhesive scaffold to integrate with surrounding tissues once injected for cartilage tissue engineering. On one side, methacrylate groups of modified CS created bonds with a hydrogel biomaterial (PEG diacrylate) through photo-crosslinking, while the aldehyde end of CS chemically bonded to tissue, Thus, a bridge between biomaterial and cartilage tissue was formed, which significantly promoted graft integration/bonding with the tissue so as to improve cartilage repair. It was reported that the repair of defected cartilage was significantly improved, when CS adhesive was used together with hydrogel.

One of the most extensively investigated tissue adhesives for tissue engineering applications is fibrin glue. One reported application of injectable fibrin glue is in cardiac tissue engineering, where damaged cardiac tissue was shown to benefit from using compliant adhesive scaffold to facilitate graft integration, reduce mechanical irritation and inflammation, and promote tissue regeneration. In one study fibrin glue was used as an injectable wall support and scaffold in myocardial infarction (MI) in a rat model [91]. The results indicated that fibrin glue could prevent wall thinning, especially after myocardial infarction. In another study by the same author, it was shown that using fibrin glue enhanced cell transplant survival, decreased infarct size, and facilitated blood flow to ischemic myocardium by improving neovascularization in a rat myocardial infarction model [92]. Fibrin glue was also used as an injectable scaffold containing adipose-derived stem cells to maintain the cardiac function in a rat model after MI [93]. It was reported that using fibrin glue together with the stem cells increased the cells

retention, enhanced the graft size, improved heart function, and significantly increased arteriole density in the infracted area, when compared to the case of injecting the stem cells alone [93].

Another reported off-label application of bioadhesives is to prevent seroma, which is a common postsurgical complication. Interruption of lymphatic system and vasculatures during surgery causes drainage and accumulation of serous fluids in the space created by surgery.[94, 95] If not treated, seroma can cause massive complications.[94] Biodegradable bioadhesives, particularly fibrin glue, are the most widely investigated materials against seroma formation. The role of fibrin glue in seroma prevention is believed to be twofold: first, by reducing the flow of body fluid into surgically-created space through sealing the damaged vessels and lymphatic systems; and second, through eliminating the generated dead space by gluing injured tissues in the surgical area [94]. The biomaterials used in sermoa prevention must be biodegradable and bioabsorbable within limited period of time to avoid complications related to the prolonged degradation. In the case of fibrin glue this period is in the range of 1-2 weeks [31].

In another capacity bioadhesives have been playing a major role in controlled and site-specific drug delivery. Adhesion of a drug loaded vehicle to the surface of a biological target, not only increases the residence time of drug and improves its absorption by the targeted biological system, but can also influence the rate of drug release, thus, improving the efficacy of medications [96]. In this context the adhesion is due to interfacial forces between the bioadhesive on one side, and either cell membrane or its coating, such as mucus, on the other. The bioadhesive drug delivery systems have been investigated in many applications such as mucoadhesives for drug delivery to gastrointestinal tract, bioadhesives in nasal drug administration, and ocular drug delivery systems.

1.7 Summary

As discussed in this chapter, tissue adhesives and sealants are important elements of medical practitioners' tools box in the modern medicine. They play a crucial role in bleeding control and wound closure to minimize patients' blood loss, which otherwise could lead to severe complications or even death. Tissue adhesives are especially applicable in the places

where other wound closure techniques, such as stitching, are not practical or accessible. Other advantages include possible reduction in morbidity and mortality rate due to rapid bleeding control, ease of use with no or little training, and possible containment of healthcare cost through shortening hospital stay by accelerating healing process and eliminating the need for readmission for removing sutures. There are currently a number of FDA-approved tissue adhesives and sealants, which are clinically used, such as fibrin-based glues and sealants and cyanoacrylates. Despite of many advantages, the current bioadhesive systems have some shortcomings, which limit their utilizations. These limitations are weak wet tissue adhesion, risk of transmitting blood-borne disease, toxicity of adhesive raw materials and their degradation products, prolonged degradation period, high costs of some of these products. To address these problems, numerous studies have focused on improving upon already available adhesives as well as on tackling these problems by developing totally new adhesive systems using new bioadhesion strategies, such as urethane chemistry and nature-inspired adhesives (mussel adhesives for example). Despite of all the efforts and breakthroughs, there exist no product that have all the necessary requirements of an ideal tissue adhesive, which can be used in versatile applications with no concerns and limitations. Thus, the pursuit of ideal tissue adhesive continues. In addition, the applications of tissue adhesives are expanding to other areas of bioengineering and pharmaceutical applications. In their new functions, adhesive systems are utilized to improve biomaterials-tissue interaction and integration in order to enhance regeneration of new tissue and tissue engineering. In addition, they play an important role in targeted and controlled drug delivery by adhering and releasing a drug load to a specific target. Numerous additional off-label medical applications have been reported for bioadhesives as well, which highlights the importance of this family of biomaterials in today's medicine [3].

1.8 Specific Aims and Hypotheses

As elaborately discussed in the previous sections, despite of offering numerous advantages the currently available tissue adhesives encounter several limitations, which restrict their applications. The major problems include inadequate adhesion strength to wet tissue

surface, possibility of transmitting blood-borne disease, allergic reactions of patients to the animal-extracted products used in some adhesives, cell- and tissue- toxicity of some adhesive materials and their degradation products, non-degradability or prolonged degradation time, and high cost, which limit the broad clinical acceptance of these tissue adhesives. Thus, developing surgical adhesives with strong wet tissue adhesion, controlled biodegradability and mechanical properties, and excellent biocompatibility in a facile and cost-effective manner has been a significant challenge.

To address these challenges, in the present research, we aim to introduce a new family of tissue adhesives, which offer superior properties over the existing tissue adhesives. These properties include: 1) strong adhesion to wet tissue surface; 2) biocompatibility of both adhesive materials and degradation products; 3) readily biodegradable and bioabsorbable with tunable rate; 4) facile and cost-effective preparation from safe constituents. These new biodegradable citric acid(CA)-based tissue adhesives are designed based on the adhesion strategy of sea mussels, which enables them to strongly and exceptionally adhere to non-specific surfaces in aqueous condition. Using this strategy enables our synthesized adhesives to form strong binding to tissues even under wet condition. Another important feature of our approach is utilizing safe and biocompatible constituents, including poly(ethylene glycol), dopamine or L-3,4-dihydroxyphenylalanine (L-DOPA), and especially CA, which is a non-toxic metabolic product of the body (Krebs cycle). Possessing multifunctional groups, which can be utilized as sites for chemical binding and conjugations without any need for complex and harsh synthesis techniques and toxic reagents, and excellent bio/hemo-compatibility confer CA unique advantages for biomaterials syntheses. To summarize, the governing hypotheses of this research are: a) the ability of mussels to adhere to non-specific surfaces in wet/dry conditions can be translated though mimicking their adhesion mechanism by incorporating the chemical components responsible for this exceptional adhesion properties into the structure of synthesized adhesive polymers; b) the multifunctional citric acid can be used to prepare water soluble and biodegradable adhesive pre-polymers through a one-step synthesis technique; c)

the resulted pre-polymers can adhere to various wet/dry surfaces and undergo crosslinking and hydrogel formation upon addition of an initiator; d) the solubility in water and tunable crosslinking of these pre-polymers make them suitable candidates for in-situ delivery; e) the controllable and pH-sensitive swelling and degradation of the crosslinked polymers can be used to fabricate hydrogel for controlled delivery of medicines and other biological agents. Our strategy is to prepare a novel family of biodegradable strong wet tissue adhesives and hydrogels, with tunable material properties, and use these materials for fast and effective sutureless wound closure and hemostasis. Furthermore, these injectable hydrogel materials can be used for controlled drug delivery system and as a carrier for cell/drug delivery with in-situ crosslinking feature. The impacts of this research proposal are that this family of bioadhesives should address many of the existing challenges in preparing and using soft tissue adhesives and help advancing the field. In addition, a new family of injectable in-situ crosslinkable composites with attractive properties for various orthopedic applications is introduced, which is developed based on addition of hydroxylapatite to our adhesive polymer system. To achieve these goals, we set the following specific aims:

Aim 1: Develop a methodology to synthesize a new family of injectable and biodegradable tissue adhesives and hydrogels with strong wet tissue adhesion:

1.1 Synthesize and characterize a new family of injectable citrate-based mussel-inspired biodegradable adhesives (iCMBAs) and hydrogels;

1.2 Study the physical, mechanical, crosslinking, and adhesion properties of iCMBAs;

1.3 Evaluate the biocompatibility and performance of iCMBAs through in vitro cell culture and in vivo studies on a rat model for sutureless wound closure and healing applications.

Aim 2: Preparation and application of injectable iCMBA-based/Hydroxyapatite(HA) composite materials for orthopedic applications:

2.1 Prepare a new injectable and in-situ crosslinkable composite from iCMBA and HA with various compositions;

2.2 Study the physical and mechanical properties of iCMBA-HA composites and governing parameters;

2.3 Evaluate the biocompatibility and in-vivo performance of iCMBA/HA composites through in vitro cell culture and in vivo study on a rabbit comminuted fracture model.

Aim 3: Prepare iCMBA hydrogels and nanoparticles for pH-sensitive controlled drug delivery system (CDDS) applications:

3.1 Prepare and characterize iCMBA hydrogels and determine their swelling ratio and degradation profile at various influencing parameters such as pre-polymer and environmental pH;

3.2 Determine the drug release profile of drug-loaded iCMBA hydrogels and governing parameters;

3.3 Fabricate and characterize nanoparticles (nanogels) from iCMBAs and investigate their drug release properties.

In the next three chapters the strategies and experiments that were designed to achieve each of the described specific aims are discussed in details.

CHAPTER 2

SYNTHESES AND CHARACTERIZATION OF INJECTABLE CITRATE-BASED MUSSEL-INSPIRED BIODEGRADABLE ADHESIVES (iCMBA) WITH HIGH WET STRENGTH FOR SUTURELESS WOUND CLOSURE

2.1 Introduction

As discussed in chapter one a few tissue adhesives have already been approved by FDA for indicated applications and are clinically utilized. Nevertheless, the performance inefficacy, safety concerns and limitations associated with these adhesives and sealants have motivated researchers to develop new adhesives with better performance in biological environment, broader applications and fewer drawbacks. Tissue adhesives must effectively function in aqueous environment in order form strong adhesion to wet biological surfaces, which is inevitable when dealing with open wounds or internal elements of the human body. To achieve this goal, researchers developed a new family of adhesives, which can adhere to non-specific surfaces in aqueous condition. This approach was inspired by the adhesion strategy employed by some maritime creatures, such as blue mussel *Mytilus edulis*, which can firmly stick to any surfaces under harsh condition of sea water and resist separation through secreting a adhesive-like protein called mussel adhesive proteins (MAPs) [65, 97]. The strong adhesion ability of the mussels has been ascribed to the presence of a catechol-containing amino acid called L-3,4-dihydroxyphenylalanine (L-DOPA), a post-translational hydroxylation of tyrosine, found in the structure of secreted mussels adhesive foot proteins [65-67]. Although the adhesion and crosslinking mechanisms of MAPs are not completely known, it has been proposed that, under oxidizing or alkaline condition, L-DOPA can promote the crosslinking reactions of these adhesive proteins through the oxidation of catechol hydroxyl groups to ortho-quinone, which subsequently triggers intermolecular crosslinking, rendering cohesion and bulk

elastic properties to the network of proteins. Recent studies revealed that oxidized DOPA also contributes to strong adhesion to biological surfaces, through the formation of covalent bonds with available nucleophile groups on these surfaces such as –NH2, –SH, –OH and –COOH groups [66, 68-70, 98, 99]. In addition, hydroxyl groups of DOPA are able to generate chemisorption to polar surfaces such as formation of hydrogen bonds to the hydrophylic surfaces [65].

Considering the outstanding and unique properties of mussel adhesives such as fast curing and strong adhesion to non-specific surfaces, even in wet condition, researchers have tried to mimic the adhesion strategy of mussels to make bioadhesives that can robustly function in wet/dry condition. Initial studies were focused on direct extraction and isolation of adhesive protein from mussels and other organisms as well as on genetically engineering these proteins [100, 101]. In one study adhesive the strength of extracted MAPs crosslinked by different curing agent has been measured and compared with some cyanoacrylate-based adhesives [102]. It was concluded that, depending on the curing system, the adhesion strength of MAPs could be higher than that of some cyanoacrylates with longer side chain (e.g. butyl and octyl cyanoacrylates) but was inferior to short-side-chain cyanoacrylate such as ethyl cyanoacrylate [102]. Since isolation and purification of MAPs from mussels is a complicated procedure with relatively low yield (10,000 mussels to obtain 1g of MAP) [75], there have been numerous investigations concerning synthesis of polymer adhesive mimetic of MAPs. In addition to studies about synthesizing DOPA-containing polypeptides [78, 103-106], researchers have also investigated the functionalization of other monomers/polymers with DOPA or compounds analogous to DOPA. By incorporating catechol-containing species into the structure of polymers, wet tissue adhesive hydrogel materials have been synthesized [75, 79, 84, 107-109]. A group of researchers reported modification of poly(ethylene glycol) (PEG) by DOPA [110]. They conjugated amine-terminated linear- and branched- PEG with DOPA and studied the crosslinking behavior and hydrogel formation of DOPA-functionalized PEG using different oxidation agent such as horseradish peroxide, hydrogen peroxide, sodium periodate and

mushroom tyrosinase [83, 110, 111]. The reported gel times varied from seconds to hours depending on structure of pre-polymer, its spatial architecture, and the oxidation agent used. In a recent study, in-vivo performance of a synthetic glue based on branched-PEG functionalized with 3,4-dihydroxyhydrocinnamic acid (a catechol containing compound), which was crosslinked using sodium periodate solution, was evaluated in extrahepatic islet transplantation of a mice model. Minimal acute or chronic inflammation was reported while the interface with the tissue remained intact for up to one year, according to the reported results [84]. However, the syntheses of these catecholic polymers require costly multi-step preparation/purification techniques and the use of toxic reagents, which must be avoided or minimized when preparing biomaterials. Furthermore, in spite of the appealing wet tissue adhesion properties, existing mussel-inspired adhesive polymers [112, 113] are essentially non-degradable, hence substantially limiting their potential uses in a variety of medical applications, including tissue adhesives, tissue engineering and drug delivery. Inspired by another natural adhesion mechanism - gecko adhesion which is mainly effective on dry surfaces, biodegradable elastomer, poly(glycerol sebacate acrylate) (PGSA) was fabricated into adhesive tape with nano-pillar structures to simulate the nano-scale setae on gecko food pads [114]. To improve wet tissue adhesion, a strategy has been recently developed to coat wet tissue adhesives such as mussel-inspired adhesives [88] and aldehyde-functionalized starch [114] on a gecko-adhesive-like nanostructures to achieve mechanical interlocking and covalent chemistry simultaneously. Despite these exciting progresses, none of the existing bioinspired adhesives alone possess sufficient wet tissue adhesion strength and controlled degradability for sutureless wound closure application.

2.2 Significance and Rationale

To address the portrayed issues, such as inadequate wet tissue adhesion strength, difficulties associated with biodegradability, and complex and expensive syntheses methods, we, hereby, introduce new methodology for facile and cost-effective syntheses of a new family of injectable citrate-based mussel-inspired bioadhesives, iCMBAs, and hydrogels (Figure 2.1),

which was designed based on the adhesion strategy that is employed by sea mussels to exceptionally adhere to non-specific surfaces in aqueous condition [115]. The rationale behind the iCMBA strategy was to react citric acid, poly(ethylene glycol) (PEG), and catechol-containing monomers such as dopamine or L-DOPA via a one-step polycondensation reaction. Such an approach allows us to fabricate new adhesive materials with great wet adhesion strength, controllable degradability, improved biocompatibility, and substantially reduced manufacturing costs. Citric acid, a non-toxic metabolic product of the body (Krebs cycle), was a key in the established methodology in the development of citrate-based biodegradable polymers (CBBPs) including poly(diol citrates) [116-119], crosslinked urethane-doped polyesters (CUPE) [120, 121], poly(alkylene maleate citrates) (PAMC) [122-124], and biodegradable photoluminescent polymers (BPLP) [125, 126] for applications in tissue engineering, drug delivery, medical devices, and bioimaging. Citric acid was mainly used to facilitate degradable ester-bond formation in biomaterials, while enhancing hemocompatibility and hydrophilicity of the polymers and providing pendant binding sites for bioconjugation to confer additional functionality such as optical properties. For iCMBA synthesis, citric acid was used to not only form degradable polyesters with PEG, but also provide valuable pendant reactive carboxyl groups to conjugate dopamine or L-DOPA. Thus, using highly reactive multifunctional citric acid enables a one-step synthesis to prepare biodegradable polyesters with pendant catechol functionalities via a facile condensation reaction. All the monomers used for iCMBA syntheses are inexpensive, readily available, and safe for in vivo uses and have been documented in many FDA- approved devices and applications.

2.3 Synthesis and Characterization of iCMBAs

2.3.1 Synthesis of iCMBAs

All chemicals, cell culture medium, and supplements were purchased from Sigma Aldrich (St. Louis, MO), except where mentioned otherwise. All chemicals were used as received.

iCMBAs are oligomers based on citric acid (CA) and PEG that have been functionalized by catechol-containing compounds, such as dopamine and L-DOPA (L-3,4-dihydroxyphenylalanine) , using a polycondensation technique, as illustrated in Figure 2.1. CA and PEG were placed in a 250ml three-necked round-bottom flask and heated to 160℃ using an oil bath until a molten clear mixture was formed under stirring. Next, under nitrogen gas flow, a calculated amount of dopamine or L-DOPA was added to the mixture. After allowing enough time for a clear solution to form, the temperature was reduced to 140℃ and the reaction was continued under vacuum for the required time until the desired molecular weight was achieved. The prepared pre-polymer was dissolved in deionized (DI) water and purified by extensive dialysis using a 500 and 1000 –MWCO (molecular weight cut-off) dialysis tube, depending on the molecular weight of PEG used. The dialyzed solution was then lyophilized to obtain the pure adhesive pre-polymer. By using different PEG lengths and various amounts of dopamine different pre-polymers of iCMBAs were synthesized as shown in Table 2.1.

2.3.2 iCMBA Pre-polymers Characterization

In order to characterize the functional groups present in the pre-polymers, iCMBAs were analyzed by Fourier Transform Infra Red (FT-IR) spectroscopy. For this purpose, 1% (w/v) solution of pre-polymers in 1,4-dioxane were cast on potassium bromide crystal discs and allowed to completely dry in a hood. The spectroscopy was then performed using a Nicolet 6700 FT-IR (Thermo Scientific, Waltham, MA) equipped with OMNIC software.

For proton analysis, 1% (w/v) solution of iCMBA pre-polymer in deuterium oxide was placed into a 5-mm-outside diameter tube and analyzed by Proton Nuclear Magnetic Resonance spectroscopy (^{1}H-NMR) using a 250 MHz JNM ECS 300 (JEOL, Tokyo, Japan).

Furthermore, the presence of unoxidzied –OH groups of catechol (2-hydroxyphenol) in the structure of iCMBA pre-polymers was determined by UV-VIS spectroscopy [127], where absorbance of 0.02 % (w/v) solution of various pre-polymers in DI water were measured using Shimadzu UV-VIS spectrophotometer machine across the wavelength of 700-200 nm.

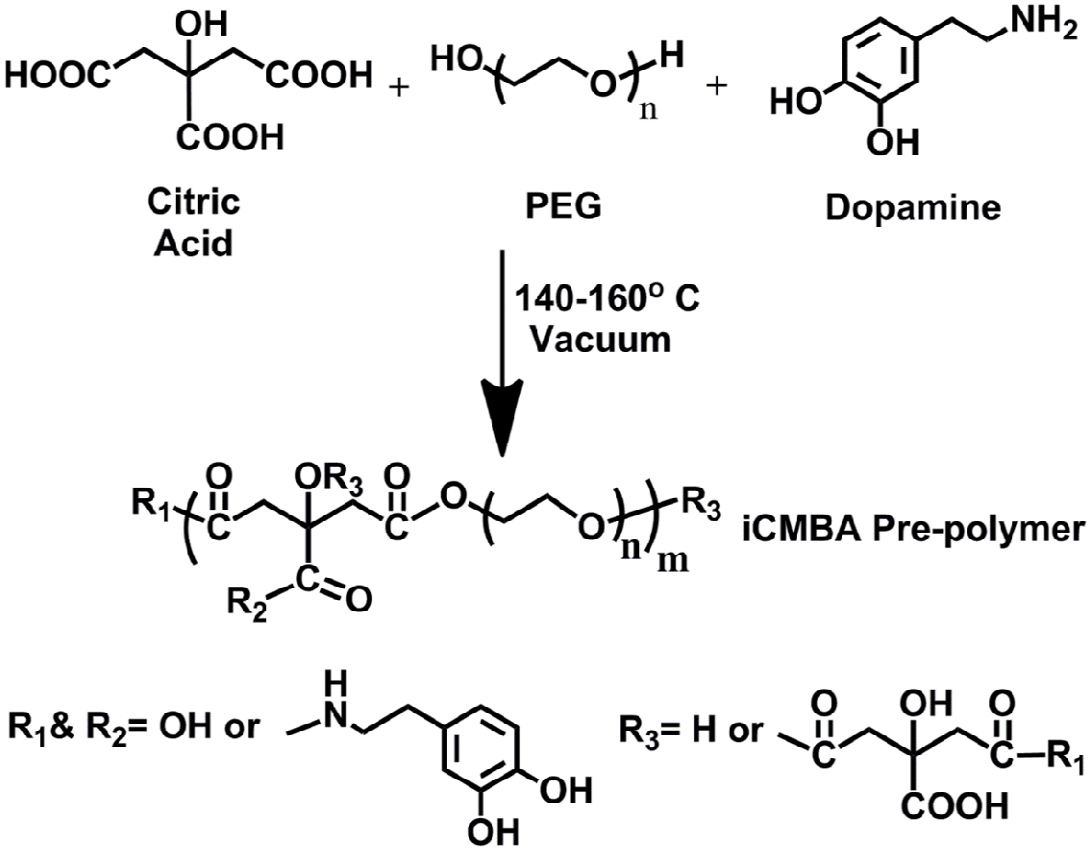

Figure 2.1 Schematic representation of iCMBA pre-polymers synthesis through polycondensation reaction.

Table 2.1 Nomenclature, feeding ratio, and final composition of pre-polymers

Polymer name	Mol weight of used PEG (Da)	CA:PEG:Dopamine (moles)	CA:PEG:Dopamine Feeding Ratio	CA:PEG:Dopmaine Composition Ratio
iCMBA-P_{400} $D_{0.1}$	400	1.1:1:0.1	0.50:0.45:0.05	0.49:0.46:0.05
iCMBA-P_{400} $D_{0.3}$	400	1.1:1:0.3	0.46:0.42:0.12	0.46:0.43:0.11
iCMBA-P_{400} $D_{0.5}$	400	1.1:1:0.5	0.42:0.38:0.20	0.41:0.42:0.17
iCMBA-P_{200} $D_{0.3}$	200	1.1:1:0.3	0.46:0.42:0.12	0.46:0.44:0.10
iCMBA-P_{1000} $D_{0.3}$	1000	1.1:1:0.3	0.46:0.42:0.12	0.45:0.46:0.09

2.3.3 Crosslinking of iCMBAs and Gel Time Measurement

In order to crosslink the pre-polymers of iCMBAs and make adhesive hydrogels, pre-polymers were first dissolved in DI water and then mixed with sodium (meta)periodate (PI) solution in DI water. PI is an oxidizing agent, which triggers oxidation and consequently crosslinking reaction of catechol-containing iCMBAs upon mixing. The amount of PI, defined as the PI-to-prepolymer w/w ratio, was varied between 2% and 8%.

Gel or set time, which was defined as the time from mixing pre-polymer solution with initiator to the beginning of crosslinking, was determined by a viscometry technique based on modified ASTM D4473 method using a cone and plate Brookfield viscometer (Brookfield Engineering Labs, Inc, MA) equipped with temperature control unit. For this purpose 1mL of 50% (w/w) solution of pre-polymer in DI water was mixed with equal volume of PI solution with different concentrations to achieve various PI/pre-polymer ratios. Immediately after mixing, the mixture was transferred to the viscometer cup and the change in viscosity of the mixture was measured versus time, using a CP-42 spindle at spinning speed of 12 revolutions per minutes. The time from the start point till onset of abrupt increase in the viscosity of the mixture, determined according to ASTM D4473, was defined as the gel time of polymer adhesives. The measurements were done at 25℃ for all samples except for iCMBA-$P_{400}D_{0.5}$ PI:8%, which was measured at two temperatures, 25℃ and 37℃, to evaluate the influence of temperature on the gel time. Different iCMBA formulations and various ratios of PI to iCMBA pre-polymers were tested to study the effect of PEG molecular weight, the amount of dopamine in the structure of the pre-polymers, and the effect of initiator-to-prepolymer ratio on the crosslinking, gel time and properties of iCMBAs.

2.3.4 Properties of Crosslinked iCMBAs

Mechanical properties of crosslinked polymers, including ultimate tensile strength, modulus and elongation at break, were measured by tensile mechanical testing according to ASTM D412A on an MTS Insight 2 fitted with a 10 N load cell (MTS, Eden Prairie, MN). Briefly, the dog bone shaped samples (25 mm × 6 mm × 1.5 mm, length × width × thickness) were

pulled at a rate of 500 mm/minute, and elongated to failure. Values were converted to stress-strain and the initial modulus was calculated from the initial slope of the curve (0-10% elongation). In order to evaluate the effect of hydration on the mechanical properties of crosslinked iCMBAs, the mechanical tests were also conducted on the fully swollen samples, i.e. samples that have been hydrated and swollen in water for 4 hours.

After the crosslinking reaction took place, the sol-gel content, which determines non-crosslinked/crosslinked fractions of polymer, and swelling ratio was measured by the mass differential before and after incubation of the polymer network in a solvent or water. For the sol (soluble) content measurement, cylindrical discs of polymers (5 mm diameter; 2 mm thick) were cut from unpurified crosslinked films. The discs were weighed to find the initial mass (W_i), and suspended in 1,4-dioxane for 48 hours while the solvent was changed every 6 hours. Next, the samples were removed from the solvent and lyophilized for 72 hours. The dried samples, absent of any non-crosslinked polymer and solvent, were weighed to find the dry mass (W_d). The sol-gel fraction was then calculated using the formula from equation (2.1):

$$\text{Sol}\ (\%) = \frac{W_i - W_d}{W_i} \times 100 \qquad \text{Equation (2.1)}$$

To measure swelling ratio, the leached and dried samples were then suspended in water for 24 hours. Next, samples were removed from the water, blotted dry with filter paper, and weighed (W_s). The swelling percentage was calculated using the formula from equation (2.2):

$$\text{Swelling}\ (\%) = \frac{W_s - W_d}{W_d} \times 100 \qquad \text{Equation (2.2)}$$

Degradation studies were conducted in PBS (pH 7.4) and at 37°C. Cylindrical disc specimens (7 mm in diameter; 2 mm thick) were cut from purified crosslinked films. The purified samples were weighed (W_0), placed into test tubes containing 10 ml of PBS, and incubated at 37°C for pre-determined time points and till complete degradation of polymers. PBS was changed every 12 hours. After incubation for pre-determined time points, samples were

thoroughly and gently washed with DI water, lyophilized for 72 hours, and weighed. The mass loss was calculated by comparing the initial mass (W_0) with the mass measured at the pre-determined time points (W_t), as shown in equation (2.3):

$$\text{Mass loss}\,(\%) = \frac{W_0 - W_t}{W_0} \times 100 \qquad \text{Equation (2.3)}$$

2.3.5 Adhesion Strength Measurement

The adhesion strengths of different formulations of iCMBAs were determined by lap shear strength test according to modified ASTM D1002-05 method. Briefly, strips of porcine-derived, acellular small intestine submucosa (SIS) material (OASIS®, HealthPoint Ltd. Fort Worth, TX) were prepared in 40x4 mm dimension. After mixing the iCMBA solution with determined amount of PI solution, 10 µL of the mixture was dispensed and spread over an area of 6x4 mm of one strip, which was pre-soaked in water. A second wet strip was subsequently brought in contact with the first one to form a contact area of 6x4 mm. The adhered strips were then placed in a highly humid chamber for 2 hours. The lap shear strength of bonded strips specimens were subsequently measured using MTS Insight 2 fitted with a 10 N load cell and crosshead speed of 1.3 mm/min (MTS, Eden Prairie, MN). Besides various formulations of iCMBAs, fibrin glue (Tisseel, Baxter healthcare Corp.) was also tested as a control.

2.3.6 In vitro Biocompatibility Tests of iCMBAs

In vitro cell compatibility of pre-polymer and crosslinked iCMBAs were evaluated both quantitatively and qualitatively. To quantitatively assess in vitro iCMBA pre-polymer cytotoxicity a Methlythiazoletetrazolium (MTT) cell proliferation and viability assay was performed. First, the solution of different iCMBA pre-polymers in Dulbecco's modified eagle's medium (DMEM), containing 10% (v/v) fetal bovine serum (FBS) and 1% (v/v) streptomycin, were prepared in 3 different concentrations: 10, 1, and 0.1mg/mL (pre-polymer/medium). Next, to each well of a 96-well cell culture plate, 200µL of solution of NIH 3T3 fibroblast cells in DMEM, with concentration of $5x10^4$ cells/mL, was added and incubated for 24 hours at 37℃, 5% CO_2 and 95% relative humidity. The medium of each well was then replaced by pre-polymer-containing DMEM

solutions with various concentrations and incubated for another 24 hours followed by MTT assay analysis as per the manufacturer's protocol. Poly(ethylene glycol) diacrylate (PEGDA, M_n=700) solutions with similar concentrations were used as control as previously described [122]. Viability of cells in the DMEM containing pre-polymers and PEGDA were normalized to that of cells cultured in blank medium (DMEM without pre-polymers) as control. The results were reported as cells viability in percentage point. In this manner 100% cell viability means the cell viability in pre-polymer was exactly identical to that of blank medium.

Cytotoxicity of sol content or leachable fraction of crosslinked iCMBAs, referred to as sol-cytotoxicity, was also assessed by incubating equal mass of crosslinked iCMBA samples in 5mL cell culture medium for 24 hours. Next, three different solutions were prepared: 1X, 10X and 100X (1X was the solution of leached products with no dilution; 10X and 100X means 10 times and 100 times dilution of 1X by medium, respectively) which were used for cell culture. Fibrin glue (Tisseel, Baxter Corp.) and blank medium were used as controls. The cell culture and MTT assay were carried out as explained above. To evaluate the degradation products cytotoxicity, various formulations of crosslinked iCMBAs films (equal weight of each polymer) were fully degraded in 10 mL complete cell culture medium. The resultant solutions were diluted to three concentrations (1X, 10X and 100X) using DMEM, and used for cell culture and subsequent MTT analysis as already explained. All the above solutions were pH-neutralized and passed through a 0.2µm filter prior to use for cell culture. Qualitative cytotoxicity evaluation was also carried out by observing the adhesion of NIH 3T3 fibroblast cells to crosslinked iCMBAs films, using light microscopy. Briefly, crosslinked iCMBA films were cut in disc shape (5mm diameter and 1mm thickness) and sterilized by incubation in 70% ethanol for 3 hours followed by exposure to UV light for another 3 hours. 200µL of 3T3 fibroblast cell solution ($5x10^4$ cells/mL) was then seeded on each film. Using a photomicroscope, Nikon Eclipse Ti-U equipped with DS-Fi1 camera (Nikon Instruments Inc, Melville NY) the proliferation and morphology of cells on the films were observed and pictured at different time points of 1st, 3rd, and 5th day post cell culture.

2.3.7 In Vivo Study

The in vivo biocompatibility and wound healing properties of the iCMBAs were tested using rat skin incision model [128]. All experiments were performed with the approval of the University of Texas at Arlington Animal Care and Use Committee (IACUC). For this purpose, Sprague-Dawley rats (female, average weight of 300±50 g, 5 animals/group) were sedated with intraperitoneal injection of ketamine (40mg/kg) and xylazine (5mg/kg). Skin surgical area was sterilized with betadine and followed by 70% ethanol. Six full-thickness wounds (2 cm long × 0.5 cm deep) were made on the dorsum of each rat. Three of the wounds on each rat were closed by dropping sterilized iCMBA-$P_{400}D_{0.5}$ PI:8% into the wounds followed by finger-clamping for about 2 minutes while three other wounds were closed by conventional suturing as control. To minimize variations in surgical intervention, one surgeon performed all the procedures in a uniform fashion. On the 7th and 28th day post-wounding, the test animals were sacrificed and skin tissue at wound sites were excised for histological analyses. These sections were stained with hematoxylin and eosin (H&E) for morphological assessment and Masson trichrome staining was used to assess the collagen production. To evaluate inflammatory cells, immunohistochemistry was performed to quantify the number of CD11b positive cells using established procedures. The tissue sections were stained with inflammatory cell marker CD11b (rabbit anti-rat Integrin αM, H-61, Santa Cruz Biotechnology), and peroxidase-conjugated goat anti-rabbit secondary antibodies (Santa Cruz Biotechnology). All histological imaging analyses were performed on a Leica microscope (Leica, Wetzlar, Germany). Cell infiltration into the incision area was quantified using Image J software [129] by calculating cell density (number of cells per unit area) in random areas in the proximity of incision line with area held constant for all samples. The number of CD11b positive cells in the incision area was also determined by counting the cells in the cell infiltration area. Collagen density (as %) was determined through Masson trichrome staining images by calculating the ratio of blue-stained area (collagen) to total area using Image J. The healing and reconstruction of tissue in the incision area after four weeks was also evaluated by measuring the tensile mechanical strength of the regenerated

tissue treated with iCMBA and comparing it with suture-closed wounds and healthy skin tissue [128].

2.3.8 Statistical Analysis

All data were presented as means ± standard deviations, with sample number of at least 5. The significance of differences between results was evaluated by One-Way ANOVA test. In some tests, the difference with the value of p <0.05 (*) and in some others p <0.01(**) were considered to be statistically significant.

2.4 Results

2.4.1 Synthesis and Characterization of iCMBA Pre-polymers

iCMBA pre-polymers were synthesized in a convenient one-step polycondensation reaction between citric acid, PEG, and dopamine without requiring any organic solvent or toxic reagent during synthesis or purification. The FTIR spectra of some iCMBA pre-polymers as well as the spectrum of poly (citrate-PEG), CA-PEG, are shown in Figure 2.2A. The peak at 1527 cm^{-1} were assigned to amide group, C(=O)-NH, which was not observed in CA-PEG. Peaks between 1700-1750 cm^{-1} were assigned to carbonyl group, C=O, in amide and ester bonds. The relatively broad peaks centered at 2931 cm^{-1} were assigned to methylene groups which were observed in all the spectra of the iCMBA pre-polymers. The broad peaks centered at 3435 cm^{-1} were assigned to the hydroxyl group stretching vibration and hydrogen bonded unreacted-carboxyl groups [130].

A representative spectrum of ^{1}H-NMR analysis of purified iCMBA pre-polymer is depicted in Figure 2.2B. The chemical shifts at 6.4-6.7 ppm were assigned to protons of phenyl group which is a characteristic of catechol group present in the structure of iCMBAs [131]. The multiple peaks between 2.55 and 2.90 ppm were assigned to the protons in methylene groups from citric acid and dopamine [132]. The large peak at 3.45 ppm was attributed to the protons signal of –OCH2– CH2– from PEG and the shifts detected at 4.1-4.2 ppm were from methylene groups of PEG adjacent to ester bond. The final composition of the iCMBA pre-polymers, shown

in Table1, was calculated by comparing the area under peaks of phenyl protons shifts with that of assigned to protons of citric acid and PEG methylene groups.

The results of UV-VIS photospectroscopy showed the absorption of UV light at 280 nm wavelength for all samples, as displayed in Figure 2.2C. iCMBA-$P_{400}D_{0.5}$ and iCMBA-$P_{200}D_{0.3}$ showed the highest absorption of UV at 280 nm followed by iCMBA-$P_{400}D_{0.3}$, iCMBA-$P_{1000}D_{0.3}$ and iCMBA-$P_{400}D_{0.1}$.

2.4.2 Crosslinking and Gel Time of iCMBAs

The gel time of different compositions is shown in Table 2.2, which has been derived from viscosity measurements (Figure 2.2D) of iCMBAs during crosslinking reaction after mixing with initiator. The measured gel time was in the range of 18 seconds for iCMBA-$P_{400}D_{0.5}$ PI:8% at 37℃ up to slightly over 5 minutes for iCMBA-$P_{400}D_{0.3}$ PI:2%. Higher amount of dopamine in the structure of pre-polymer decreased the gel time as did higher initiator-to-prepolymer ratio. iCMBA pre-polymers made from PEG with higher molecular weight exhibited longer gel time, when crosslinked with the same amount of PI.

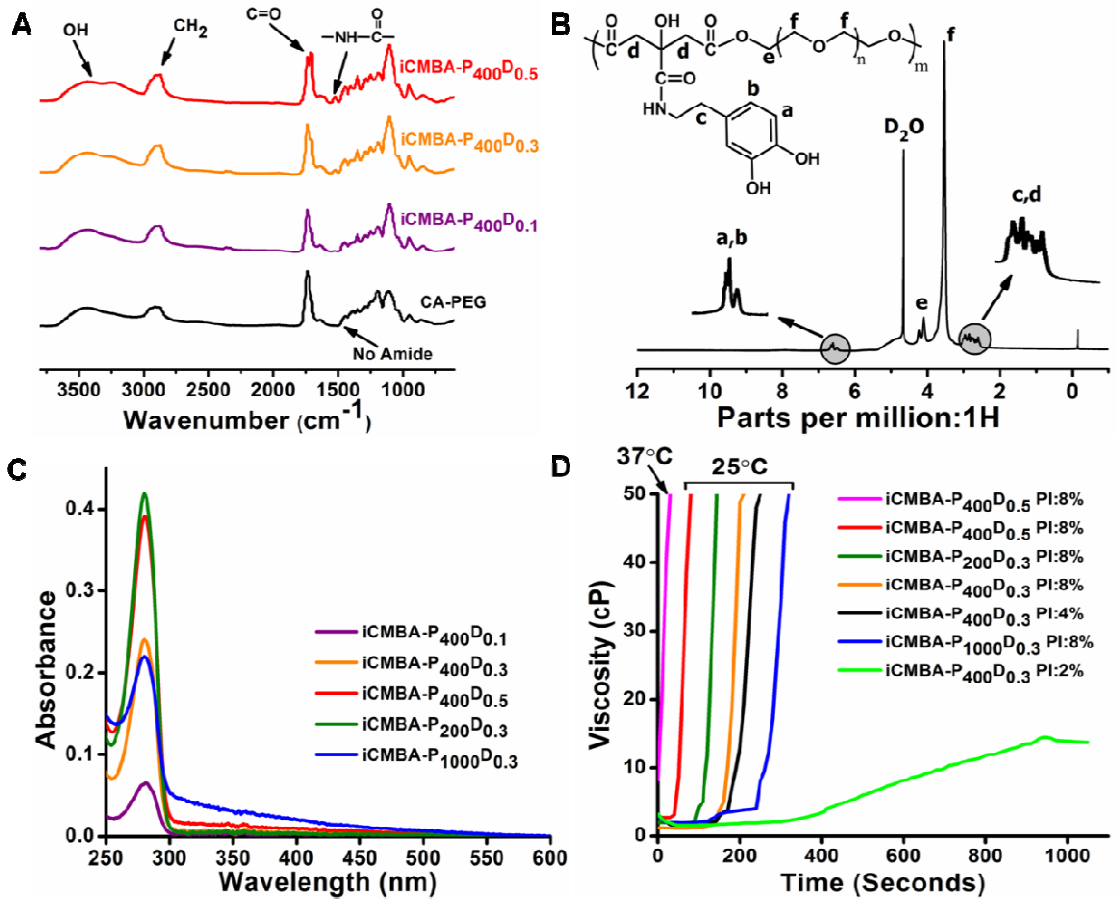

Figure 2.2 Characterization and gel time measurement of iCMBAs. A) FTIR spectra of different iCMBAs. B) 1H-NMR spectrum of a representative iCMBA. C) UV-VIS absorption spectra of iCMBAs, measured on 0.02% pre-polymer solutions in deionized water. D) Viscosity changes versus time for different iCMBAs being crosslinked with various ratios of sodium periodate (PI).

Table 2.2 time of iCMBAs crosslinked by various PI ratios (measured by viscometry)

Polymer name	PI to pre-polymer ratio (w/w%)	Test temperature (℃)	Measured gel time (Sec)
iCMBA-P_{400} $D_{0.5}$	8%	37	18±2
iCMBA-P_{400} $D_{0.5}$	8%	25	46±4
iCMBA-P_{200} $D_{0.3}$	8%	25	97±3
iCMBA-P_{400} $D_{0.3}$	8%	25	163±9
iCMBA-P_{400} $D_{0.3}$	4%	25	175±13
iCMBA-P_{1000} $D_{0.3}$	8%	25	244±11
iCMBA-P_{400} $D_{0.3}$	2%	25	313±10

2.4.3 Properties of Crosslinked iCMBAs

Mechanical properties of crosslinked iCMBAs in dry and fully hydrated states are listed in Table 2.3. In the dry state, the highest measured values for tensile strength, elongation at break and tensile modulus were 8515.1±1167 kPa (iCMBA-$P_{200}D_{0.3}$ PI:8%), 1582.5±144.6 % (iCMBA-$P_{400}D_{0.3}$ PI:4%) and 35.7±6.7 MPa (iCMBA-$P_{200}D_{0.3}$ PI:8%), respectively. The stress-strain curves of crosslinked iCMBAs are also shown in Figure 2.3A. All iCMBAs demonstrated a rubber-like (elastomer) behavior. As shown in Table 2.3, the mechanical properties decreased when samples were hydrated and swollen, which is expected for hydrophilic iCMBAs.

The degradation studies of the polymers revealed that the disintegration rate of crosslinked iCMBAs was inversely related to the degree of crosslinking, as expected. As shown in Figure 2.3B, iCMBA-$P_{400}D_{0.5}$ PI:8% exhibited the slowest rate of degradation, 25 days for complete degradation in PBS at 37℃. For the same reason, iCMBA-$P_{400}D_{0.1}$ was rapidly disintegrated within less than one day. On the other hand, using PEG with higher molecular weight accelerated the degradation of polymers as can be observed from faster degradation of iCMBA-$P_{1000}D_{0.3}$ (PEG 1000) compared to iCMBA-$P_{400}D_{0.3}$ (PEG 400) and iCMBA-$P_{200}D_{0.3}$ (PEG 200) with an identical PI-to-prepolymer ratio (8%).

Table 2.3 Mechanical properties of different iCMBAs crosslinked at various prepolymer- to-sodium periodate (PI) ratios, in dry and fully hydrated (swollen) states

Polymer name	PI to pre-polymer Ratio (w/w%)	Tensile strength (kPa)		Elongation at break (%)		Modulus (MPa)	
		Dry	Swollen	Dry	Swollen	Dry	Swollen
iCMBA-P_{400} $D_{0.3}$	2	1082.6±166.4	-	962.2±78.1	-	0.356±0.05	-
iCMBA-P_{400} $D_{0.3}$	4	1644±84.3	-	1582.5±144.6	-	0.73±0.05	-
iCMBA-P_{400} $D_{0.3}$	8	2067.3±732	69±7	911.8±405.8	143.5±46	1.61±0.66	0.068±.007
iCMBA-P_{400} $D_{0.5}$	8	2931.4±514.9	216±57.2	296.1±83.9	41.6±6	2.61±0. 57	0.69±0.14
iCMBA-P_{200} $D_{0.3}$	8	8515.1±1167	242.4±52.3	397.4±26.4	210±97.2	35.7 ±6.7	0.202±0.07
iCMBA-P_{1000} $D_{0.3}$	8	3496±806.2	82.8±3.6	201.4±49	132±32.1	33.4±11.9	0 .091±.005

Sol contents of different crosslinked iCMBAs are shown in Figure 2.3C. iCMBA-$P_{400}D_{0.5}$ and iCMBA-$P_{200}D_{0.3}$, both crosslinked with PI:8% (w/w PI/pre-polymer), showed the lowest amount of sol content of 2.37% and 2.86%, respectively, meaning that only 2.37% and 2.86% of those polymers were not crosslinked. With about 35%, iCMBA-$P_{400}D_{0.3}$ PI:2% had the highest sol content.

The evaluation of swelling ratios of crosslinked polymers showed that iCMBA-$P_{400}D_{0.5}$ PI:8%, having the highest amount of dopamine content and crosslinked with high PI-to-iCMBA ratio, demonstrated the lowest swelling percentage with 471.8% as shown in Figure 2.3D. On the other hand iCMBA-$P_{1000}D_{0.3}$ PI:8%, which consists of PEG 1000, displayed the highest swollen ratio at approximately 3400%.

2.4.4 Adhesion Strength

The lap shear adhesion strength of different iCMBA formulations varied between 33.4±8.9 kPa (for iCMBA-$P_{200}D_{0.3}$ PI:2%) and 123.2±13.2 kPa (for iCMBA-$P_{1000}D_{0.3}$ PI:8%), which were at least two folds stronger than commercially available fibrin glue with the adhesion strength measured at 15.4±2.8 kPa, as shown in Figure 2.4 and Table 2.4.

2.4.5 In Vitro Cell Viability and Proliferation

The results of cytotoxicity of pre-polymers are shown in Figure 2.5A. At the concentration of 10mg/mL (pre-polymer/cell culture medium) the cell viability was between 66±6 and 78±11 % of that in the blank medium, which was comparable to the value for control solution (PEGDA 700) at 78±7 %, and there were no significant differences between different pre-polymers.

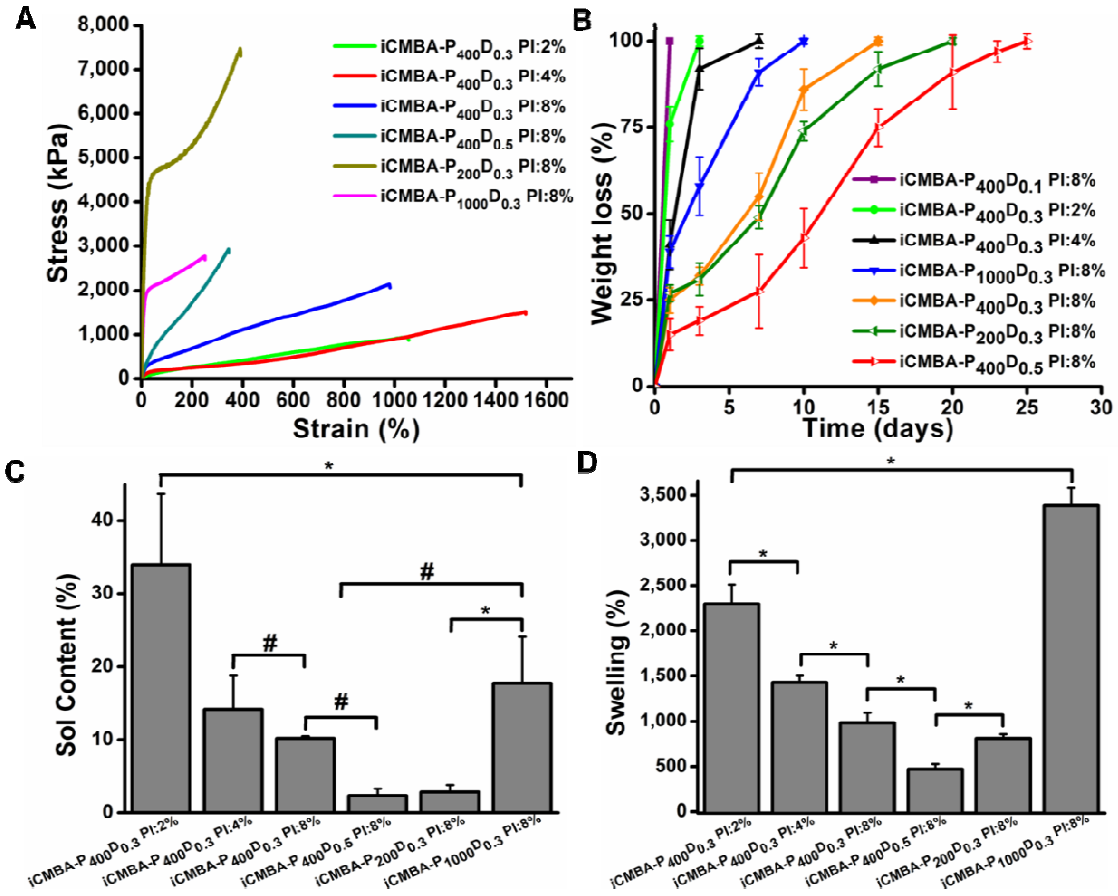

Figure 2.3 Mechanical properties, degradation, sol content and swelling of crosslinked iCMBAs. A) Stress-strain curve of crosslinked iCMBAs. B) Degradation profile of crosslinked iCMBAs incubated in PBS (pH7.4) at 37℃. C) Sol content, a nd D) Swelling ratios of iCMBAs crosslinked with various sodium periodate (PI) to pre-polymer ratios.

Table 2.4 Adhesion strength of iCMBAs and fibrin glue to wet porcine small intestine submucosa measured through lap shear strength test

Polymer name	PI to pre-polymer Ratio (w/w%)	Lap shear strength(kPa)
iCMBA-P_{400} $D_{0.3}$	2%	39.09±7
iCMBA-P_{400} $D_{0.3}$	4%	40.4±2.79
iCMBA-P_{400} $D_{0.3}$	8%	50.73±2.43
iCMBA-P_{400} $D_{0.5}$	8%	61.3±10.87
iCMBA-P_{200} $D_{0.3}$	2%	33.41±8.93
iCMBA-P_{200} $D_{0.3}$	4%	33.84±5.26
iCMBA-P_{200} $D_{0.3}$	8%	44.99±5.76
iCMBA-P_{1000} $D_{0.3}$	2%	49.34±6.49
iCMBA-P_{1000} $D_{0.3}$	4%	90.25±11.25
iCMBA-P_{1000} $D_{0.3}$	8%	123.23±13.23
Fibrin glue	-	15.38±2.82

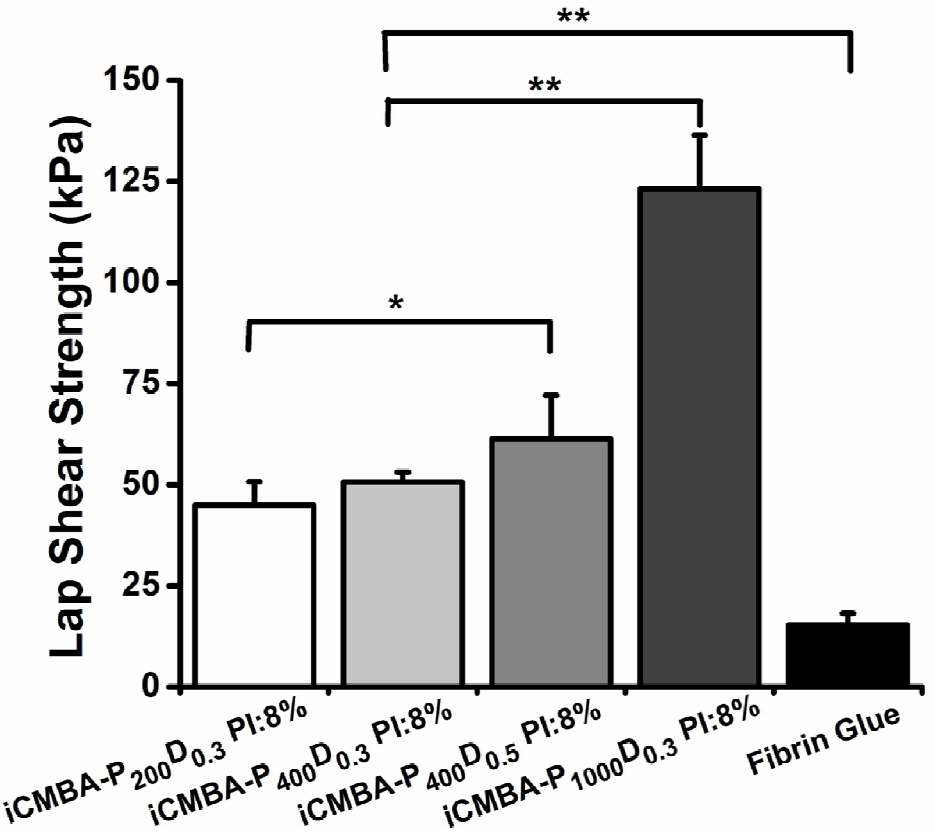

Figure 2.4 Adhesion strength of iCMBAs and fibrin glue to wet porcine small intestine submucosa measured through lap shear strength test (** $p<0.01$, * $p<0.05$).

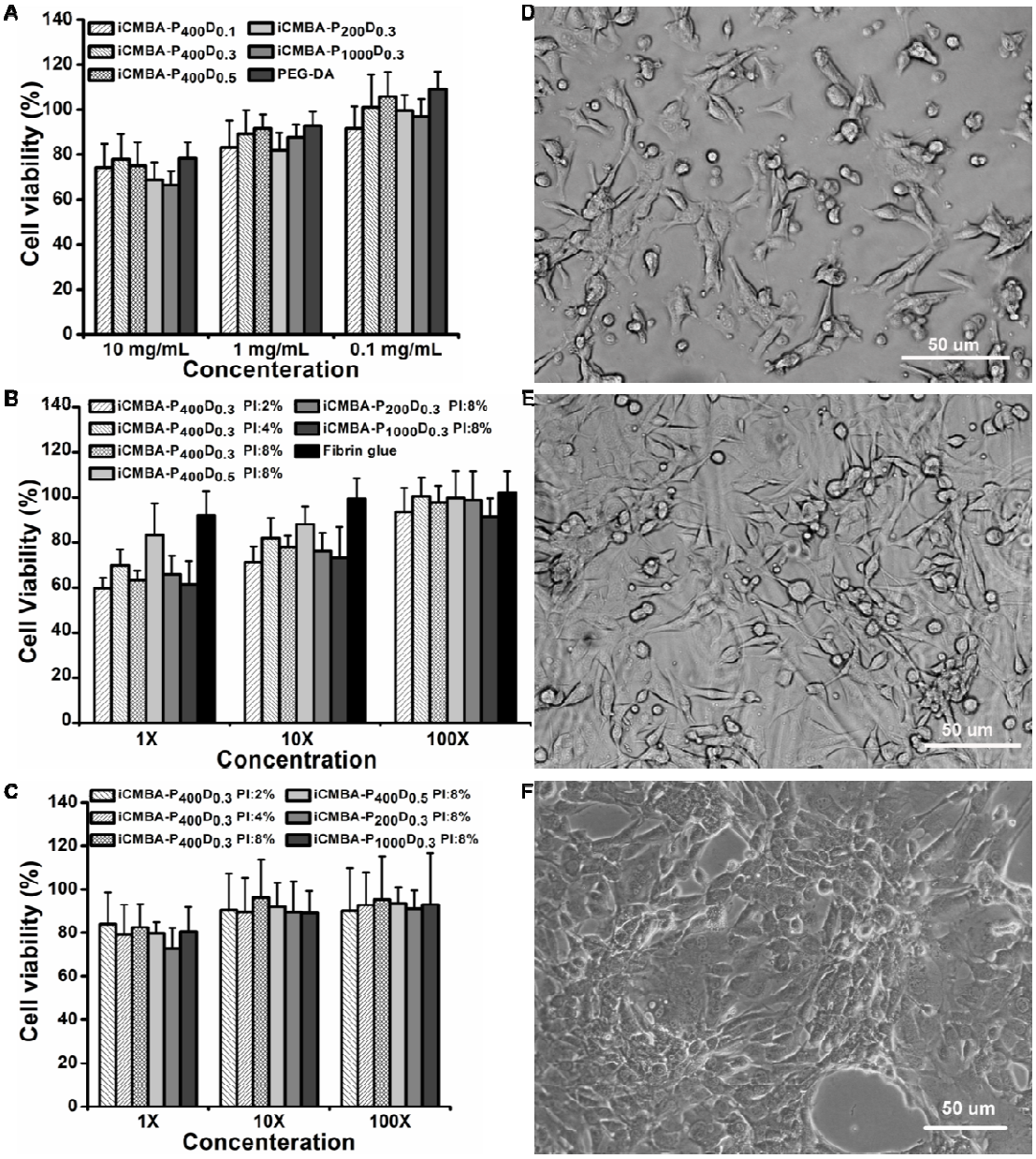

Figure 2.5 In vitro cytotoxicity evaluation of iCMBAs. Cytotoxicity study using NIH 3T3 fibroblast cells by MTT assay for: A) iCMBA pre-polymers and poly(ethylene glycol) diacrylate (PEGDA) control, B) Leachable products (sol content) of crosslinked iCMBAs and fibrin glue control, and C) Degradation products of crosslinked-iCMBAs. All data were normalized to cell viability in blank medium. D, E, and F) Light micrographs of NIH 3T3 fibroblast cells seeded on iCMBA films at 1st day, 3rd day, and 5th day post seeding, respectively.

In diluted solutions of 1 and 0.1 mg/mL the cell viability was approximately similar to what measured for blank medium and PEGDA. The cells viability in the presence of leachable

content (sol content) of crosslinked iCMBAs at 1X concentration was between of 60±4 and 83±14 %, showing minor to moderate cytotoxicity, which was directly proportional to the sol content of each polymer and the amount of PI (8%) (Figure 2.5B). The cells viability increased as diluted solutions of sol content (10X and 100X) were used. Furthermore, iCMBA degradation products (1X) showed a cell viability of at least 72.9±9 %, suggesting that the degradation products of all crosslinked iCMBAs did not induce significant cytotoxicity (Figure 2.5C). The qualitative examination of NIH 3T3 fibroblast cells by light microscopy demonstrated an excellent cell attachment to the iCMBA films with a spindle-shape morphology. The proliferation of the cells was also observable through the increase in the number of cells throughout three time points (Figure 2.5D-F).

2.4.6 In Vivo Study

During animal study, upon applying iCMBAs, the bleeding caused by creation of wounds on the dorsum of Sprague-Dawley rats was immediately stopped and the wound openings were closed within two minutes (Figure 2.6A). Furthermore, the visual examination and comparison of iCMBA-treated and sutured wounds at different time points demonstrated the high efficiency of iCMBAs in the wound healing process (Figure 2.6B, C and 2.7A-C). The histological evaluation (H&E staining) at day seven showed only minor acute inflammation when iCMBA was utilized. The difference between total cell densities in the incision area treated by iCMBA (7th day= 3996±264 #/mm^2; 28th day= 3202±227 #/mm^2) and suture (7th day: 4117±269 #/mm^2; 28th day: 2992±163 #/mm^2) was not significant (Figure 2.6D-G, P). Similarly the number of CD11b positive inflammatory cells in the incisions area at seventh day post treatment was not significantly different in iCMBA-treated wounds (1771±242 #/mm^2) and sutured wounds (1592±142 #/mm^2). By day 28th there was a negligible number of inflammatory cells for both groups (iCMBA: 92±42 #/mm^2; suture: 107±50 #/mm^2) (Figure 2.6H-K, Q). In addition, on day 28th, a higher amount of collagen was found at the sites of wound treated by iCMBA (7th day= 15±12 %; 28th day= 63±4 %) than those treated with suture (7th day= 17±9 %; 28th day= 58±7 %) (Figure 2.6L-O, R).

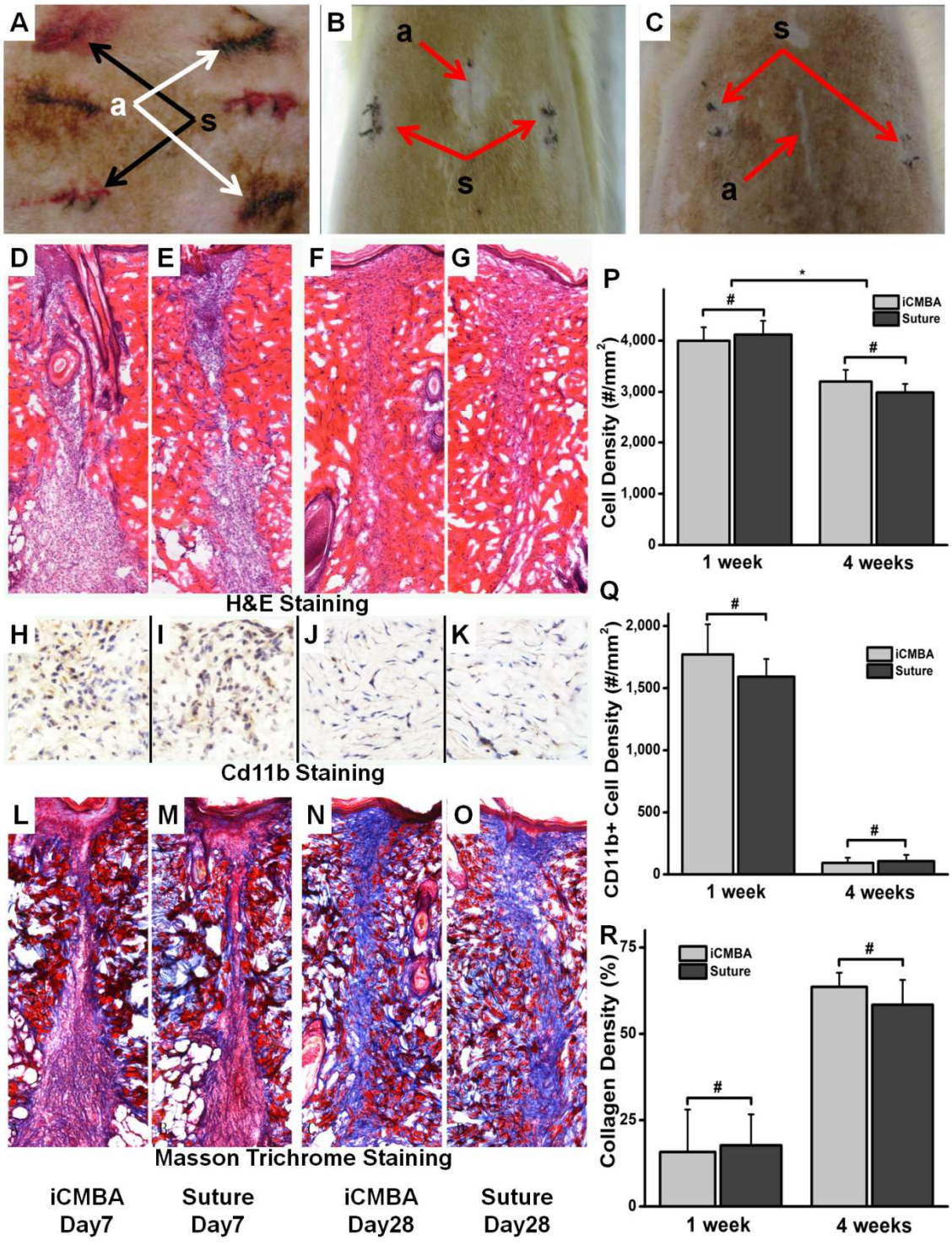

Figure 2.6 Histological evaluation of rat skin closure and wound repair. Images of a rat's dorsum skin with created wounds that were closed by iCMBA (a) and suture (s): A) 2 minutes, B) 7days, and C) 28 days post operation. D-O) Images of H&E (hematoxylin and eosin), immunohistochemical (for CD11b), and Masson trichrome staining of sections of wounds at 7th

day post treatment with iCMBA (D, H and L) and suture (E, I, and M); and at 28th day post treatment with iCMBA (F, J, and N) and suture (G, K, and O) (original magnification: 200X for D-G, and L-O and 400X for H-K). P) Total cell density infiltrated into the area surrounding the incision 1 week and 4 weeks post treatment with iCMBA and suture. Q) Number of CD11b positive cells in the vicinity of wounds treated with iCMBA and suture. R) Collagen density in the wound area at 1- and 4-week time points (# p>0.05).

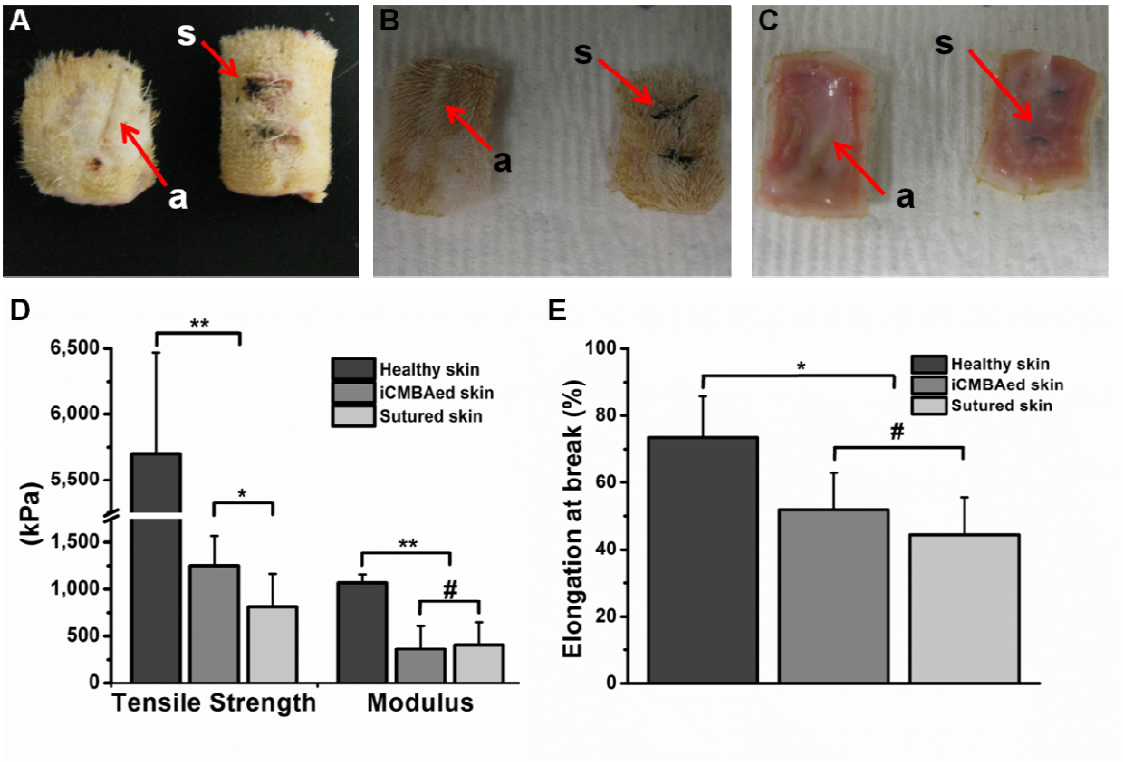

Figure 2.7 Tensile tests on healed skins closed by iCMBA (a) and suture (s). The pieces of excised skin tissue of sacrificed rats at the site of wounds treated with iCMBA and suture at 7th day (A) and 28th day (B and C: reverse side) post operation. Note the enhanced healing of the wounds closed by iCMBA over sutured wounds. D) Tensile strength and Young's modulus of healthy skin and healed skin closed by iCMBA and suture at 28th days. E) Elongation at failure for the same study groups (** p<0.01, * p<0.05 and # p>0.05).

The measurement of mechanical properties of rat skin revealed that the iCMBA-treated skin had higher tensile strength (1250±315 kPa) than suture-closed skin (810±355 kPa), while modulus and elongation at break were similar for both groups (Figure 2.7D, E). The examination of the healed wounds after 28 days showed no trace of polymer at the location of healed tissue, suggesting that iCMBAs were fully degraded in the rat body (Figure 2.7C).

2.5 Discussion

iCMBAs were synthesized by a single-step polycondensation reaction between citric acid, polyethylene glycol and dopamine (Figure 2.1). The FTIR and ^{1}HNMR characterizations confirmed the esterification reaction between carboxyl groups of CA and hydroxyl groups of PEG on one hand, and the formation of amid linkage between the unreacted –COOH groups of CA and dopamine's $–NH_2$ groups (Figure 2.2A, B). ^{1}HNMR also revealed that the compositional ratio of iCMBA pre-polymers was consistent with the feeding ratio, a sign of high yield of this synthesis method (Table 2.1).

The UV-VIS photospectroscopy proved the availability of catechol hydroxyl groups in the pre-polymers structure through the observation of UV light absorption at 280 nm wavelength for all samples (Figure 2.2C) [127]. The presence of unoxidized catechol groups is essential for adhesion and crosslinking processes to take place [65, 66, 68-70, 98, 99]. The intensity of the absorption for each composition was related to the amount of dopamine in that composition. However, in the pre-polymers with high molecular weight PEG (M_n=1000, for example) the UV absorption was weaker than expected, which can be related to the reduced amount of available unoxidized hydroxyl groups, presumably due to the possible partial oxidation of the catechol groups over the course of longer synthesis time of these pre-polymers compared to those with shorter synthesis duration. This was evident from the smaller absorption peak of iCMBA-$P_{1000}D_{0.3}$ at 280 nm compared to iCMBA-$P_{400}D_{0.3}$ and iCMBA-$P_{200}D_{0.3}$. Oxidation of catechol hydroxyl groups to quinone could also be verified by UV absorption of quinone group at around 390 nm [127].

Based on proposed crosslinking mechanisms of mussel adhesive proteins [131], the plausible crosslinking and adhesion mechanisms for iCMBAs are shown in Figure 2.8. The gel time ranged between 18±2 and 313±10 seconds (Figure 2.2D and table) and was a function of multiple factors. Increasing the amount of initiator, i.e. PI-to-prepolymer ratio, incorporating more dopamine in the pre-polymer structure, and using PEG with smaller molecular weight resulted in faster gel formation. These factors could increase the available pendant catechol

groups as crosslinking sites, resulting in faster formation of quinone-initiated crosslinking of iCMBAs.

The sol content and swelling data also confirmed the crosslinking of the pre-polymers, which were in agreement with the expected degree of crosslinking (Figure 2.3C, D). When the number of sites for the formation of crosslinks between two iCMBA pre-polymer chains, i.e. unoxidized catechol groups, increases and the distance between consecutive crosslink points decreases, the number of non-crosslinked polymer chains will be fewer, which means less sol content. The shorter distance between crosslink points also means less space for diffusing molecules, such as water, which will translate into lower amount of swelling. This can explain the lower swelling ratio of iCMBA-$P_{400}D_{0.5}$ PI:8% compared to iCMBA-$P_{400}D_{0.3}$ PI:8% or the difference in swelling between iCMBA-$P_{200}D_{0.3}$ PI:8% and iCMBA-$P_{1000}D_{0.3}$ PI:8%, in addition to the fact that iCMBAs made from PEG with higher molecular weight were generally more hydrophilic, as expected, which can cause absorption and retention more water into the iCMBA polymer network.

The evaluation of mechanical properties of crosslinked iCMBA suggested that these materials demonstrated elastomer-like behavior with typical characteristics of elastomeric stress-strain curve (Figure 2.3A), which is especially important for soft tissue adhesives, which must mechanically remain in harmony with flexible soft tissues for better load bearing and stress transferring. Tensile strength, elongation at break and modulus of iCMBAs varied with the molecular weight of PEG and the degree of crosslinking, which was itself a function of the amount of dopamine in the pre-polymer structure and the amount of crosslinking initiator (PI) (Table 2.3). Thus, the mechanical properties can be easily tuned according to requirements. The higher mechanical properties of iCMBA-$P_{200}D_{0.3}$ PI:8% can be related to the shorter PEG length, which could result in shorter distance between two successive catechol groups attached to citric acid, as sites for crosslinking, and a possible increase in crosslinking density. The shorter the distance between two crosslink points, the higher will be the mechanical properties. In the case of iCMBA-$P_{1000}D_{0.3}$ PI:8%, the tensile strength and modulus could be affected by

possible intermolecular forces between the chains of PEG portion of iCMBA, which is longer in PEG 1000 than PEG 400.

The degradation profile of the crosslinked iCMBAs exposed one of the unique features of our synthesized adhesives: the degradability of these adhesive biomaterials within a limited period of time (Figure 2.3B). The degradation rate was inversely related to the level of crosslinking, as expected. iCMBA-$P_{400}D_{0.5}$ PI:8% exhibited the slowest rate of degradation, 25 days for complete degradation in PBS at 37℃, due to higher crosslinking level. On the contrary, iCMBA-$P_{400}D_{0.1}$ PI:8%, which was inadequately crosslinked due to low catechol (dopamine) content, rapidly disintegrated within less than one day. The presence of higher-molecular-weight PEG in the polymer structure, which conferred more hydrophilicity to the polymer, accelerated the degradation of polymers, as can be observed from faster degradation of iCMBA-$P_{1000}D_{0.3}$ compared to iCMBA-$P_{400}D_{0.3}$ and iCMBA-$P_{200}D_{0.3}$, all crosslinked with the same PI-to-prepolymer ratio (8%).

With the formulations investigated, the wet tissue bonding strength of the iCMBAs was 2.5-8.0 folds higher than that of fibrin glue ($p<0.01$) (Figure 2.4 and Table 2.4). Thereof, the lowest bonding strength among iCMBAs belonged to iCMBA-$P_{200}D_{0.3}$ PI:2% (33.41±8.93 kPa), which was at least two folds higher than that of the gold standard, fibrin glue, measured at 15.38±2.82 kPa. Adhesives based on iCMBA-$P_{1000}D_{0.3}$ demonstrated the strongest adhesion to SIS adherents, followed by iCMBA-$P_{400}D_{0.5}$. Bonding strength of iCMBA-$P_{400}D_{0.3}$ adhesive polymers were higher than iCMBA-$P_{200}D_{0.3}$ polymers ($p<0.05$). However, there were no significant differences within iCMBA-$P_{400}D_{0.3}$ group or iCMBA-$P_{200}D_{0.3}$ group when crosslinked with different PI ratios (Table 2.4). The higher adhesion strength of iCMBAs prepared from PEG with greater molecular weight, i.e. 1000 or 400, can be ascribed to the enhanced intermolecular forces and possible entanglement between polymer chains, the chance of which increased as the molecular weight of PEG was raised.

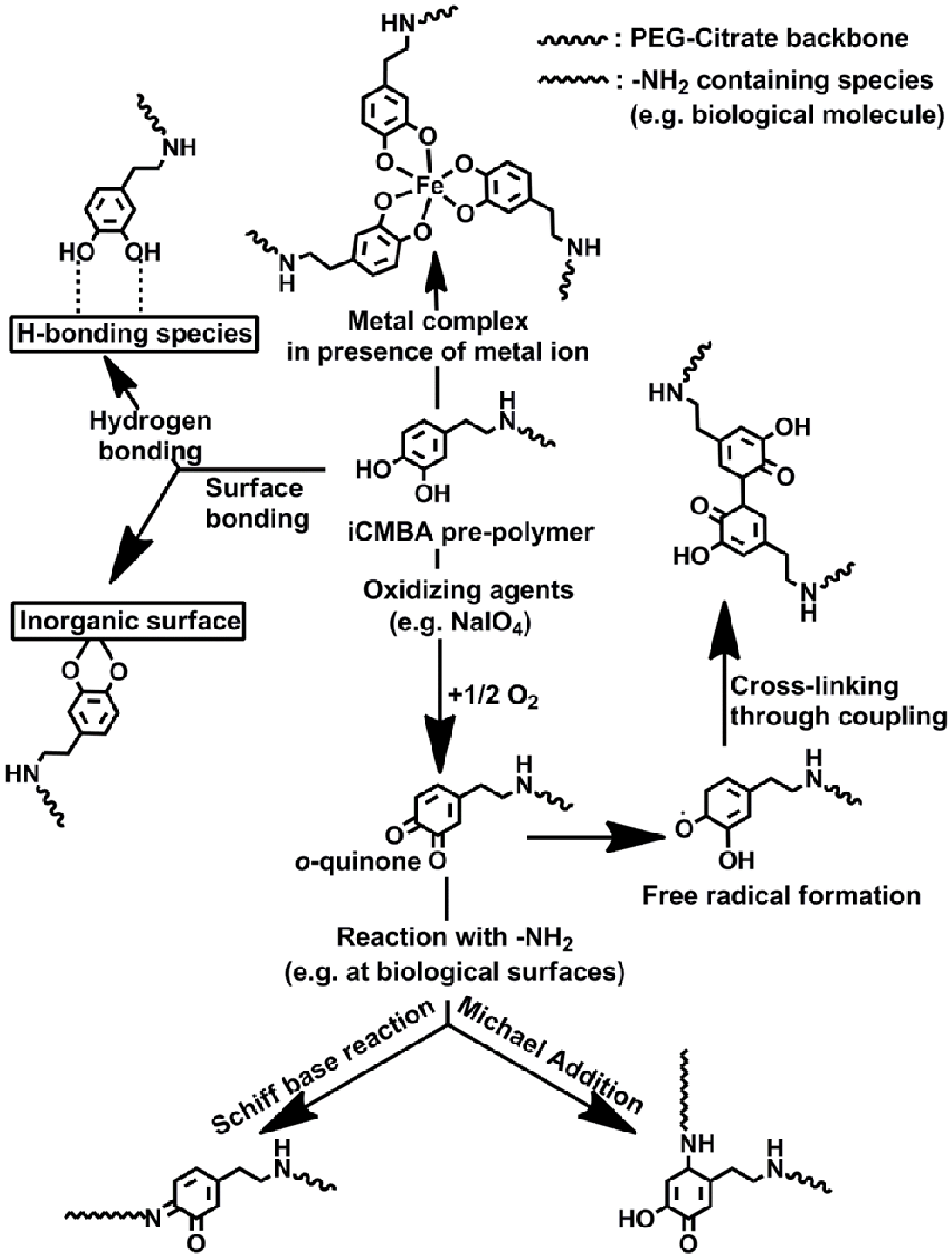

Figure 2.8 Schematic representation of possible crosslinking and adhesion pathways of iCMBA pre-polymers.

The quantitative in-vitro cytotoxicity evaluations of iCMBA pre-polymers, and sol (leachable) content and degradation products of crosslinked iCMBAs exhibited that the tested formulations did not induce significant cytotoxicity to NIH 3T3 fibroblast cells (Figure 2.5A-C). These results, in addition to qualitative proliferation and morphological assessment (Figure 2.5D-F), support that this family of bioadhesive polymers is suitable candidates for biological and biomedical applications.

In vivo studies confirmed the effectiveness and convenience of using iCMBAs in wound closure and bleeding control. The proposed tissue adhesion mechanisms of iCMBAs are schematically shown in Figure 2.9. Upon dropping iCMBA solution inside the full-thickness cutaneous incisions, created on the back of Sprague-Dawley rats, the bleeding was immediately ceased and the wound opening was closed within a few minutes (Figure 2.6A). In contrary to suture, no blood leakage was then sighted, which could be related to superior hemostatic property of iCMBAs to suture. In addition to the formation of a mechanical barrier against blood loss due to the bulk of adhesive, the hemostatic effects of iCMBAs could also partially attributed to the rich carboxyl groups on iCMBAs, which can readily interact with blood protein to form insoluble interpolymeric complexes. In addition, using iCMBA lead to an improved and accelerated wound healing when compared to suture (Figure 2.6B, C, 2.7A-C). The histological evaluation (H&E staining) at 7^{th} day post application of iCMBAs showed only minor acute inflammation, while total cell infiltration into the incision area at both 7^{th} and 28^{th} day time points, defined by cell density, was not significantly different for iCMBA-treated and sutured wounds (Figure 2.6D-G, P). Moreover, the insignificant difference between number of CD11b positive inflammatory cells in the proximity of iCMBA-treated and sutured wounds at 7^{th} day post treatment indicated the minimal inflammatory response to iCMBA. After 28 days the number of inflammatory cells for both groups was negligible (Figure 2.6H-K, Q). The existence of slightly higher amount of collagen at the sites of iCMBA-treated wounds compared with sutured wounds (Figure 2.6L-O, R) suggests that iCMBAs may be used to improve wound healing with better outcome than suture stitches. The measurement of mechanical properties of the healed rat skin

revealed that the iCMBA-treated skin had superior tensile strength (1250±315 kPa) over suture-closed skin (810±355 kPa), while modulus and elongation at break were similar for both (Figure 2.7D, E). These findings suggested that the healing process and tissue reconstruction was facilitated by iCMBA polymers, which presumably provided a suitable scaffold for cell growth and tissue repair, accelerating the tissue regeneration process. Interestingly, after 28 days no trace of polymer was observed at the location of healed tissues, a sign of complete in-vivo degradation of the iCMBAs (Figure 2.7C). These results support that this family of bioadhesive polymers is suitable candidates for biological applications, particularly where the employed biomaterial is required to be degraded and absorbed after intended time of service with minimal toxicity on the host body. Another observed advantage of iCMBA adhesive over suture was the absence of needle holes (wounds), inevitably created in suturing, when using the adhesive, as evident from Figure 2.7A-C.

2.6 Conclusion

The experimental results presented above demonstrate the syntheses of a novel family of injectable citrate-based mussel-inspired biodegradable adhesives, iCMBAs, from safe and inexpensive constituents and via a one-step and cost effective synthesis technique without involvement of any toxic reagents, and their applications in hemostasis and sutureless wound closure. The syntheses of iCMBA enrich the methodology of citrate-based biomaterial development and represent an innovation for tissue adhesive biomaterial design. The properties of iCMBAs such as gel time, adhesion strength, mechanical properties, and degradation profile were shown to be easily tunable. The wet tissue bonding strength of the investigated iCMBAs to SIS substrates was significantly higher than that of fibrin glue. The pre-polymers, sol content, and especially degradation products of iCMBAs did not pose significant cytotoxicity to NIH 3T3 cells. In vivo studies also confirmed the effectiveness and easiness of using iCMBAs to close wounds, while only triggering minor acute inflammation. iCMBAs were also degraded and absorbed in vivo within 28 days [115].

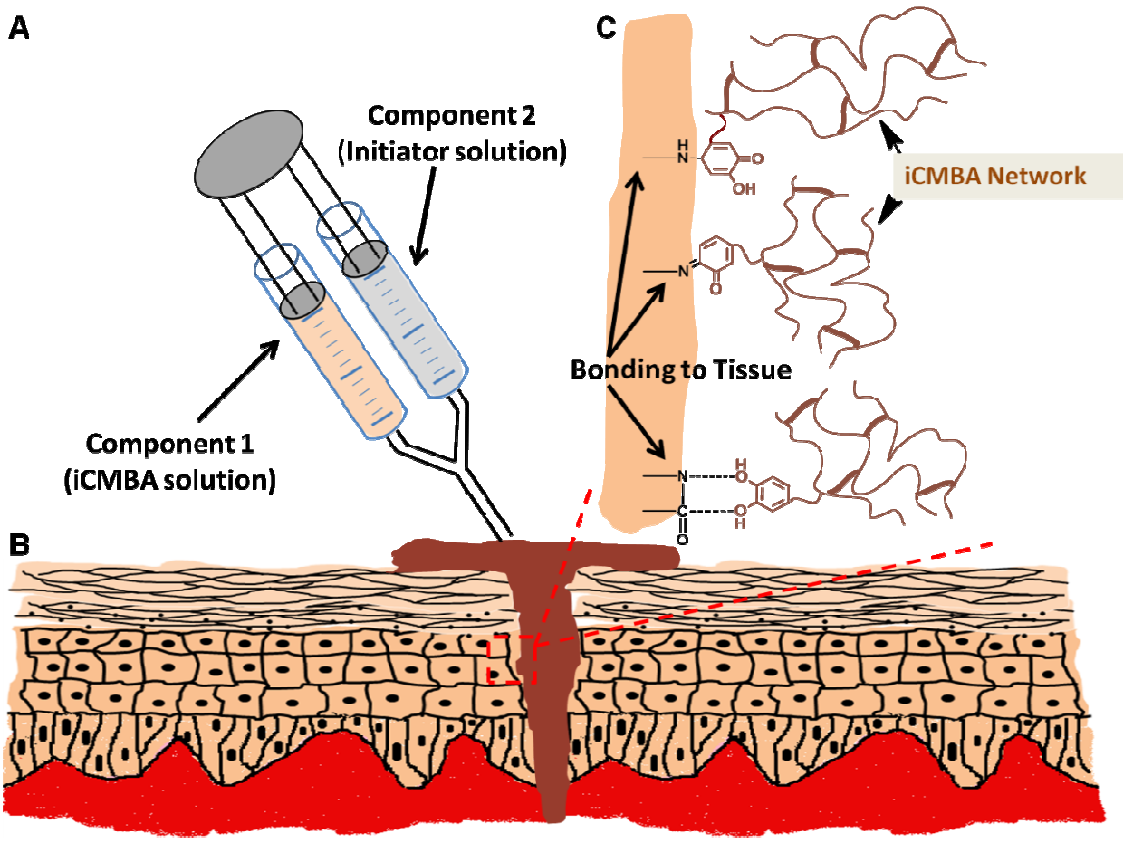

Figure 2.9 Schematic illustration of iCMBA application on wound and tissue adhesion. A) Preparation and application of 2-component adhesive: iCMBA and oxidizing (sodium periodate) solutions. B) Schematic representation of iCMBA utilized for sutureless wound closure. C) Proposed mechanisms of iCMBAs adhesion to tissues.

The superior mechanical strength of the incised skin closed by iCMBA to those of suture-closed skin supported that the healing process and tissue reconstruction was facilitated by iCMBA polymers, which presumably provided a suitable scaffold to facilitate cell growth and the wound healing process. iCMBAs were shown to be biodegradable strong wet-tissue adhesives that could effectively seal a bleeding open wound, instantly stop bleeding, and promote tissue regeneration without the aid of other surgical tools, such as suture and staples, or other adhesive mechanisms. The sutureless wound closure may be particularly very useful for those wounds on which sutures are hard to be placed due to the lack of surrounding healthy collagenous structure and fascia supports. The convenient handling procedures, strong tissue

adhesion, controlled degradability, and elastomeric mechanical properties make iCMBA promising for any topical and non-topical applications across all disciplines of surgical practice ranging from suture/staple replacement; tissue grafts to treat hernias, ulcers, and burns; hemostatic wound dressing for laparoscopic partial nephrectomy (LPN); waterproof sealants for vascular anastomoses; and treatment of gastrointestinal (GI) fistulas, leaks, mucosal oozing or bleeding, and perforation [115].

CHAPTER 3

INJECTABLE iCMBA-HYDROXYAPATITE (HA) COMPOSITES FOR ORTHOPEDIC APPLICATIONS

3.1 Introduction

3.1.1 Injectable Biomaterials for Bone Tissue Regeneration

Bone has multiple functions including production of red/white blood cells, storage of minerals such as calcium, protecting body organs, and providing mechanical-structural supports for the body. Although bone has a self-healing property, sometimes treatment of bone defects, which can occur due to trauma or bone disease, require a reconstruction strategy [133]. This is especially important in the case of large bone defects, multi-fragmental fractures, or in the skeletal regions with high mechanical load bearing such as lower extremities. Bone tissue engineering and regeneration strategy is increasingly being utilized in treatment of orthopedic injuries and bone-related disease such as bone fracture and osteonecrosis [134]. For instance, complex bone defects such as comminuted fracture require different and, sometimes, multiple approaches for treatment. Comminuted fracture, also termed multi-fragmented fracture, is a very serious case of bone defects. In this type of fracture the affected bone is broken into three or more pieces due to crushing of a bone. It may occur due to an accident, such as fall from height, or in people with weak bone tissues such as in the elderly or those suffering from diseases that weaken bones, like cancer and osteoporosis. To heal this type of fracture without causing any deformity, the fragments of the broken bone must be re-aligned to their normal anatomical position. This process, also termed as reduction, and immobilization of the bone fragments in the case of comminuted fracture is associated with serious difficulties. Using pin fixation, such as Kirschner wires, might not be effective in holding the bone fragments together [135]. Furthermore, using plates and screws are also ineffective because there are either too

large in size or fail to fix the multiple small fragments. In addition, the external fixator would require prolonged application, which can cause complications [136]. Exploiting a system that can effectively binds and holds the pieces of broken bone together and in their anatomical position while providing adequate mechanical strength would be an ideal remedy. As a solution, injectable bone-like materials, with the ability of binding the bone fragments and concurrently filling in the irregularities caused by fracture, would help and accelerate the healing process of the fracture [136]. Another type of complex bone defects is osteonecrosis, which is a bone disease caused by the lack of enough blood supply to bone tissue, which may lead to complete bone death and collapse, if its progression is not ceased. It is especially critical in weight-bearing regions, such as femoral head [137]. There are different approaches for treating osteonecrosis from noninvasive treatments such as using medications [138] to surgical procedures including core decompression [139], autologous/allogenic bone graft [140], and eventually total hip replacement. A replacement method is using bone tissue engineering, which typically involves using 3-D biocompatible biomaterials as scaffold, which provides an environment for cells to grow, differentiate, and function. These constructs occasionally include growth factors, such as vascular endothelial growth factor (VEGF) and bone morphogenetic protein (BMPs), and drugs to support growth of new tissue through vascularization [141]. Various natural and synthetic biomaterials have been used to fabricate these scaffolds. Naturally-derived materials include collagen[142-144], alginate [145], demineralized bone matrix (DBM) [146, 147], hyaluronic acid derivatives [148], chitin/chitosan [149], and silk [150, 151], which have demonstrated excellent biocompatibility, and biodegradablity. However, inconsistent and variable properties, and difficulties associated with their processability and fabrication have limited their utilizations.

Ceramics, especially those consist of calcium phosphates, which is very similar to bone mineral composition, have also been widely investigated. Calcium carbonate, calcium phosphates (Hydroxyapatite or HA), tricalcium phosphate (β-TCP) and biphasic calcium phosphate, and bioglass are among the most studied ceramics for bone reconstruction

applications [141]. Nevertheless, the lack of flexibility and brittleness render ceramics unsuitable for applications in regions under high load bearing and dynamic loading.

Synthetic polymers are another class of materials that have been investigated for this application due to their appealing properties such as flexibility in design and biodegradation. Properties of polymers can be reproducibly customized to meet specific requirements of bone graft materials through manipulation of their structure and composition [134]. poly(a-hydroxy esters) (such as poly(L-lactic acid)(PLLA), poly(glycolic acid) (PGA), and poly(lactic-co-glycolicacid) (PLGA)), poly(ethylene glycol), polydioxanone, poly(orthoesters), polyanhydrides, polyurethanes, and poly(propylene fumarate)(PPF) [134, 141]. Relatively low compressive modulus and strength of most polymers, and brittleness of ceramics make them unsuitable to be used as bone graft materials. Thus, as alternative, polymer/ceramic composites, which benefit from high modulus of ceramics and elasticity and flexibility of polymers, have been investigated. PLGA/HA [152], PLLA/HA [153], PLGA/TCP, PLGA/Bioglass [154] are examples of the polymer/ceramic composites that have been investigated for bone applications.

Implantation of prefabricated scaffolds requires invasive procedures, which is usually not desirable. Considering the advances made in the field of arthroscopic procedure, recently using injectable bone graft materials for the treatment of bone defects has gained more popularity due to their minimally invasive procedures. In addition, possibility of filling cavities with irregular shapes and fitting the contours of the wound are further advantages of injectable materials, which have created promising outcomes [155]. Following the injection into the bone cavity or fracture area, the injected bone materials harden within a few minutes through a solidifying and/or crosslinking mechanisms, and provide a much-needed mechanical support to the bone.

Various types of materials have been investigated for injectable bone applications. Calcium phosphate cement (CPC) is a well known synthetic bone graft ceramic. After mixing with water, the material forms a workable paste which can be shaped during surgery to fit the contours of a wound. The product of hardening reaction is hydroxyapatite, $Ca_5(PO_4)_3(OH)$, the

primary inorganic component of natural bone, which makes the hardened cement biocompatible and osteoconductive [156]. Nevertheless, due to its brittleness, CPC is approved and used only for non-load-bearing bone defect applications. Numerous studies have focused on developing injectable ceramic-based bone materials with desirable properties. However, most of these ceramics lack required tensile strength comparable to the bone tissue and show prolonged degradation /resorprtion time, which can hinder growth of new bone tissue [155].

To address these problems polymers were chosen as alternative due to their adjustable and controllable mechanical and degradation properties, which can be tailored based on requirements. Polymeric injectable bone materials are either in the form of monomers, which polymerize in situ following injection, or, more commonly, are polymers/prepolymers, which undergo crosslinking reaction after they are injected into the place of interest. Different polymers have investigated for this purpose [155]. Poly(methyl methacrylate) (PMMA) is a commonly used bone injectable cement, which can be crosslinked using a chemical pathway or by photo-initiation, following placing into the defected bone cavity. However, disadvantages such as high crosslinking temperature, release of toxic methyl methacrylate, and non- biodegradability, which can cause stress shielding and hinder the bone healing process, have limited its utilization [155, 157]. To address these concerns, a group of investigators developed photopolymerizable acrylate-modified poly(ahydrides), which are crosslinked upon exposure to light [158]. Although this family of injectable polymers exhibit promising properties for bone applications, they depend on light for the photo-crosslinking to occur, which might not be accessible in deep tissue defects. In another attempt, researchers reported development of a linear polyester called poly(propylene fumarate), a chemically crosslinkable polymer, which showed attractive properties [155, 159].

To combine desirable properties of ceramics (high compression strength and modulus) and polymers (high flexibility and tensile properties), and eliminate their individual disadvantages, injectable polymer/ceramic composites have attracted researchers' attention [160] . Different research groups have reported the fabrication of the composites based on

PPF/β-TCP with desirable properties [160, 161]. Despite of all these developments and progresses, the pursuit of ideal injectable bone materials with necessary rheological, mechanical and degradation properties continues.

Regardless of the nature of materials, scaffolds used in orthopedic applications must fulfill many requirements. An ideal orthopedic biomaterial for bone regeneration should:

1) possess enough mechanical and structural strength to provide required supports throughout the healing process, without interfering with new bone tissue regeneration through stress-shielding;

2) contain adequate porosity with required pore size to allow neovascularization and ingrowth of cells and new tissue;

3) allow and promote cells adhesion, growth, and differentiation;

3) be biocompatible in the manner that initial materials, final synthetic bone graft, and degradation products should cause no/minimal cytotoxicity, immunogenicity, and inflammatory response;

4) in case of injectable materials, have suitable handling properties, such as flowability and curing time without causing any significant change in the local temperature;

5) be sterilizable;

6) be biodegradable with controlled rate, which should be in harmony with the growth of new tissue [133, 155].

Biodegradability of implanted bone graft biomaterials is of immense importance because of multiple reasons. First, it eliminates the need for a second surgery to remove the implant. Second, gradual degradation and removal of biomaterial support reduces the risk of stress shielding as load-bearing is slowly taken over by newly-formed bone tissue. And finally, as the degradation continues with time, it provides a porous structure that can accelerate the ingrowth of new bone tissue into the pore of degrading bone biomaterial scaffold.

3.1.2 iCMBA-HA; An Injectable and Biodegradable Composite for Bone Repair and Regeneration

In chapter 2 the attractive properties of iCMBAs have been extensively discussed. Some of these properties such as flowability, in-situ crosslinking with adjustable time in the range of tens of seconds to a few minutes, minimal cytotoxicity and inflammatory response in a rat model, and controlled biodegradability can be beneficial for applications as injectable bone materials for treatment of bone defects caused by traumas or diseases, such as comminuted fracture or osteonecrosis. To improve the mechanical strength of iCMBAs, hydroxylapatite was chosen to fabricate iCMBA-HA composites. These composites seem to possess important characteristics of injectable, in-vivo crosslinkable, and biodegradable synthetic bone graft, which were highlighted in the previous section. In addition, the adhesion properties of iCMBA can provide iCMBA-HA composites with an extra advantage over other existing systems by improving the interaction between injectable bone composite and native bone tissue in the interface region to not only enhance the mechanical support to the defected bone but also to facilitate the growth of new bone tissue into the composite scaffold. This property can be of significant importance in tissue engineering, because one of the biggest challenges of using biomaterials in regeneration of damaged tissues is the discontinuity in the interfacial region between biomaterials and tissue, which can cause the failure of the integration between the two. To prevent this separation from occurring, various integration techniques, such as suturing or tissue adhesives, are employed. In an attempt to minimize the risk of failure, investigators employed adhesive moieties to promote graft integration in tissues like cartilage [162]. They used a biodegradable injectable adhesive scaffold to improve integration with surrounding tissues. The adhesive was reported to create a bridge between biomaterial and cartilage tissue, which significantly promoted graft integration/bonding with the native tissue so as to improve cartilage repair. Similarly, the integration between injectable iCMBA-HA composites and native bone tissue can benefit from possible adhesion between of iCMBAs and native bone, and eventually might improve bone defect treatment.

Another very important characteristic of iCMBA-HA composite is the presence of citrate groups in the structure of iCMBA. Natural bone tissue is an organic-inorganic nanocomposite where thin nanocrystals of apatite are embedded in collagen. The small nanocrystals (3 nm thick) control the mechanical properties of bone and prevent crack propagation [163]. It was believed that the stabilization of these apatite nanocrystals was regulated by the citrate molecules, which was found to form 5 wt% of the organic component of the natural bone [164]. In Another recent study solid-state nuclear magnetic resonance (NMR) was used to show that the surface of apatite nanocrystals is studded with strongly bound citrate molecules [165]. Citrate is a strongly bound integral part of the bone nanocomposite and is not a dissolved calcium-solubilizing agent [163]. Although the function of citrate groups on natural bone development is still largely unknown, the design of bone biomaterials and scaffolds may benefit from the existence of such groups in their structures. This hypothesis and strategy was recently investigated in a study on poly(diol citrate)/HA composites. As a citrate-based biodegradable elastomer, poly(diol citrate) can potentially be utilized in tissue engineering and other biomedical applications [116, 166]. Poly(diol citrate)/HA demonstrated excellent osteoconductivity and induced rapid mineralization. Surprisingly, it elicited no chronic inflammatory response at the tissue-composite interface in vivo [166]. It was ascribed to that the rich –COOH from citrate units of poly(diol citrate) prompt calcium chelation thus facilitating poly(diol citrate)/HA interaction, enhancing mechanical properties, and promoting mineralization. Clear understanding on why poly(diol citrate)/HA exhibited excellent in vivo tissue/bone-compatibility is still unknown. Although poly(diol citrate)/HA was not developed under an hypothesis that the existence of citrate in bone may implicate the bone development, its excellent in vivo performance prompts further systematic study on the development of citrate-based orthopedic biomaterials. Since iCMBAs also possess citrate groups in their structure, a composite based on iCMBA-HA is also expected to demonstrate the much desired properties of a synthetic bone material such as excellent osteoconductivity and enhanced mineralization with satisfactory biocompatibility.

In order to investigate the efficiency and performance of injectable iCMBA-HA composites for treatment of bone defects, such as bone fracture and osteonecrosis of femoral head, the preparation and various physical, mechanical, degradation, and in vitro/vivo properties of these composites are evaluated and discussed in the current chapter.

3.2 Preparation and Properties of iCMBA-HA Composites

3.2.1 Preparation of iCMBA-HA Composites

All chemicals, cell culture medium, and supplements were purchased from Sigma Aldrich (St. Louis, MO), except where mentioned otherwise. All chemicals were used as received.

iCMBA pre-polymers were synthesized and characterized as described earlier in chapter 2. Due to its higher mechanical properties, such as tensile strength and modulus, iCMBA-$P_{200}D_{0.3}$ was chosen for composite fabrication. The injectable composites were prepared by mixing iCMBA solution in water with different amounts of HA to achieve various final composite formulations with 30, 50, and 70 wt% HA (w/w of dry composite). A calculated amount of crosslinker solution (PI in DI water) was then added to the mixture. The amount of PI was determined to provide enough ample time for preparation and injection of iCMBA-HA without compromising final mechanical properties of resulting composites. It is important that the mixture maintained enough flowability and injectability prior to completion of crosslinking. The set time of the composites was determined as the time from addition of PI to the iCMBA-HA mixture till it was not flowable. It is noteworthy to mention that for set time measurements the ratio of solid to liquid content was kept constant for all samples.

3.2.2 Physical and Mechanical Properties of iCMBA-HA Composites

Mechanical properties of iCMBA-HA composites were determined by unconfined compressive testing for the reason that compressive properties are believed to be the most relevant for cancellous bone replacements [141]. The measurements were conducted according to ASTM D695-10 on a MTS Insight 2 fitted with a 500 and 2000 N load cell (MTS, Eden Prairie, MN). Briefly, the cylindrical shaped samples (6 mm $\times$ 12 mm, diameter x height) were

compressed at a rate of 1.3±0.3 mm/minute, and deformed to failure. Values were converted to stress-strain and the initial modulus was calculated from the initial slope of the curve (0-10% elongation). The mechanical tests were conducted on the freshly-prepared samples (within1 hr after preparation) as well as on samples completely dried by lyophilization.

The sol-gel content, an indication of non-crosslinked/crosslinked fractions of the composites, and swelling ratio was measured by the mass differential before and after incubation of the polymer network in water, as described in section 2.2.4. The sol content and swelling ratio were then calculated using equations (2.1) and (2.2), respectively.

Degradation studies were conducted in PBS (pH 7.4) and at 37°C using cylindrical disc specimens (7 mm in diameter; 2 mm thick) as described in section 2.2.4. The mass loss was calculated by comparing the initial mass with the mass measured at the pre-determined time points using equation (2.3). It is important to mention that as degradation occurs predominantly due to disassociation of iCMBA, the calculated degradation rate was only based on the weight loss of iCMBA, which was measured by deducting the weight of the released HA from the total weight loss at each time point.

3.2.3 Mineralization of iCMBA-HA Composites

To evaluate in vitro mineralization on iCMBA-HA composites, disk shaped scaffolds of the composites (iCMBA-$P_{200}D_{0.3}$ PI:8%-HA70%) were immersed in simulated body fluid (SBF), which was prepared as described in the literature [167, 168]. To accelerate the mineralization process concentrated SBF was used, in which the concentration of inorganic ions was five times of those in human blood plasma (SBF-5X). The composite samples were immersed in 10mL of SBF-5X and incubated at 37℃ for up to 5 da ys while the SBF was replaced every other day. At each predetermined time point the specimens (n=5) were taken out, gently washed with DI water to remove any soluble inorganic ions from the surface of samples, and air-dried. Next, the specimens were sputter-coated with silver and examined by scanning electron microscope (SEM) using Hitachi 3000N (Hitachi, Pleasanton, CA). The elemental analysis of the mineralized composites were also conducted by Energy dispersive X-ray

spectroscopy (EDX) to determine the composition and ratio of the elements present in the minerals formed on the composites surface. In addition to composites, iCMBA-$P_{200}D_{0.3}$ PI:8% without HA was also subjected to mineralization test to find out the possible role of HA in the mineralization of iCMBA-HA composites.

3.2.4 In Vitro Biocompatibility of iCMBA-HA Composites

Various studies were conducted to evaluate the interaction between the composites and cells in vitro. The Cytotoxicity of sol content or leachable fraction of iCMBA-HA composites was assessed by incubating equal mass the composites specimen in 5mL Minimum Essential Medium (MEM) Alpha cell culture medium (Invitrogen Corp, Eugene, OR), containing 10% (v/v) fetal bovine serum (FBS) and 1% (v/v) streptomycin, for 24 hours. Next, three different solutions were prepared: 1X, 10X and 100X (1X was the solution of leached products with no dilution; 10X and 10X means 10 times and 100 times dilution of 1X by medium, respectively) were used for cell culture. To each well of a 96-well cell culture plate, 200µL of solution of MC3T3 pre-osteoblast cells in complete MEM, with concentration of 5x104 cells/mL, was added and incubated for 24 hours at 37℃, 5% CO2 and 95% rela tive humidity. The medium of each well was then replaced by pre-polymer-containing MEM solutions with various concentrations and incubated for another 24 hours followed by MTT assay analysis as per the manufacturer's protocol. The cytotoxicity of degradation products was also evaluated. iCMBA-HA composite samples with equal weight were fully degraded in 10 mL complete MEM Alpha cell culture medium. The resultant solutions were diluted to three concentrations (1X, 10X and 100X) using MEM, and used for cell culture and subsequent MTT analysis. All the above solutions were pH-neutralized and passed through a 0.2µm filter prior to use for cell culture. The cell viability results were normalized to the viability of cells in blank medium.

The viability and adhesion of MC3T3 cells to the surface of iCMBA-HA composites were also studied using fluorescent microscopy. Briefly, one drop of the iCMBA-HA composite (prior to completion of crosslinking) was uniformly spread on the surface of a glass slip cover and left to form a very thin layer of the composite. The samples were then sterilized by incubation in

70% ethanol for 24 hours followed by exposure to UV light for 3 hours. The samples were then placed in 24-well plate and seeded by MC3T3 cells with the density of 50,000 cells/cm^2. At each time point (day1 and day3 post seeding) the constructs were removed from the well plate, rinsed by PBS and stained with CFDA-SE (Carboxyfluorescein diacetate, succinimidyl ester) dye (Vybrant® CFDA SE Cell Tracer Kit, Invitrogen Corp, Eugene, OR) as per manufacturer's procedure. Next, the fluorescent images of stained samples were taken using a photomicroscope, Nikon Eclipse Ti-U equipped with Andor DR-328G camera (Nikon Instruments Inc, Melville NY).

The viability and proliferation of cells seeded on the surface of iCMBA-HA composites were determined by DNA assay. For this purpose, the composite samples were cut in disk shape to fit into the 24-well plate, and sterilized by incubation in 70% ethanol for 24 hours followed by exposure to UV light for 3 hours. MC3T3 cells were then seeded on the surface of the composites with a density of 50,000 cells/cm^2. At each time point, the samples were rinsed with TBS 1X (Tris-buffered saline), underwent 3 cycles of freeze-thaw-sonication in order to break cells and expose their DNAs. Quant-iT™ PicoGreen ® dsDNA reagent (Invitrogen Corp, Eugene, OR) was then used to quantify the double-stranded DNAs through fluorescent staining, by fluorescence excitation/emission at 480/520 nm . Using a known quantity of cells, a standard curve was also prepared as the reference to correlate between fluorescence intensity and number of cells.

The differentiation of MC3T3 osteoblast precursor cells to osteoblasts (an important type of bone cells that are in charge of producing new bone through synthesis of the organic matrix by secretion of a wide variety of extracellular matrix proteins [169]) was tracked by measuring the production of alkaline phosphatase (ALP) by osteobalsts. Cell-composite constructs were prepared as previously described. Briefly, MC3T3 pre-osteoblast cells were cultured on sterile composite samples, as well as on cell culture plate as control, with the concentration of 50,000 cells/cm^2. 24 hours after seeding, the cell culture media was replaced by a differentiation media containing 50 µg ascorbic acid and 3.06 mg of beta-glycerol

phosphate (BGP) in 1 mL of complete MEM media. The differentiation media was replaced every other day. At each time point the constructs were washed with PBS and went through 3 freeze-thaw-sonication cycles. ALP activity was then measured through incubation of 50 µL aliquots of homogenates with 4-nitrophenyl phosphate solution at 37℃ for 30 minutes. The amount of 4-nitrophenyl released due to the presence of ALP was then measured through absorption at 405nm using spectrophotometer and by comparing to a standard curve of 4-nitophenyl with various concentrations. ALP activity was normalized to the number of cells at each time point, which was separately measured by DNA assay.

3.2.5 In Vivo Study

To evaluate the in-vivo performance of the injectable iCMBA-HA composites, the composition with 70% HA was chosen. All the materials and tools were sterilized by either passing through a 0.2 µm filter, for solutions, or autoclaving, for solids. First, iCMBA-$P_{200}D_{0.3}$ dissolved in water to achieve a 40% solution. A calculated amount of HA was then added and thoroughly mixed to reach a composition of 70% w/w of HA over the total dry composite weight. Next, the required amount of sodium periodate was added to achieve a PI-to-prepolymer ratio of 6%. After vigorous mixing, the paste-like composite was injected into the area of interest as described below. New Zealand Rabbits (male, average body weight 3 kilogram) were used as animal model. All the rabbits were operated under general anesthesia, achieved with the intravenous injection of 3% pentobarbital sodium (30 mg per kilogram of body weight). Next, the surgical area were sterilized with 0.5% iodophor and then covered with surgical towel to insure clear operation field and prevent incision infection. Before skin cut, the fore limb (right side) of interest was shaved to identify the radial head of fore limb. A clear skin incision of 1.5 cm was made at the antero-lateral side of radius, which was just 1.5 cm distal to radial head. The anterior surface of the right radius was exposed by intermuscular space, saving muscles and related tendons. To make a standard and reproducible comminuted radial facture, radial osteotomy were first performed at two sites with surgical electric saw to produce a 1-cm-length bone block and then the bone block were cut into several segments(usually 3-4 fragments) with

bone rongeurs. Before the radial osteotomy, ulna should be exposed and protected from fracture to provide sufficient biomechanical support for fractured radius. After comminuted fracture was created, several bone fragments were split and then iCMBA-HA materials (at gel stage) were injected into the medullary space to unite the separate bone fragments. After making sure that the injection materials united well with the bone fragments, the deep fascia was sutured with stitches as tight as possible. After skin was sutured, external casts were performed to offer an instant stability for radius after the operation. Cotton gauze was inserted between skin and cast to keep the incision clean. All rabbits received buprenorphin (0.5 mg/kg) every 6 h for the first 3 postoperative days as analgesic therapy. Infection prophylaxis with penicillin (50000 U/kg) was maintained for the first 3 postoperative days twice a day. For control, the same procedure was repeated without using any filling material. The animals were subjected to X-ray radiology and micro-CT test at 4th week after the operation, to assess the bone tissue repair and regeneration through measuring bone mineral density (BMD) and the ratio of bone volume over tissue or total volume (BV/TV).

3.3 Results

3.3.1 Preparation of iCMBA-HA Composites

iCMBA-HA composites were prepared using iCMBA-$P_{200}D_{0.3}$ and varying amount of HA and sodium periodate (Figure 3.1). The various formulations have been listed in Table 3.1. The set time varied between 159±8 for iCMBA-P_{200} $D_{0.3}$-HA70% and 247±13 for iCMBA-P_{200} $D_{0.3}$-HA30% with PI-to-prepolymer ratios of 8% and 4%, respectively. Increasing the amount of HA in the composition slightly decreased the set time. Similarly higher amount of the initiator, PI, accelerated the crosslinking reaction, but with a greater impact.

Table 3.1 Formulation and set time of iCMBA-HA composites

Composite formulation	HA/composite ratio (dry w/w%)	PI to pre-polymer ratio (w/w%)	Measured set time (sec)
iCMBA-P_{200} $D_{0.3}$-HA30%	30	4%	247±13
iCMBA-P_{200} $D_{0.3}$-HA30%	30	8%	172±15
iCMBA-P_{200} $D_{0.3}$-HA50%	50	4%	238±9
iCMBA-P_{200} $D_{0.3}$-HA50%	50	8%	166±11
iCMBA-P_{200} $D_{0.3}$-HA70%	70	4%	231±10
iCMBA-P_{200} $D_{0.3}$-HA70%	70	8%	159±8

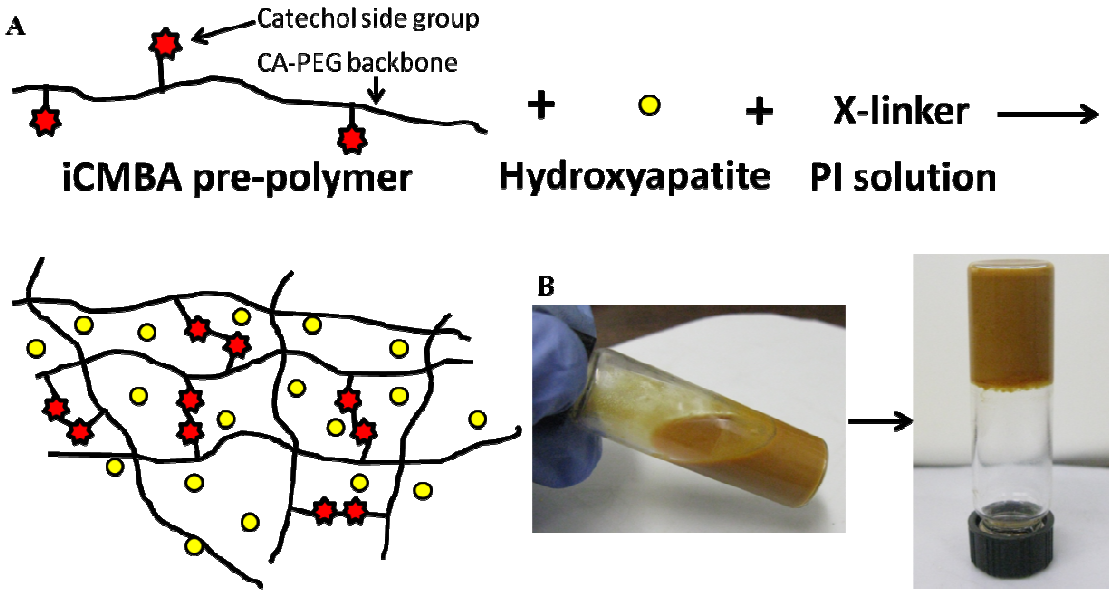

Figure 3.1 Preparation of iCMBA-HA composites. A) Schematic representative of iCMBA-HA composite preparation through mixing iCMBA with HA followed by crosslinking using PI solution. B) Images of iCMBA-HA mixture before (left) and after (right) crosslinking.

3.3.2 Physical and Mechanical Properties of iCMBA-HA Composites

Mechanical properties of iCMBA-HA composites for freshly prepared and dry samples are shown in Table 3.2 and Figure 3.2. In the dry state, the highest measured values for compressive strength, and modulus were 23.71±2.61 MPa and 178.79±14 MPa, respectively, for iCMBA-$P_{200}D_{0.3}$ PI:8%-HA70%, followed by iCMBA-$P_{200}D_{0.3}$ PI:8%-HA50% (strength: 9.26±2

MPa; modulus: 19.83±2.1 MPa) and iCMBA-$P_{200}D_{0.3}$ PI:8%-HA30% (strength: 8.03±2.3 MPa; modulus: 2.67±0.7 MPa). For the freshly prepared samples compressive strength and modulus were 2.45±0.37 MPa and 5.74±1.10 mPa (HA70%), 1.89±0.45 MPa and 4.31±0.89 MPa (HA50%), and 1.25±0.35 MPa and 1.062±0.12 MPa (HA30%), respectively. The stress-strain curves of freshly prepared composites are also shown in Figure 3.3.

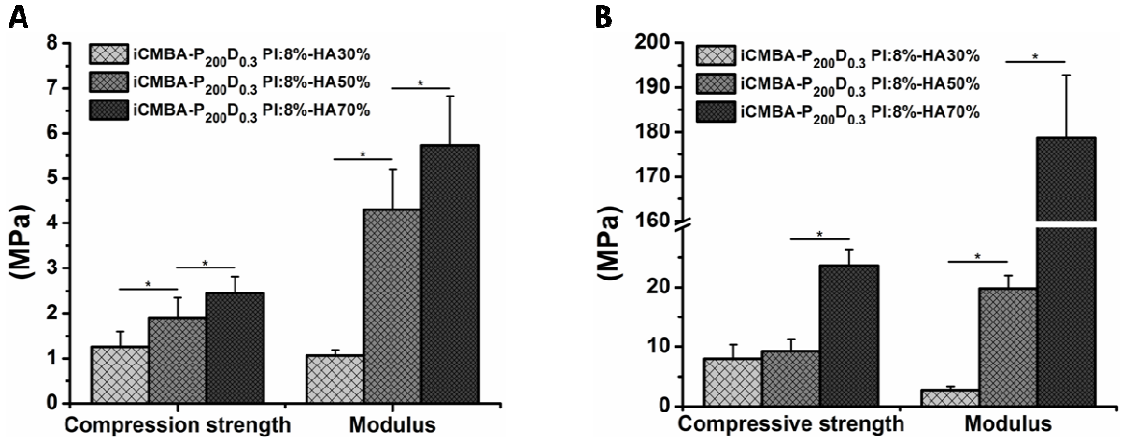

Figure 3.2 Mechanical properties of iCMBA-HA composites. Compressive strength and modulus of A) freshly prepared sample, and B) lyophilized samples.

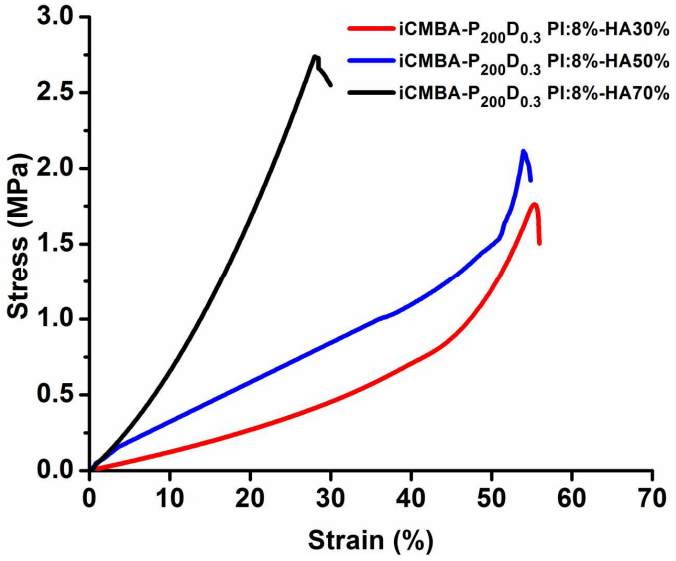

Figure 3.3 Stress-strain curve of iCMBA-HA composites measured through compressive mechanical testing one hour after preparation.

Table 3.2 Mechanical properties of iCMBA-HA composites

Composite formulation	PI to pre-polymer Ratio (w/w%)	Compressive strength (MPa)		Compressive modulus (MPa)		Strain at Break (%)	
		As prepared	Freeze-dried	As prepared	Freeze-dried	As prepared	Freeze-dried
iCMBA-P_{200} $D_{0.3}$-HA30%	8	1.25±0.35	8.03±2.30	1.06±0.12	2.67±0.70	54. 08±2.24	77.60±0.9
iCMBA-P_{200} $D_{0.3}$-HA50%	8	1.89±0.45	9.26±2.0	4.31±0.89	19.83±2.1	52±3 .71	51.70±8.0
iCMBA-P_{200} $D_{0.3}$-HA70%	8	2.45±0.37	23.71±2.60	5.74±1.10	178.79±14	29 .46±4.33	32.8±6.06

The sol contents of different iCMBA-HA composites were between 2.46% and 3.29% for the composites with 50% and 30% HA, respectively, but were not significantly different for the samples with and without HA (Figure 3.4A).

The study of the composites swelling revealed that the degree of swelling was lowest for iCMBA-$P_{200}D_{0.3}$ PI:8%-HA70% with 110±9.8, followed by samples with 50%, 30%, and no HA with the ratios of 249.5±36.8, 353.2±32.2, and 802.3±64.6, respectively(Figure 3.4B).

The degradation studies of the composites revealed that the rate of degradation decreased as the amount of HA increased in the composites. As shown in Figure 3.5, iCMBA-$P_{200}D_{0.3}$ PI:8%-HA70% exhibited the slowest rate of degradation with complete degradation in 30days incubation in PBS at 37℃, followed by compo sites 50% and 30% HA. iCMBA polymer with no HA disintegrated faster than composites.

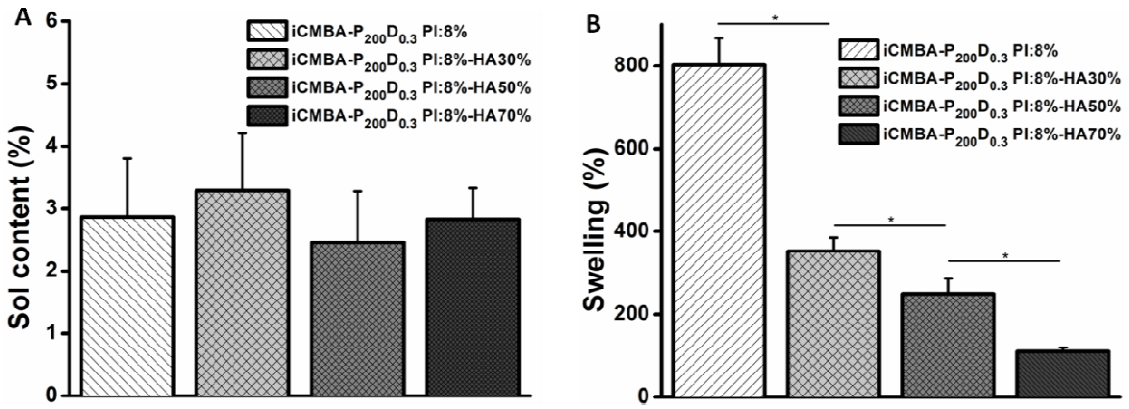

Figure 3.4 Soluble content (A) and swelling ratio (B) of iCMBA-HA composites.

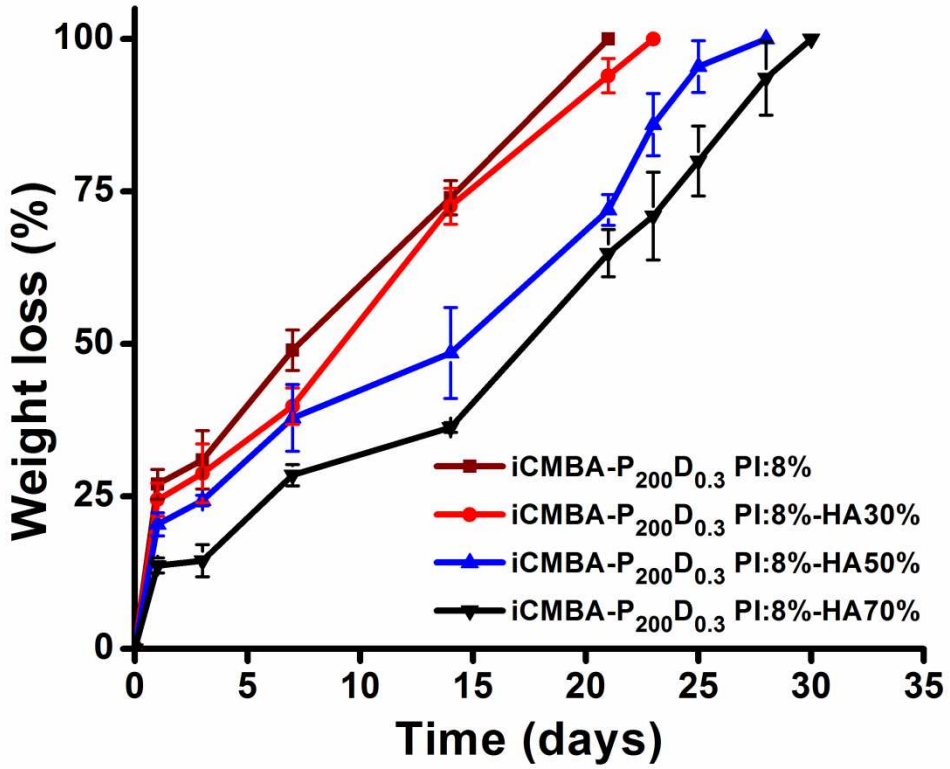

Figure 3.5 Degradation profiles of iCMBA-HA composites, measured through weight lost after incubation in PBS at 37℃.

3.3.3 Mineralization of iCMBA-HA Composites

After 1 day incubation of iCMBA-$P_{200}D_{0.3}$ PI:8%-HA70% composites in SBF-5X, no crystals on the surface of samples were observed, as shown in Figure 3.6A. As incubation continued, crystals of calcium phosphate began to form and grow. Figures 3.5B-D show the formation of the crystals on the surface of iCMBA-HA composite. In addition, EDX analysis confirmed the existence of these crystals, in which the ratio of Ca/P was around 1.61 (Figure 3.6E). In the case of iCMBA-$P_{200}D_{0.3}$ PI:8% (no HA) samples, incubation in SBF-5X did not induce any crystal formation on the surfaces as can be seen in Figure 3.6F.

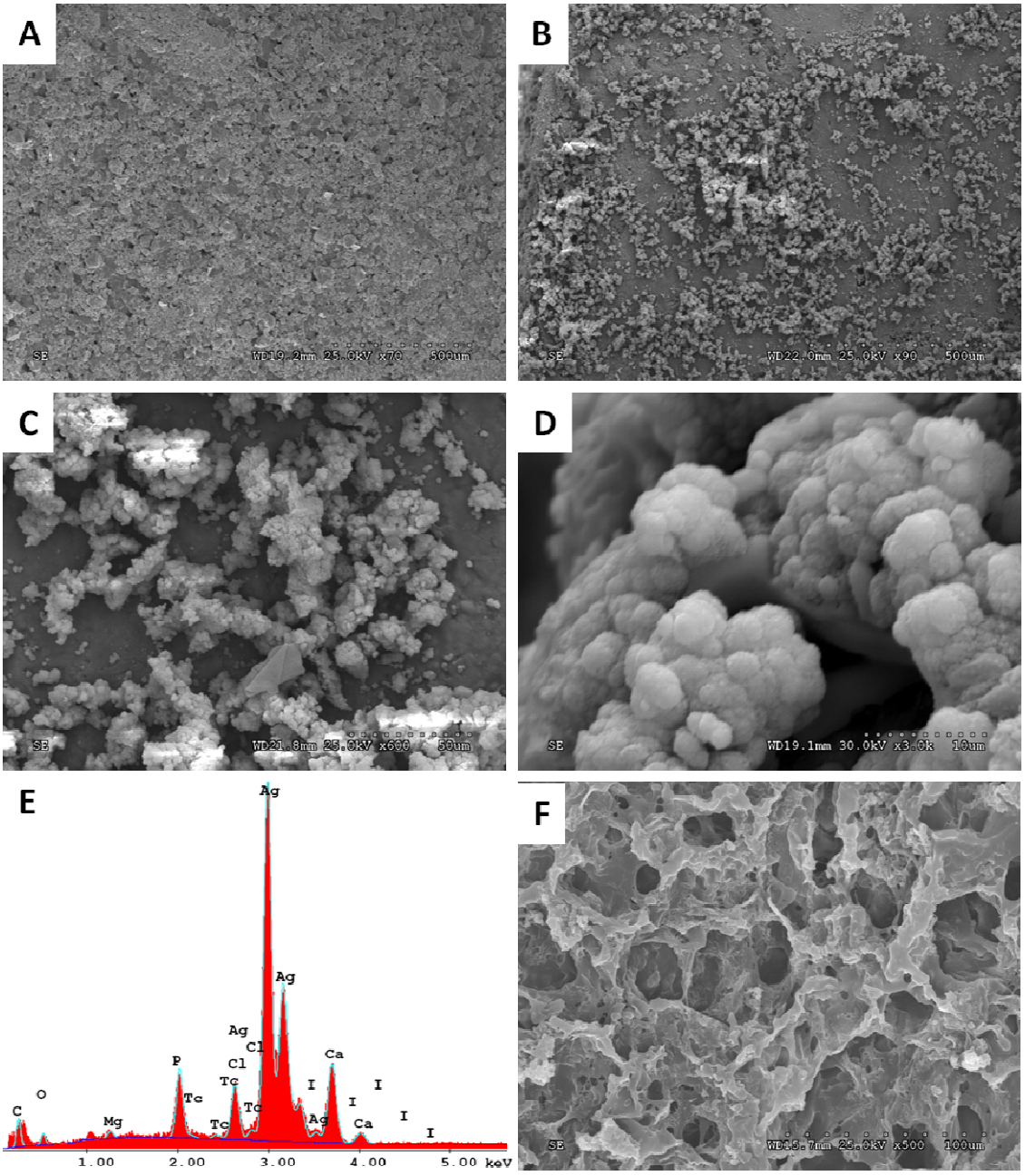

Figure 3.6 Mineralization of the composites. SEM images of iCMBA-$P_{200}D_{0.3}$ PI:8%-HA70% composites incubated in SBF-5X at 37℃ for: (A) 1 day, and (B, C, and D) 5days. E) EDX analysis of the surface of crystal-deposited composite. F) iCMBA-$P_{200}D_{0.3}$ PI:8% without HA, incubated in SBF-5X for 5days at 37℃ (no crystal is formed).

3.3.4 In Vitro Biocompatibility of iCMBA-HA Composites

The results of cytotoxicity study of the soluble (leachable) content and degradation products of various iCMBA-HA composites are shown in Figure 3.7A. The MC3T3 cells viability in the presence of soluble content of the composites at 1X concentration was between of 74.02±18.41% (30% HA) and 92.64±5.09% (no HA), showing only minor cytotoxicity. In diluted solution of 10X and 100X the minimum the cells viability was at least 87.65±7.24%. Furthermore, the degradation products (1X) showed a cell viability of at least 73.46±7.52 % (no HA), suggesting that the degradation products of all iCMBAs composites did not induce significant cytotoxicity (Figure 3.7B). The cell viability improved as the solution of degradation products was further diluted to 10X and 100X.

The evaluation of adhesion and proliferation of MC3T3 cells on the surface of the composites using fluorescent light microscopy demonstrated an excellent cell attachment to the composites films and the expected morphology, as shown in Figures 3.8. The proliferation of the cells was also observable through two time points.

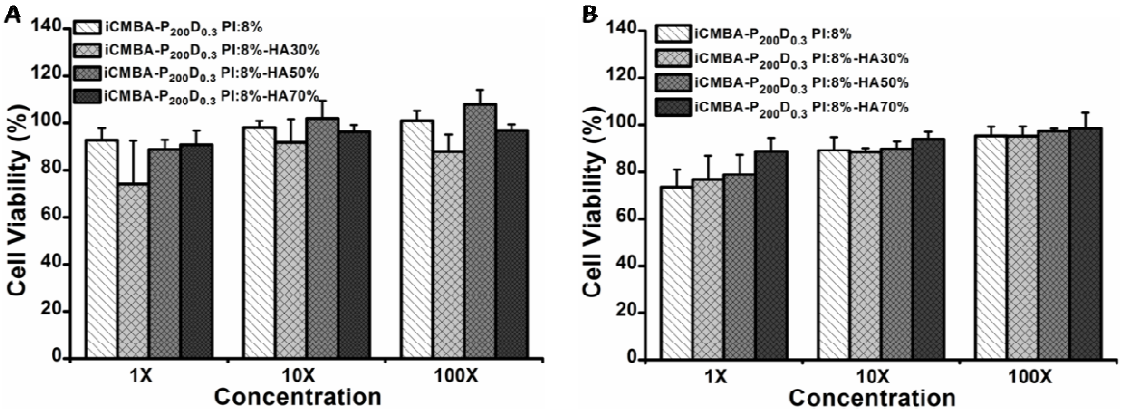

Figure 3.7 In vitro cytotoxicity of iCMBA-HA composites. Cytotoxicity study using MC3T3 pre-osteoblast cells by MTT assay for: A) Leachable products (sol content), and B) Degradation products of iCMBA and iCMBA-HA composites. All data were normalized to cell viability in blank medium.

The viability and proliferation of MC3T3 cells, quantified by DNA PicoGreen assay, confirmed the increase in the number of the cells seeded on the iCMBA-$P_{200}D_{0.3}$ PI:8%-HA70%

composites through three different time points, which was not significantly different from the cells seeded on the polystyrene cell culture plate (Figure 3.9A).

In addition, the differentiation of MC3T3 pre-osteoblast cells to osteobalsts was evident from the ALP activity of osteoblast cells seeded on the composite, which increased from 0.0127 pmol *p*-nitrophenol/cell in the 1st day to 0.0803 at day 7 and not significantly different from that of cells grew on the cell culture plate (Figure 3.9B).

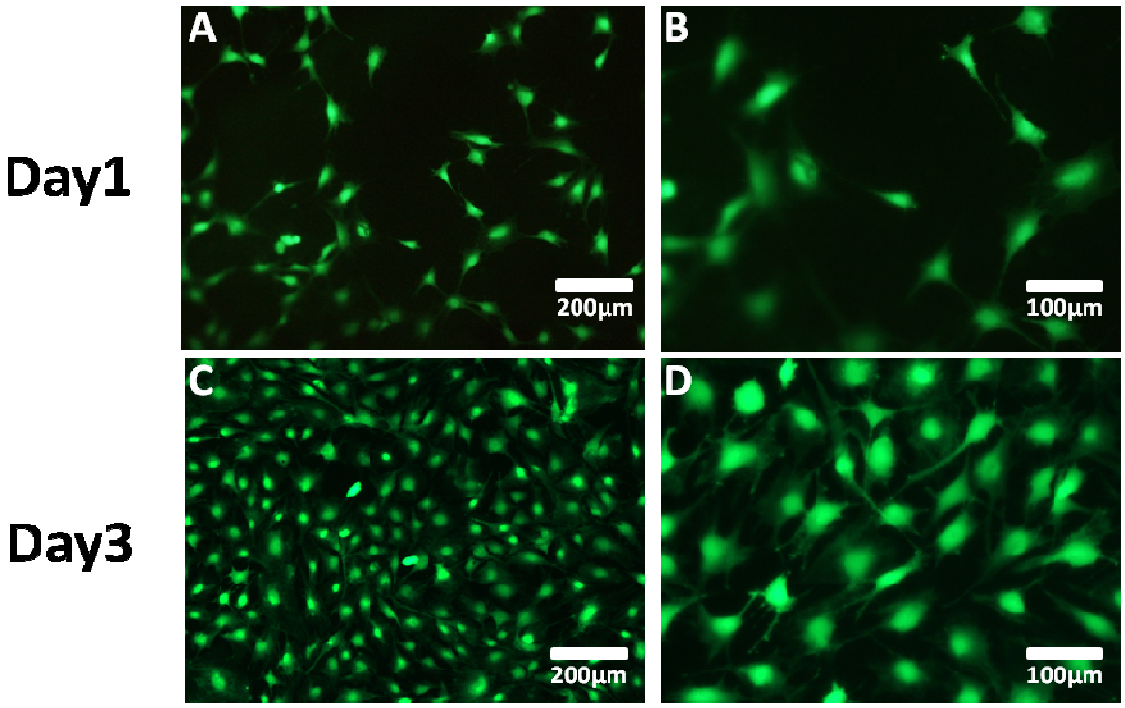

Figure 3.8 Fluorescent images of CFDA-SE stained MC3T3 pre-osteoblast cells seeded on the iCMBA-$P_{200}D_{0.3}$ PI:8%-HA70% composite films at 1st day(A,B) and 3rd day (C,D) post seeding.

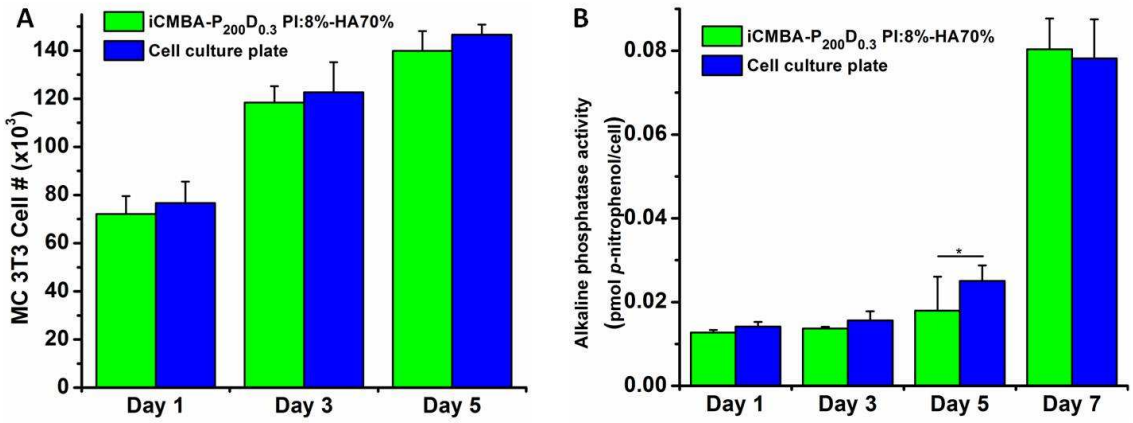

Figure 3.9 MC3T3 pre-osteoblast cells proliferation and differentiation on the iCMBA-$P_{200}D_{0.3}$ PI:8%-HA70% composite and cell culture plate (control). A) Proliferation of the cells measured through PicoGreen DNA assay at 1st, 3rd, and 5th day post seeding. B) Differentiation of pre-osteoblast cells to osteoblasts measured by ALP expression at 1st, 3rd, 5th, and 7th day post adding the differentiation medium.

3.3.5 Animal Study

The animal study was conducted on a comminuted fracture created on the New Zealand rabbit model. As shown in Figure 3.10 [170], comminuted or multi-fragmentary fracture is a complex bone fracture in which the bone is fractured into several pieces.

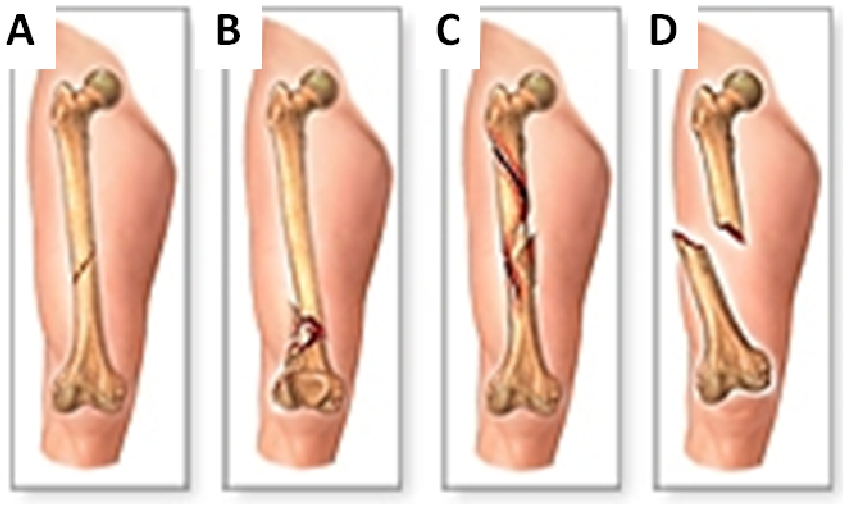

Figure 3.10 Different types of bone fracture: A) oblique, B) comminuted, C) spiral, and D) compound [170].

The iCMBA-HA composite samples showed good flowability properties and were easy to inject. The set time was adequate to allow enough time for the surgical procedure be carried out within the required time frame. The X-ray radiographs of the fractured bone right after fracture and 4 weeks after treatment are shown in Figure 3.11. The bone treated with iCMBA-HA enhanced the regeneration and healing of the fractured bone tissue compared to the control, as can be observed from Figure 3.11B, C. In addition, the results of micro-CT demonstrated that the BMD and BV/TV for the composite-filled bone fracture was 388.4 mg/cc and 62.5%, respectively, which were significantly higher ($p<0.05$) than those values for the control with BMD of 327.5 and BV/TV of 49.3% (Figure 3.12).

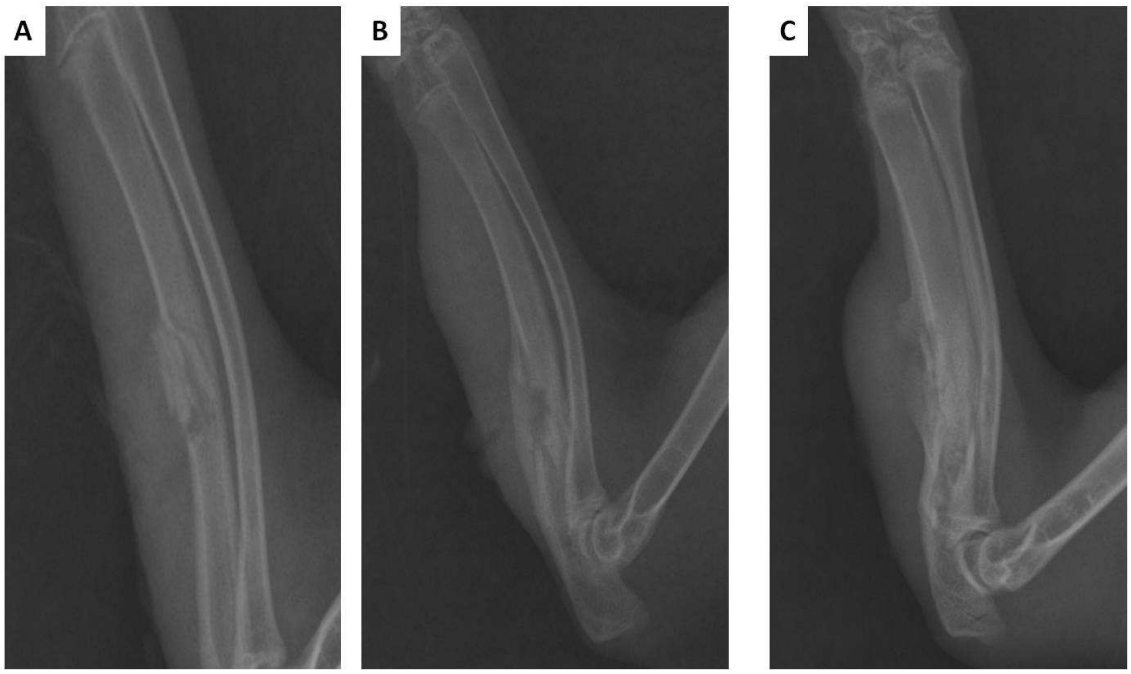

Figure 3.11 X-ray radiographs of New Zealand rabbit forelimb with comminuted radius bone fracture: A) Immediately after fracture, and 4 weeks after operation for B) control and C) treated with iCMBA-HA injectable composite.

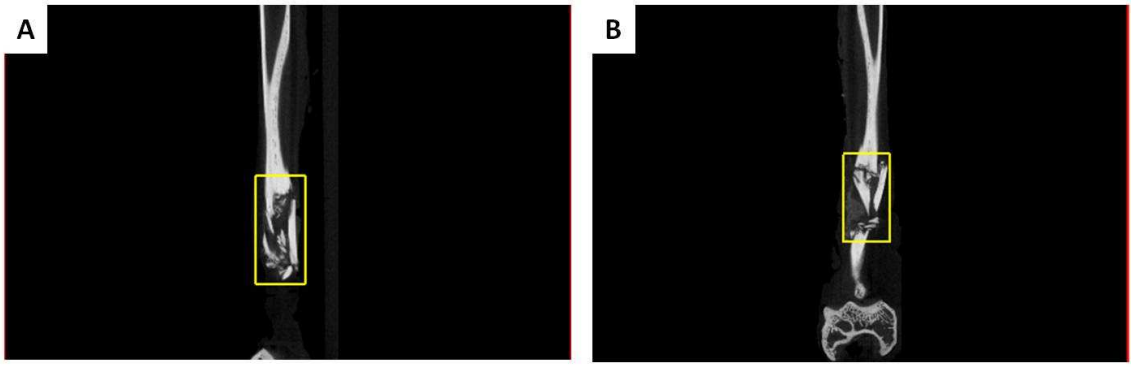

Figure 3.12 Images of micro-CT of New Zealand rabbit bone with comminuted fracture 4 weeks after operation: A) control with no filling material, and B) injected with treated with iCMBA-HA composite. Bone mineral density (BMD) and bone volume over total volume is significantly higher for iCMBA-HA treated bone fracture ($p<0.05$).

3.4 Discussion

As previously discussed in chapter one, water soluble iCMBA pre-polymers can be easily synthesized and crosslinked. The rate of crosslinking was dependent on multiple parameter, such as the amount of dopamine in the structure of polymer, length of PEG, and the amount of crosslinker initiator, sodium periodate, which could be simply tuned based on requirements. The facile preparation of iCMBAs from safe and non-hazardous constituent, their capacity to be crosslinked in-situ, and their promising in vitro and in vivo performance, confer iCMBA properties set required for applications that injectable in-situ-crosslinkable biomaterials are used. Taking advantage of these qualities, we prepared injectable iCMBA-hydroxyapatite composites for orthopedic applications in bone defects such as osteonecrosis. For this purpose iCMBA-P_{200} $D_{0.3}$, which showed the highest mechanical properties among all iCMBAs (chapter 2), was mixed with different amount of HA and crosslinked by adding the required amount of sodium periodate with PI-to-prepolymer ratio of 8%. The set time of iCMBA-HA composites were a function of not only the percentage of PI as expected, but also the amount of HA in the mixture. Higher amount of HA resulted in shorter set time, which could be due to the reduction

in the pH of mixture when more HA is present in the system. As previously mentioned in chapter one oxidation, and consequently crosslinking of catechol groups are accelerated in alkaline environment. Nevertheless, the effect of HA on the set time of composites was much less than that of the amount of the initiator, sodium periodate.

The sol contents of samples, with and without HA, did not differ significantly and was not a function of the HA amount in the composites, suggesting that the level of crosslinking was similar in all formulations. Since iCMBA polymer is the crosslinkable component of the iCMBA-HA composite, the soluble content comprised only non-crosslinked polymer and was not related to the amount of HA in the system. In contrast, the swelling ratio of iCMBA-HA composites was inversely dependent on the amount of HA. By increasing the amount of HA, or lowering the amount of iCMBA in the composites, the more hydrophilic portion of the composite, i.e. iCMBA, was in fact decreased, which resulted in a reduction in water absorption capacity of the composite, thus less swelling. The mechanical properties of the composites were directly proportional to the amount of HA in the system. Compressive strength and modulus were improved as the amount of HA increased, as expected for particulate composites. The deformation to failure, however, reduced by increasing the amount of HA, especially in composition with 70% HA, which was expected due to decrease in the fraction of flexible iCMBA polymer in the composite.

The degradation rate of iCMBA-HA composites was also dependent on the HA fraction in the system. The composites with 70wt% HA exhibited the slowest rate of degradation while the sample without HA was degraded in the fastest pace. The weight loss of the composite was primarily due to the degradation of iCMBA. The decreased rate of the degradation in iCMBA-HA composites containing higher amount of HA could be explained by possible chelation of –COOH groups of iCMBA with HA particles, resulted in enhanced interaction between iCMBA and HA particles, which could slow down the degradation of the composite [166].

Based on SEM and EDX images (Figure 3.6), iCMBA-HA composites with 70 wt% HA induced surface mineralization when incubated in SBF 5X for 5 days. Studies have shown that

HA can stimulate deposition of calcium phosphate on the ceramics implants and improve bonding to bone tissue. Bone-like apatite layer has proven to form a bone-binding interface between the biomaterial and native bone tissue [171-173]. On the other hand, samples without HA were not conductive to mineralization within the time frame studied, which is yet another indication of the role of HA in nucleation and formation of calcium phosphate crystals on the surface of iCMBA-HA composites.

In vitro study of cytotoxicity of iCMBA-HA composite showed that sol (leachable) content and degradation products of the composite did not induce significant cytotoxicity to MC3T3 preosteoblast cells (Figure 3.7A,B). In addition, the fluorescent imaging of the cells seeded on the surface of iCMBA-HA thin film demonstrated a perfect attachment, spread, and proliferation of MC3T3 cells on the composite surface, which was similar to the cells attachment to a cell culture plate used as control (Figure 3.8). The proliferation of MC3T3 cells on the surface of iCMBA-HA composites, measured by DNA assay at different time points, also proved that the composites provided suitable conditions for cells growth and proliferation, which was not significantly different from cell culture plate (Figure 3.9A). These findings support the idea that the iCMBA-HA composites are safe for possible use in biological and biomedical applications. In addition, the results of ALP assay (Figure 3.9B) revealed that MC3T3 osteoblast precursor cells, cultured on the surface of iCMBA-HA samples, were differentiated to osteoblasts, which play a crucial role in producing new bone tissue through synthesis of the organic matrix by secretion of a wide variety of extracellular matrix proteins [169]. The differentiation of MC3T3 pre-osteoblast cells to osteoblasts is a time-dependent process, and usually begins when MC3T3 cells achieve confluence [174], which can explain the jump in ALP expression at day7 after adding the differentiation media. The peak of ALP activity and, therefore, the differentiation of pre-osteoblast cells to osteoblasts, has been shown to occur within two to three weeks [174]. In the case of iCMBA-HA composites, as the samples began to degrade before reaching these time points, it was not possible to record the peak ALP activity. Nonetheless, the jump in the ALP activity at 7th day indicated that the process of cells

differentiation had already started. The differentiation of preosteoblast cells to osteoblasts marks an important stage of new bone tissue formation in the body.

The in vivo performance of the injectable iCMBA-HA composite in the treatment of the comminuted fracture of the radius bone in New Zealand rabbit model, showed that the composites were easy to prepare and use. The set time was shown to be adequate for preparation and injection of the composite to the fracture area. The preliminary results of subsequent follow-up tests, such as X-ray radiography and micro-CT, after 4 weeks proved that the iCMBA-HA improved new bone formation when compared to unfilled control fracture.

3.5 Conclusion

In the present chapter, the synthesis, preparation, properties, and applications of a new injectable biodegradable bone cement was reported. The injectable iCMBA-HA composites were prepared from a simple technique. The set time and physical and mechanical properties, and degradation rate of these composites could be simply tuned by changing the amount of HA and the initiator in the system to achieve the required setting time and properties. The in-vitro formation of calcium phosphate crystals on the surface of iCMBA-HA was also shown to take place when the composites were immersed in simulated body fluid, which could improve the binding between the injectable composite and native bone tissue. Leachable content and degradation products of iCMBA-HA composites did not induce significant cytotoxicity on MC3T3 cells during in vitro cell viability study. The cells also showed normal proliferation and adhesion when cultured on the surface of composite samples. In addition, the composites appeared to facilitate the differentiation of MC3T3 preosteoblast cells to osteoblasts, which is an important step in formation of new bone tissue. The preliminary in vivo study on a comminuted fracture of a rabbit model confirmed that injectable iCMBA-HA composites can be utilized to improve the formation of new bone tissue in a defected bone area and accelerated the healing process.

CHAPTER 4

iCMBA HYDROGELS AND NANOGELS FOR PH–SENSITIVE DRUG DELIVERY

4.1 Introduction

Among various biomaterials, hydrogels, which are three-dimensional crosslinked network of hydrophilic polymers, are gaining growing popularity in biological, pharmaceutical, and medical applications, such as wound dressing, tissue engineering, and drug delivery. This is mainly due to hydrogels attractive properties such as capability of absorbing large amount of water while maintaining good mechanical properties and biocompatibility [56, 175]. Among various applications, the utilization of hydrogels in controlled drug delivery system (CDDS) has been the focal points of numerous studies.

Controlled drug delivery has attracted immense attention in the modern medicine, because it can significantly improve the efficiency of drugs and lower the risk of drugs side effects by delivering drugs to an intended site with a predefined release rate and for a determined period of time [176]. In the conventional drug delivery, the effective therapeutic level of active pharmaceutical ingredient (API) is reached almost immediately after administration of drug, but sharply falls below the effective range within a very short time after. Thus, to keep the efficiency level the administration of drug must be repeated frequently. A controlled drug delivery, by contrast, can sustain the therapeutic level for a required period of time following administration [177-179]. A drug delivery system typically comprises a drug-loaded biomaterial, in various shapes and sizes, which releases drug when the predetermined conditions are satisfied. A wide variety of materials have been used as coating and carries for drugs. They are, for example, fabricated from hydrophilic polymers such as methyl cellulose, or from hydrophobic polymers such as ethyl cellulose, hydroxypropylmethylcellulose, and some derivatives of acrylate polymers. One of the approaches taken by scientists to determine the place, rate, and

duration of a drug release is to design and use ‘smart’ biomaterials that can sense the change in the environmental conditions and adjust the rate and/or the place of drug release according to physiological need and conditions. This requires biomaterials to sense and response to environmental stimuli, which can be physical such as temperature, light, pressure, sound, and electrical or magnetic fields, or chemical stimuli such as alteration in surrounding pH, ionic strength, or existence of a specific molecule [176, 180]. In an ideal case, a drug delivery system should be able to sense any changes in physiological conditions caused by diseases and subsequently regulate the amount the drug release based on the type and magnitude of those change. Given hydrogels desirable properties, such as high water retention capacity while keeping structural integrity, which can also improve their blood compatibility, they have been extensively investigated for drug delivery systems [176, 181]. Hydrogels can also be functionalized with specific groups to act as ‘smart’ materials in response to physical and chemical stimuli. Among various systems, hydrogels that can sense and respond to changes in surrounding temperature and pH are of immense importance in physiological environment, because these two parameters are subject to change in the body, which can be due to natural variation or caused by diseases. The pH, for example, can take different values in the human body due to various reasons. The well known example is variation of pH in different sections of gastrointestinal (GI) tract. Another example is the pH at tumor sites, which is found to be lower than healthy tissues [182]. Thus, developing pH sensitive ‘smart’ or ‘intelligent’ hydrogels, which can sense and accordingly respond to the environmental pH, have been of significant interest.

In order for a polymer to be pH-sensitive, it should contain ionizable pendant groups, which can either accept or release protons in response to changes in environmental pH [176, 180]. Therefore, the existence of pendant acidic (such as carboxylic and solfoinc) or basic (such as ammonium salt) groups renders a polymer pH-sensitivity. When a large number of ionizable groups are present in a polymer it is referred to as ‘polyelectrolytes’. Another classification of pH-sensitive polymers is based on the type of ion they form upon ionization. Polymers having pendant acidic groups are ionized to anions in solution with high pH, therefore, they are known

as anionic polymers or hydrogels (Figure 4.1A). Acrylic acid polymers such as poly(acrylic acid) (PAA) and poly(methacrylic acid) (PMAA) are examples of anionic polymers. On the other hand polymers containing basic groups are referred to as cationic polymers or hydrogels, because they form cations in low pH environment (Figure 4.1B). Some examples include polymers or hydrogels containing dimethylamino or quaternary amino groups, or vinyl pyridine [176, 180, 183].

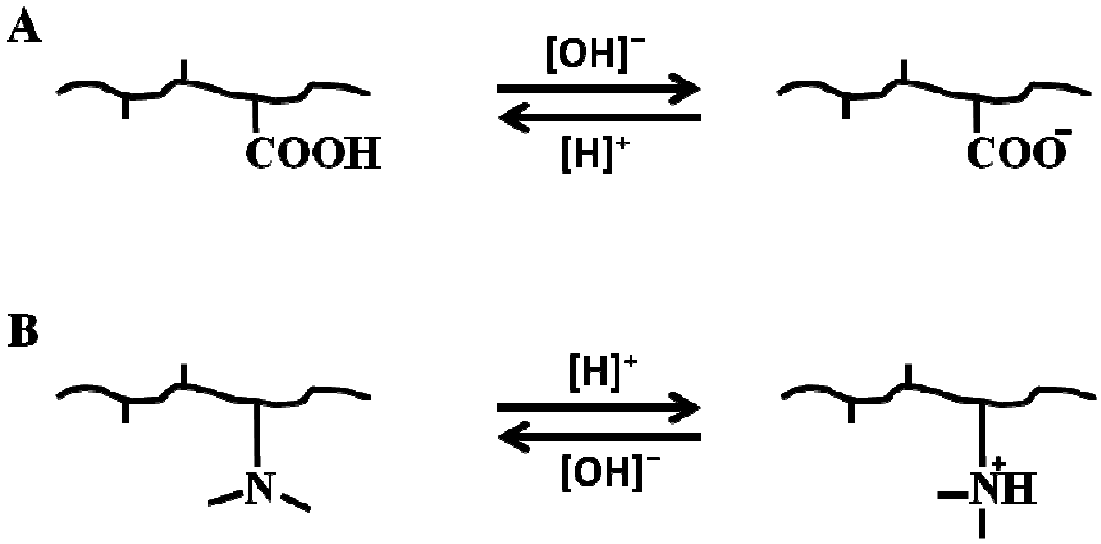

Figure 4.1 Schematic diagram of ionization and deionization of polymers with ionizable groups. A) An anionic polymer containing acidic groups, deprotonated and ionized in basic solution. B) A cationic polymer, ionized in acidic condition.

When a pH-sensitive hydrogel is subjected to a change in environmental pH, its swelling reaction is defined by the type of pendant groups, ionic strength, type of counterions, and the pH of the surroundings [176]. When acidic groups exist, the hydrogel swells more if the external pH increases and deswells when the pH is lowered. If immersed in a basic solution, the pendant acidic groups in the structure of hydrogel deprotonate and the separated protons, i.e. H^+, combine with hydroxide anions (OH^-) to form water molecule. To maintain the charge neutrality, more cations, diffuse into the hydrogel. The accumulation of cations in the gel increases the osmotic pressure, which consequently results in hydrogel swelling[180]. In polyelectrolytes the swelling is mainly attributed to electrostatic repulsion among similar charges

present on the polymer chains as well [176]. Swelling and deformation of hydrogel causes a counter elastic force by the hydrogel network. An equilibrium state is reached when the osmotic pressure and the elastic force of the network balance each other. The transition between swollen and relaxed state occurs within the range of apparent acid disassociation constant, pKa, of the ionizable group of the hydrogel. However, the presence of numerous ionizable groups in polyelectrolytes creates an electrostatic effect on other ionizable group, which causes their pKa to be different from corresponding monoacid [176].

The properties of pH-sensitive hydrogels make them appropriate for drug delivery application, particularly in oral drug administration. The diverse external conditions that are imposed to a drug in the GI tract, provides a tool for controlling the drug release. The change in environmental pH along GI tract can determine the place and rate of drug release in a drug-loaded pH-sensitive hydrogel [177]. This facilitates the release of an API in a section with optimum uptake and prevents its release in the regions that it might cause adverse side effects [183]. to As shown in Table 4.1, pH varies in the GI tract from 2.0 in the stomach up to 8.0 in the colon [183]. Several models have been proposed to explain the mechanisms of drug release in pH-sensitive hydrogels. Depending on the rate-limiting parameter, the release can be controlled by diffusion, swelling, or chemical reactions. Diffusion is the most cases are explained by Fick's diffusion laws, which uses constant or variable diffusion coefficients and the driving force is concentration gradient. When the diffusion of drug molecules is faster than hydrogel swelling rate, the latter is the limiting factor and controls the drug release. In the third mechanism, the release of drug requires a chemical reaction to take place. This reaction can be the enzymatic or hydrolytic degradation of hydrogel polymers network, in which the drug is entrapped, or the breakage of a chemical link between drug and polymer chain, on which the drug has been conjugated [176, 180, 183].

pH-controlled drug delivery systems are either prepared by coating a preformed drug form, i.e. tablet, capsule, pellet, or particle, using a pH-sensitive polymer or embedding of drugs active agents in a polymer hydrogel. Various polymer systems have been used to prepare pH-

sensitive coatings. The most widely used coating systems are polymers based on methacrylic acid, methyl methacrylates, and their copolymers (with the general trade name of Eudragit, Evonik Rohm, Darmstadt, Germany). By functionalizing these polymers with negatively or positively charged moieties, the coatings can be designed to be removed in acidic or basic environment, respectively, and expose the drug core. pH-sensitive polymeric hydrogels are swellable and biodegradable materials, which are utilized for drug delivery, particularly in GI tract sections with neutral or basic pH, such as small or large intestine, or colon. These hydrogels are based on anionic polymers with no or low swelling in acidic environment of stomach and enhanced swelling in neutral or basic condition of lower GI tract. Poly(acrylic acid), poly(methacrylic acid), poly(acrylamid), and dextran are among widely investigated polymers to prepare this type of hydrogels [176, 184]. In contrast, hydrogels from cationic polymers, such as N,N´-dimethylaminoethylmethacrylate (DMAEM) and chitosan, are used to protect drug in neutral or basic pH but they swell or degrade and release drug in a acidic environment of stomach [176, 183]. Neutral hydrogels can also be pH-sensitized through incorporating ionizable groups into the structure of hydrogels [185, 186].

Table 4.1 pH of various sections of gastrointestinal tract of the human body

Section of GI tract	**pH (fasted)**
Oral cavity	7.0
Esophagus	6.0-7.0
Stomach	Men: 2.1, Women: 2.8
Small intestine	5.5-8.0
Large intestine	5.5-7.0
Colon	8.0
Rectum	7.0

The release of drug in pH-sensitive swellable hydrogels can be enhanced by disruption of the drug-loaded hydrogel matrix thorough the rupture of polymer backbone or crosslinks by

hydrolytic or enzymatic degradation [184]. For a hydrogel to be susceptible to degradation by enzymes, specific chemical bonds must be introduced to hydrogels structure. For example in one study polyanions hydrogels crosslinked by azoaromatic groups were prepared. Following the equilibrium swelling of these hydrogels, which exposed azoaromatic crosslinks, the crosslinks were cleaved by enzymes produced in the colon [184].

Despite of significant breakthroughs in designing pH-responsive hydrogels, there are some limitations. Non-biodegradability of hydrogels prepared based on synthetic polymers is one these limitations[176]. This may not cause any serious problems in applications such as oral drug delivery, as the non-degraded materials can be physiologically repelled from the body. However, degradation of hydrogel is advantageous as it enhances the drug release and delivery efficiency, as discussed earlier. In addition, for applications rather than oral drug delivery, such as implantable drug delivery systems, of which the drug release is dependent on the degradation of hydrogel, the problem of non-biodegradability needs to be addressed. For this purpose, researchers developed biodegradable hydrogels based on polysaccharides. Dextran was first activated by 4-nitrophenyl chloroformate. Next, it was conjugated with aminobutyric acid and crosslinked by 1,10-diaminodecane, to prepare a pH-sensitive hydrogel [187]. Carboxylpropyl groups enhanced swelling in high pH conditions. The hydrophilicity of dextran and hydrogen bonding with water molecules resulted in slower rate of swelling/desewlling in response to change in external pH. Using dextranase enzyme reportedly enhanced the model drug release from the hydrogel through breaking down of dextran [187]. Due to absence of required enzyme in the human body or certain part of it, the biodegradation of dextran might not always be possible [176]. Some studies focused on preparing hydrogels based on proteins and synthetic polypeptides. In an attempt, a polypeptide hydrogel was prepared using poly(L-glutamic acid) (PLG) crosslinked by PEG [188]. The resulted hydrogel was highly hydrophilic and exhibited fast swelling/desewlling properties in reaction to environmental pH change. Other synthetic polypeptides such as poly(hydroxyl-L-glutamate), poly(L-ornithine), poly(aspartic acid), and poly(L-lysine) have also been investigated for preparing pH-sensitive hydrogels [176].

However, preparing these polypeptides may require complex synthesis routes. In addition, depending on the type of bacteria available in the organ targeted for drug delivery, a specific type of polypeptide might be required to be susceptible to attack and degradation by those bacteria

To address the described issues and prepare a readily biodegradable material, pH-sensitive, hydrolytically degradable hydrogels with controllable degradation rate based on iCMBA polymers have been proposed. It was shown in chapter two that iCMBAs can form hydrophilic polymer network, with high swelling ratio of at least 470% (while maintaining the structural integrity) and controllable degradation, using facile syntheses and preparation method. The degradation of iCMBA was shown to be easily manipulated by variation in the PEG length, amount of dopamine in the iCMBA structure, and the amount of crosslinking initiator, sodium periodate. The presence of pendant unreacted carboxylic groups of citric acid on the chain of iCMBA polymers (Figure 2.1) is believed to render iCMBA hydrogels pH sensitivity, which can be utilized to prepare pH-responsive swellable and biodegradable controlled drug delivery system. To evaluate this hypothesis, the focus of this chapter will be on the preparation and characterization of iCMBA hydrogels, their swelling and degradation dependency on environmental pH, and the drug release properties of iCMBA hydrogels.

4.2 Preparation and Properties of iCMBA Hydrogels and Drug Loading

4.2.1 Preparation of iCMBA Hydrogels

All chemicals, cell culture medium, and supplements were purchased from Sigma Aldrich (St. Louis, MO), except where mentioned otherwise. All chemicals were used as received.

iCMBA pre-polymers were synthesized and characterized as described earlier in chapter 2. Among various formulations, iCMBA-$P_{200}D_{0.3}$ was chosen for hydrogel preparation and study. The hydrogel were prepared by dissolving iCMBA pre-polymer in water, followed by of a calculated amount of crosslinker initiator solution (PI in DI water) to achieve the required prepolymer-to-PI ratio, i.e. 4% or 8%. To investigate the influence of pre-polymer pH on the

swelling and degradation of iCMBA hydrogels, pre-polymers with three different values of pH, i.e. pH: 2.0, 5.0, and 7.0, were prepared by drop wise addition of the required amount of sodium hydroxide solution or hydrochloric acid to the pre-polymer solution.

4.2.2 Swelling and Degradation Measurement

The swelling ratio and degradation rate of crosslinked iCMBAs were measured in PBS with different values of pH including 2.0, 4.0, 6.0, 7.0, 7.4, and 8.0, using the procedures already described in chapter 2 and equations (2.1) and (2.3).

4.2.3 Calculation of iCMBA Hydrogel Network Parameters

One of the key features of hydrogels, especially in drug delivery and tissue engineering applications, is their permeability to solute molecules, which is a function of hydrogels network structure parameters such as polymer volume fraction in the swollen state, average molecular weight of polymer between two adjacent crosslinking points, $\overline{M}_c$, and crosslinking density [189]. Among different experimental methods for determining these parameters, equilibrium swelling theory and rubber elasticity theory are the most prominent [190]. The parameters of iCMBA hydrogels were calculated using rubber elasticity theory. The elastic behavior of the hydrogel at low strain values was examined under tensile test to measure the tensile stress and the amount of deformation, which was then used to calculate $\overline{M}_c$of iCMBA hydrogel. For this purpose, we will use equation (4.1), which has been developed and modified for hydrogels prepared in the presence of a solvent [190]:

$$\tau = \frac{\rho RT}{\overline{M}_c}\left(1 - \frac{2\overline{M}_c}{\overline{M}_n}\right)\left(\alpha - \frac{1}{\alpha^2}\right)\left(\frac{v_{2,s}}{v_{2,r}}\right)^{1/3} \qquad \text{Equation (4.1)}$$

where, τ is the tensile stress applied to the hydrogel sample in the swollen state, ρ is the density of the polymer, R is the universal gas constant (8.314 J/K.mol), T is the absolute experimental temperature, $\overline{M}_c$ is the average molecular weight between crosslinks, $\overline{M}_n$is the number average molecular weight of the polymer, α is the extension ratio of hydrogel, $v_{2,s}$ and $v_{2,r}$ are the

polymer volume fraction in the swollen state and the polymer volume fraction in the relaxed state, which is defined as the state of the polymer immediately after crosslinking but before complete swelling, respectively. The methods of measuring these parameters are briefly described in the following sections.

The crosslinking density, ρ_x, was also calculated using following equation (4.2) [116]:

$$\rho_x = \frac{\rho}{\overline{M}_c} \qquad \text{Equation (4.2)}$$

where, ρ is polymer density and $\overline{M}_c$ average molecular weight of polymer between two adjacent crosslinking points. All the experiments were carried out at room temperature (23℃). In the equation (4.1) the unit for density of polymer is g/m^3.

4.2.3.1 Measurement of $\overline{M}_n$

Matrix-assisted laser desorption/ionization mass spectroscopy (MALDI-MS) was used to measure the number average molecular weight of iCMBA pre-polymers using a Shimadzu Biotech Axima Performance MALDI TOF-TOF mass spectrometer. N-diisopropylethylammonium α-cyano-3-hydroxycinnamate (CHCA-DIPEA) was used as the matrix to mix with the pre-polymer in a 1:10 pre-polymer:matrix molar ratio.

4.2.3.2 Determining the Density of iCMBA

The density was determined using two different techniques: through liquid displacement and via measuring the volume and the weight of the regularly shaped specimens of the dry hydrogel. In the first technique the dry weight of a piece of crosslinked iCMBA was measured. The hydrogel was then fully submerged in a graduate cylinder with known volume of 1,4-dioxane. The volume of the iCMBA hydrogel was then calculated by subtracting the initial volume of the liquid from its final volume. The density was then calculated by dividing the weight over the volume. The density calculated from the second technique, i.e. dividing the measured weight over mathematically-calculated volume of a cylindrically-cut crosslinked iCMBA (using the equation for calculating the volume of a cylinder), was identical to what measured through water displacement technique.

4.2.3.3 Measurement of $v_{2,s}$ and $v_{2,r}$

The polymer volume fraction in the relaxed state,$v_{2,r}$, was calculated by dividing the pre-polymer volume over the total volume of pre-polymer plus the volume of the water in pre-polymer solution and PI solution. The volume of pre-polymer was calculated by dividing the weight of pre-polymer over its density. The total volume of water in the system, from pre-polymer solution and PI solution, was also known. To calculate the polymer volume fraction in fully swollen state, $v_{2,s}$, the volume of polymer in the system was divided over the sum of the volume of polymer, the volume of water in polymer solution and PI solution, plus the volume of absorbed water to the hydrogel. The weight of the water absorbed by the iCMBA hydrogel in fully swollen state was calculated by subtracting the weight of iCMBA hydrogel right after hydrogel formation from the weight of fully swollen hydrogel. The calculated weight of absorbed water was then converted to the volume by dividing it over the density of water. To determine the equilibrium or fully swollen state, the weight of the iCMBA hydrogel was measured at different time points of incubating in water. The equilibrium state was considered the point when there was no further change in the weight of hydrogel. The total volume of fully swollen hydrogel was also calculated using liquid displacement method by measuring the increase in volume of water upon immersing the fully swollen iCMBA hydrogel into a water-containing graduated cylinder. The difference between the calculated values using these two techniques was not significant.

4.2.3.4 Mechanical Testing

The iCMBA hydrogel in fully swollen state was subjected to tensile test to determine the tensile stress and extension ratio within the linear and elastic deformation region. The samples were cut to prepare 6 mm-wide specimens to match ASTM standard width and were pulled at the rate of 25.4 mm (1 in)/min [191] using an MTS Insight 2 fitted (MTS, Eden Prairie, MN). The tensile stress at 10% strain was recorded for the fully swollen sample. The extension ratio, α, was calculated from following equation:

$$\alpha = \frac{L}{L0} = \text{strain} + 1 \qquad \text{Equation (4.3)}$$

where L and L_0 are elongated and initial length of sample, respectively.

4.2.4 Preparation of Drug-Loaded iCMBA Hydrogels and Drug Release Study

The study of drug release behavior of iCMBA hydrogels was carried out by preparing drug-loaded hydrogels and measuring the drug release rate over time. The drug of interest was Doxorubicin (DOX), a well-established anti-cancer drug, which has been utilized for the treatment of various cancers for decades [192]. To prepare the drug-loaded hydrogels, a measured amount of drug was solubilized in a 50% w/w solution of iCMBA in DI water by vigorous mixing using a vortex. The total amount of drug was 1% w/w of iCMBA pre-polymer. Upon complete dissolution of DOX, a calculated amount of crosslinker solution (PI) was added to the mixture to form an iCMBA network, into which DOX was entrapped. To evaluate the release rate of DOX under various pH conditions, the drug-loaded iCMBA gel was cut into disk shape using a core borer, weighed, and incubated in PBS, with different pH in the range of 2 to 8, at 37℃. At predetermined time points, the extra cts were removed and the amount of drug release was determined by measuring the amount of DOX in the extract through fluorescent spectrometry. DOX is a fluorescent material with excitation in the range of 470-480 nm and emission of 580-590 nm [193, 194]. For this experiment the best combination for excitation/emission was found to be 470/585 nm respectively. To correlate the intensity of fluorescent emission to the amount of DOX, a standard curve of the intensity versus known concentrations of the drug solution was prepared. The resulted polynomial equation was then used to convert the intensity of the DOX released from the hydrogels to corresponding drug weight. The drug release was then reported in percentage of release over time. In addition to the effect of environmental pH, the impact of pre-polymer pH on the rate of drug release was also evaluated, by preparing drug-loaded gels using iCMBAs pre-polymers with 3 different pH of 2.0, 5.0, 7.0.

4.2.5 Preparation and Characterization of iCMBA Nanoparticles

The nanoparticles (NPs) of iCMBA hydrogels or nanogels were fabricated using a simple technique. A 1% or 0.5% solution of iCMBA in DI water was prepared. Next, the pH of the solution was brought to approximately 2.0 using hydrochloric acid, which caused the solution to be turned into a cloudy suspension, most likely due to the reduction in ionization of acidic groups available on the polymer chain, which resulted in decreased solubility of anionic iCMBA polymers [176]. The cloudy suspension was then sonicated for 2 minutes at 20W power using an Ultrasonic Hemogenizer model 300 VT (BioLogics Inc, Manassas, VA). Next, a calculated amount of crosslink initiator (PI) solution was added under sonication. The mixture was then sonicated for another 4 minutes at 40W, while kept in ice bath. The mixture was then passed through a 0.2 µm filter and spun-down using ultra centrifuge at 15,000 rpm for 20 minutes to obtain the NPs. The size and size distribution of iCMBA NPs were measured by dynamic light scattering (DLS) technique, using a ZetaPals machine (Brookhaven Instruments Corp, Novato, CA). For this test a very dilute suspension of iCMBA particles in DI water (<0.1%) was prepared and transferred into a cuvette and placed into the machine. The test was then run three times for each sample. The stability of iCMBA nanoparticles was also investigated by measuring the zeta potential of the particles For this purpose the NPs of iCMBA were resuspended in DI water, place into a cuvette and the charge of particles was measured by ZetaPals machine equipped with zeta potential analyzer software.

4.2.6 Evaluation of Drug Release from iCMBA Nanoparticles

The drug release pattern of iCMBA NPs was investigated using DOX as test drug. For this purpose a measured mass of iCMBA NPs was suspended in a known volume of 1% solution of DOX in DI water. The mixture was stirred for 24 hours to allow enough time for drug to be loaded into the particles, followed by centrifugation at 15,000 rpm for 20 minutes. The resulted drug-loaded particles were then collected and placed into a dialysis tube with MWCO 1000 Da and incubated in PBS at three different pH of: 2.0, 6.0, and 7.4 at 37℃. At each predetermined time point the medium replenished and the drug release was measured by

fluorescent spectrophotometer of the collected solutions, as previously described. The initial drug loading efficiency of the nanoparticles was also calculated by comparing the fluorescent intensity of the initial drug solution and the amount of drug in the supernatant after iCMBA NPs incubation using the following equation:

$$\left(\frac{\text{Initial amount of drug} - \text{Amoutn of drug in the supernatant}}{\text{Initial amount of drug}}\right) \text{x } 100$$

4.3 Results

4.3.1 Drug-loaded iCMBA Hydrogel

The synthesis of iCMBA and the preparation of hydrogels were possible using a facile effective method, which was described in details in chapter 2. Preparation of iCMBA hydrogel in presence of DOX solution, caused the drug molecules to be entrapped in the hydrogel, as illustrated in Figure 4.2.

4.3.2 Swelling and Degradation

The swelling ratios of iCMBA hydrogels showed a clear dependency on the pH of medium, in which they were immersed. As shown in Figures 4.3 and 4.4, the swelling ratio of iCMBA hydrogels mildly increased from 1.2 to 2.6 when the pH of incubation medium changed from 2.0 to 5.0. However, the rate of increase in swelling ratio was much steeper when the medium pH varied between 5.0 and 7.0, showing a jump in swelling from 2.6 to 8.01. The rate of increase in swelling ratio was again decelerated when the pH of medium was raised to 7.4 and 8.0.

The iCMBA hydrogels degradation study showed that the degradation rate was primarily dependent on the pH of the PBS medium, in which they were incubated. As indicated in Figures 4.5 through 4.6, for the hydrogels prepared from pre-polymers with the same pH, i.e. pH 2.0, 5.0, or 7.0, the degradation was accelerated as the pH of PBS medium was increased.

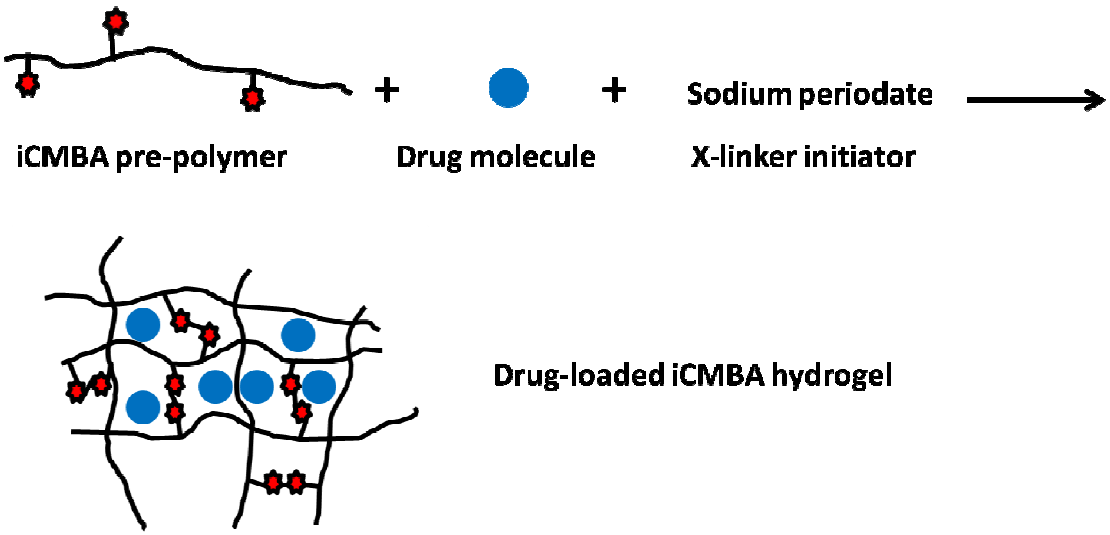

Figure 4.2 Schematic illustration of iCMBA hydrogel formation and drug entrapment.

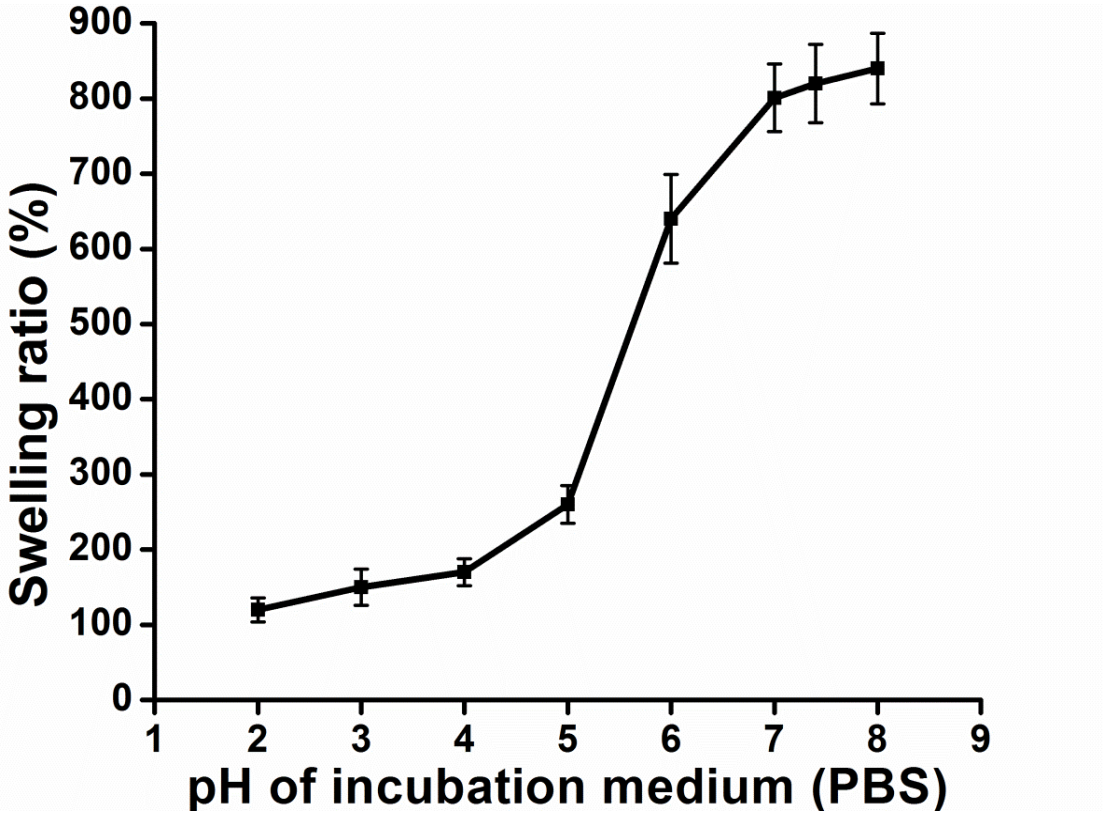

Figure 4.3 Swelling ratio of iCMBA-$P_{200}D_{0.3}$ PI:8% incubated in phosphate buffer saline with various pH at 37℃.

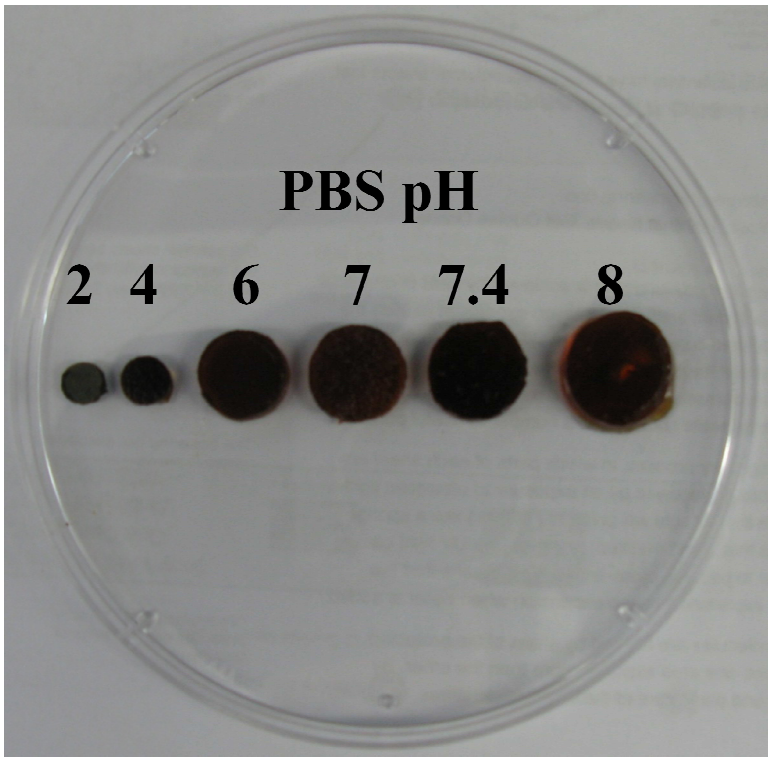

Figure 4.4 iCMBA hydrogel pellets swollen in PBS with different pH.

The complete degradation of iCMBA hydrogel (prepared from pre-polymer with pH 2.0) incubated in PBS with pH 2 and 37℃ was achieved in 27 days, while the full degradation took only 10 and 8 days when the same hydrogels incubated in PBS with pH 7.4 and 8.0, respectively. The same trend was observed when the hydrogels were prepared from pre-polymers with pH 5.0 and 7.0. Degradation was also, up to lesser extent, dependent on the pH of iCMBA pre-polymer, from which the hydrogel was prepared (Figures 4.5 to 4.8). When incubated in the PBS with identical pH, for example pH 2.0, it took the hydrogel, prepared from pre-polymer with pH 2.0, to completely degrade in 27 days, while when pre-polymers with pH 5.0 and 7.0 were used, the degradation was accomplished in 25 and 24 days, respectively. Similarly in PBS with pH 7.4, the full degradation was achieved in 6, 8, and 9 days, when the pre-polymer pH was 7.0, 5.0, and 2.0, respectively, as shown in Figure 4.8.

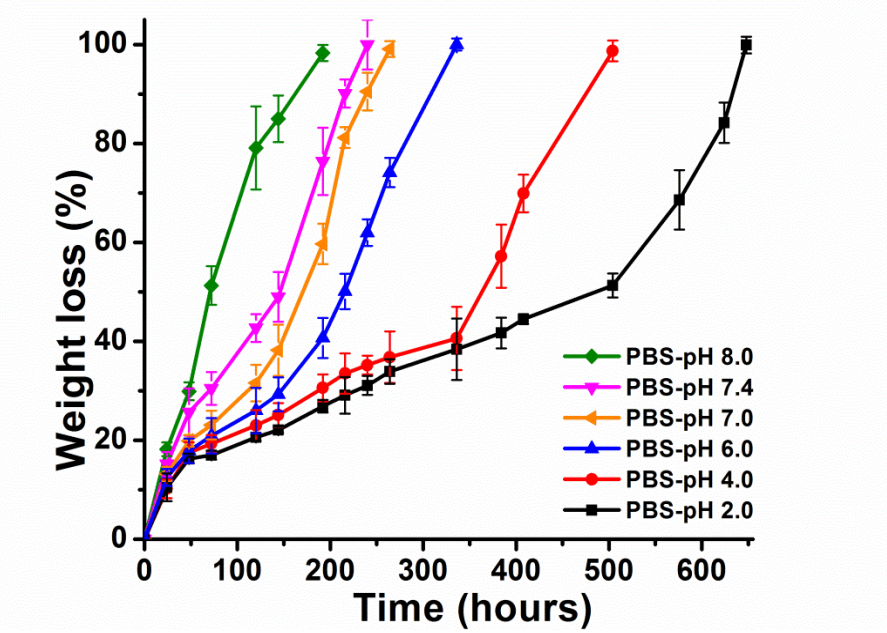

Figure 4.5 Degradation profiles of hydrogels prepared from iCMBA-$P_{200}D_{0.3}$ pre-polymer with pH 2.0, crosslinked with 4wt% PI-to-prepolymer ratio, and incubated in PBS with various pH at 37℃.

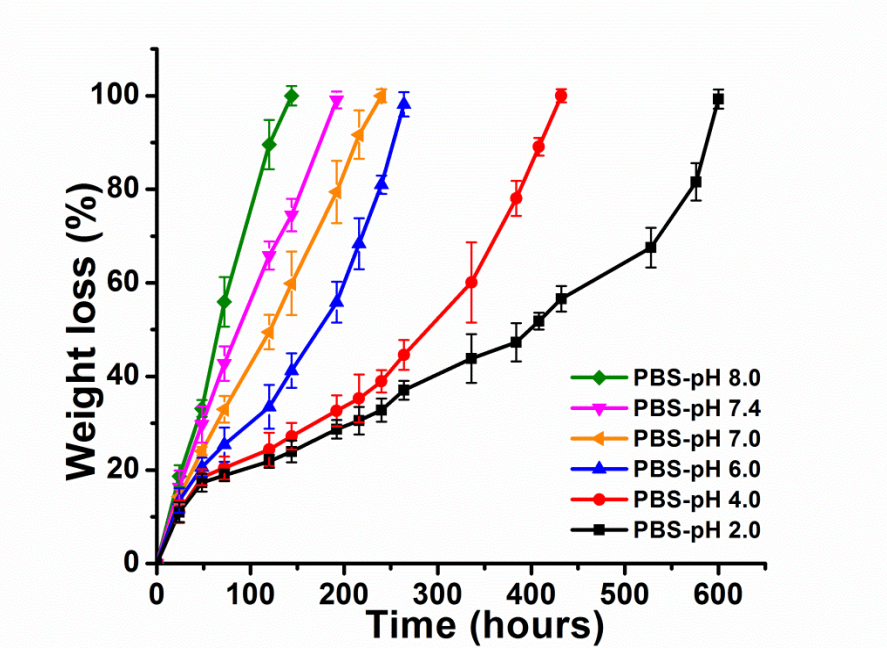

Figure 4.6 Degradation profiles of hydrogels prepared from iCMBA-$P_{200}D_{0.3}$ pre-polymer with pH 5.0, crosslinked with 4wt% PI-to-prepolymer ratio, and incubated in PBS with various pH at 37℃.

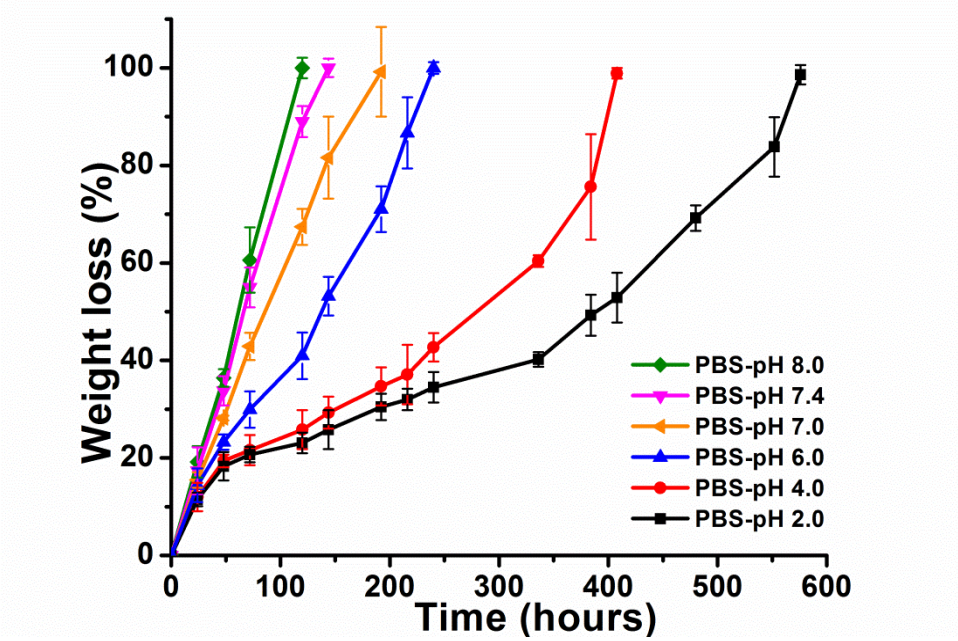

Figure 4.7 Degradation profiles of hydrogels prepared from iCMBA-$P_{200}D_{0.3}$ pre-polymer with pH 7.0, crosslinked with 4wt% PI-to-prepolymer ratio, and incubated in PBS with various pH at 37℃.

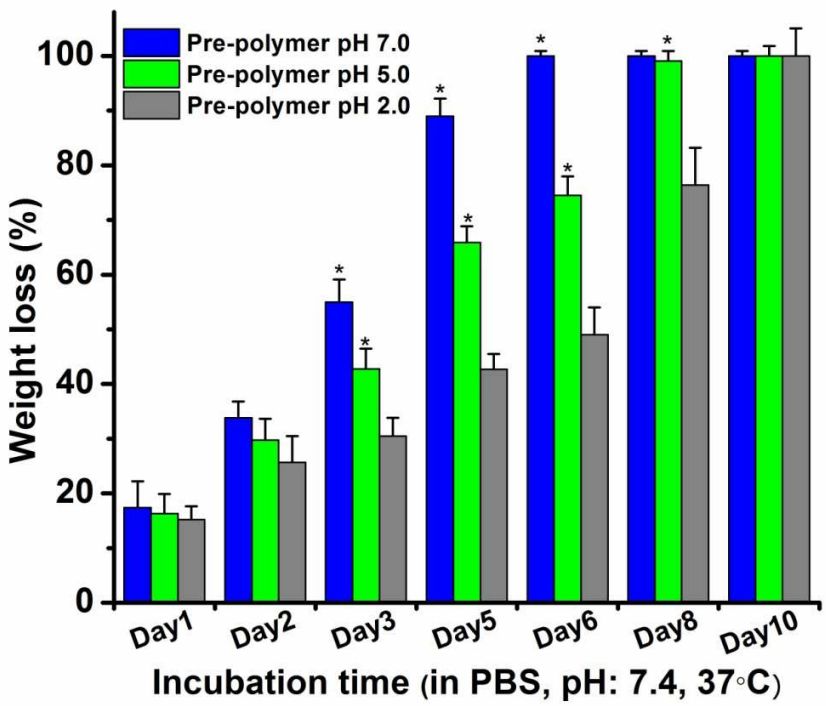

Figure 4.8 Dependency of iCMBA hydrogel degradation on the pH of pre-polymer.

4.3.3 iCMBA Hydrogel Network Parameters

The properties of iCMBA-P_{200} $D_{0.3}$, such as density and number average molecular weight, had to be measured prior to calculating the iCMBA hydrogel network properties. The number average molecular weight, measured by MALDI-MS, was 1347.36 ± 68.11. A typical MALDI diagram of iCMBA-P_{200} $D_{0.3}$ is shown in Figure 4.9.

The network parameters of the iCMBA hydrogels, which were calculated using equation (4.1) through (4.3), are listed in Table 4.2. The molecular weight between two successive crosslink points ($\overline{M}_c$) was 643.48 and 630.46 g/mol for iCMBA-P_{200} $D_{0.3}$ crosslinked with PI-to-prepolymer ratios of 4% and 8%, respectively. The crosslinking density (ρ_x) was calculated to be1943.02 and 1992.99 mol/m^3 for those two samples.

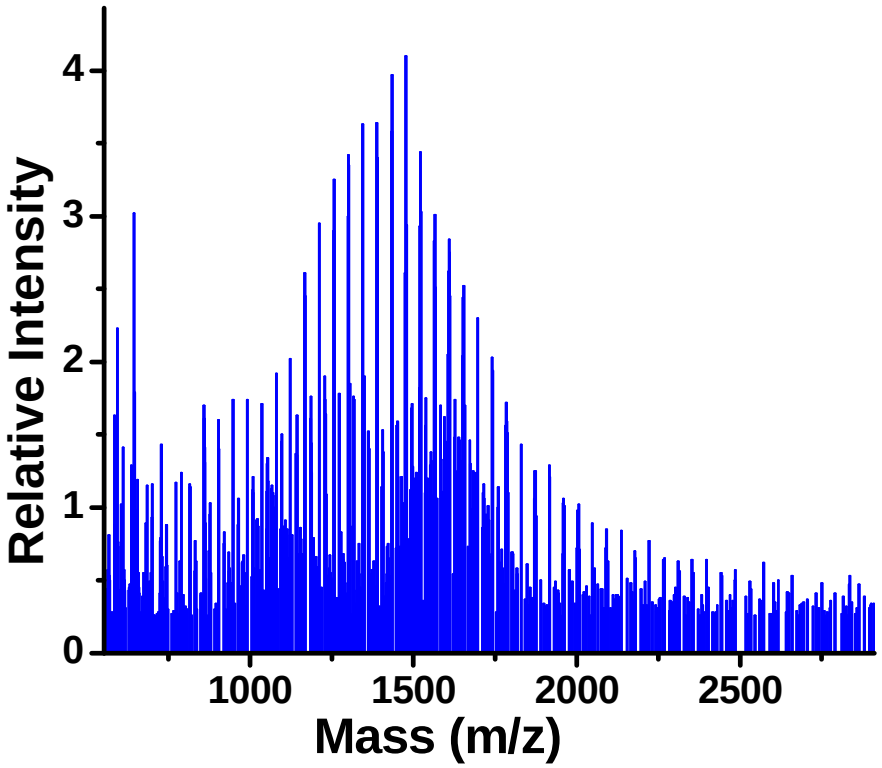

Figure 4.9 Representative MALDIi-MS diagram of iCMBA-P_{200} $D_{0.3}$.

Table 4.2 The properties of iCMBA and the formed hydrogel network

Polymer name	Prepolymer molecular weight ($\overline{M}_n$)	PI-to-prepolymer Ratio(w/w%)	Density (g/cm^3)	$v_{2,s}$	$v_{2,r}$	$\overline{M}_n$ (kPa)	α	$\overline{M}_c$ (g/mol)	ρ_x (mol/m^3)
iCMBA-P_{200} $D_{0.3}$	1299.98	4	1.2503±0.06	0.03425	0.2161	7.1±1.9	1.1	643.48	1943.02
iCMBA-P_{200} $D_{0.3}$	1299.98	8	1.2565±0.04	0.04795	0.2167	24.4±6.9	1.1	630.46	1992.99

4.3.4 Drug Release Study

The amount of drug release from iCMBA hydrogel at each time point was calculated from the fluorescent intensity using a polynomial equation of order 3, which was developed from standard curve from known concentrations of drug. The cumulative drug release profiles of hydrogels prepared from iCMBA pre-polymers with pH of 2.0, 5.0, and 7.0 are shown in Figures 4.10, 4.11, and 4.12, respectively. The DOX release rate was a function of pH of both pre-polymer and incubation medium. The drug release was faster when the drug-loaded hydrogel was incubation in medium (PBS) with higher pH. In the case of hydrogel made from pre-polymer with pH 2.0, Figure 4.10, the drug was completely unloaded within 120 hours in slightly basic PBS with pH of 8.0. In pH 2.0, however, it took close to 600 hours for the drug to be fully released. The raise in the rate of drug release with increasing the pH of medium, in which the iCMBA hydrogel was incubated, was further accelerated when the pH was between 7.0 and 8.0. Although the pH of pre-polymer, from which the hydrogel was fabricated, had an effect on the rate of drug release (higher pH increased the release rate), this impact was not as strong as the influence of alteration in the environmental pH through changing the pH of medium. For instance, when both incubated in PBS with pH 7.4, the complete drug release was achieved in 122 hours for hydrogel made from pre-polymer with pH 2.0, but in approximately 100 hours for hydrogel from pre-polymer with pH 7.0 (Figures 4.10 and 4.12).

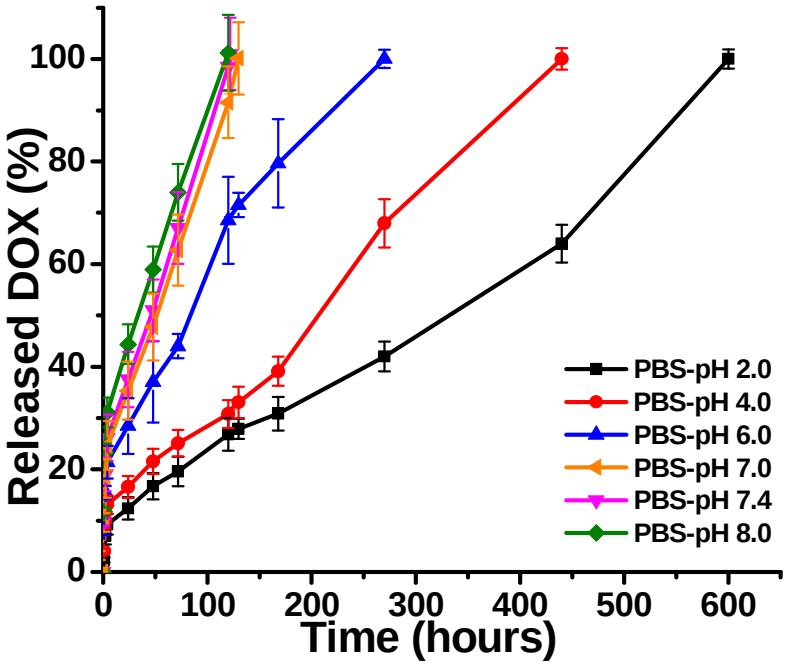

Figure 4.10 pH dependency of drug (doxorubicin) release from hydrogels prepared from iCMBA-P_{200} $D_{0.3}$ pre-polymer with pH 2.0 and incubated in PBS with different pH at 37℃.

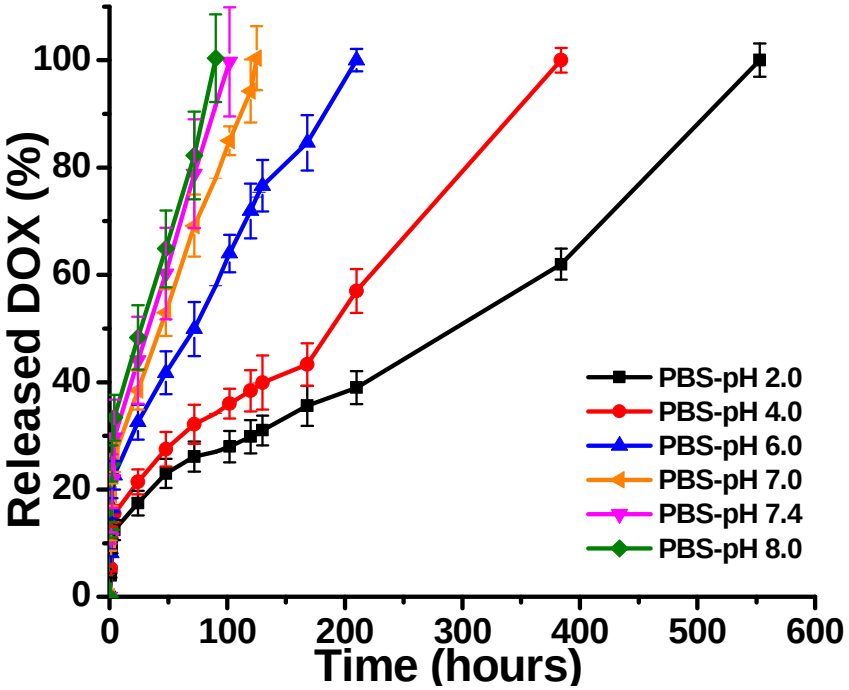

Figure 4.11 pH dependency of drug (doxorubicin) release from hydrogels prepared from iCMBA-P_{200} $D_{0.3}$ pre-polymer with pH 5.0 and incubated in PBS with different pH at 37℃.

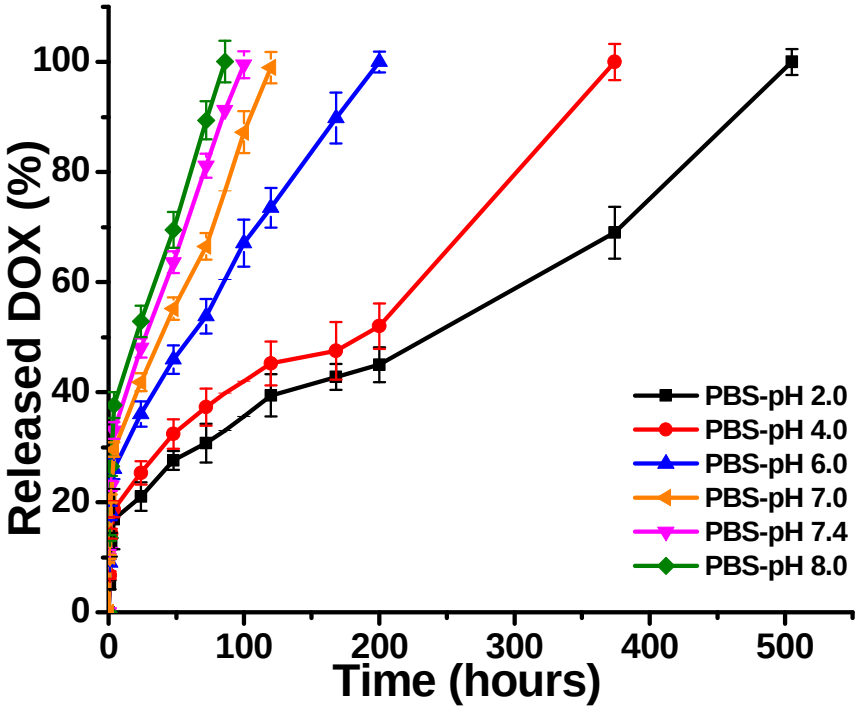

Figure 4.12 pH dependency of drug (doxorubicin) release from hydrogels prepared from iCMBA-P_{200} $D_{0.3}$ pre-polymer with pH 7.0 and incubated in PBS with different pH at 37℃.

4.3.5 Nanoparticles of iCMBA Hydrogel

The results of particles size measurement through dynamic light scattering (DLS) confirmed the formation of iCMBA nanoparticles and determined the size and size distribution of the fabricated nanoparticles. When a 0.5% solution of iCMBA was used, the average diameter of iCMBA NPs was measured at 244±56 nm (Figure 4.13). In the case of 1% solution the size of NPs increased to the average size of 327±83 nm. (Figure 4.14) The zeta potential of iCMBA NPs were found to be around -29 mV, which shows a moderate stability of particles against aggregation (Figure 4.15).

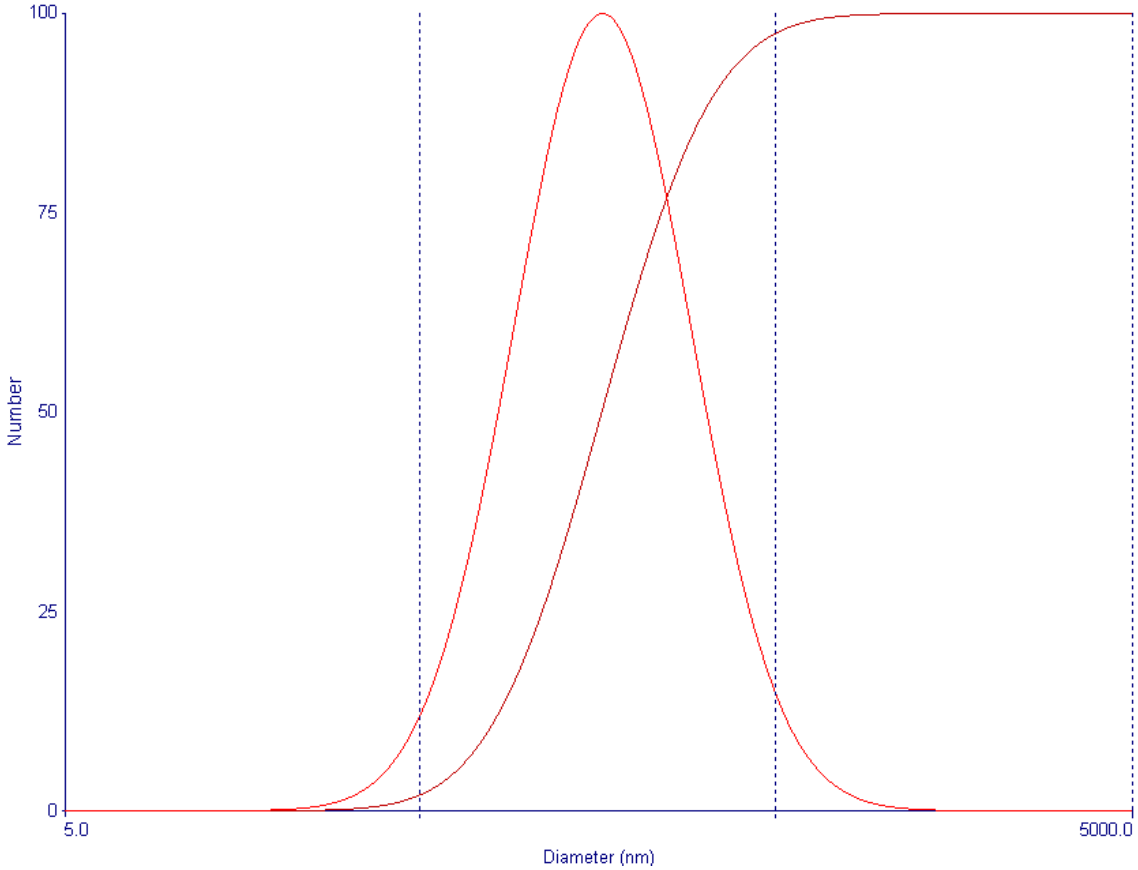

Figure 4.13 Particle size and distribution of nanoparticles prepared from 0.5% solution of iCMBA-P_{200} $D_{0.3}$, measured by dynamic light scattering.

4.3.6 Drug Release from iCMBA Nanoparticles

Based on the amount of DOX absorbed by nanoparticles the drug loading efficiency of iCMBA NPs was calculated to be 47.1 %. The results of drug release study are shown in Figure 4.16. It is noteworthy to mention that the drug release study was carried out using nanoparticles prepared from iCMBA with pre-polymer pH of 2.0. As illustrated in Figure 4.16, the rate and profile of DOX release from drug-loaded iCMBA NPs (nanogels) was not significantly different from that of iCMBA bulk hydrogel (Figure 4.10).

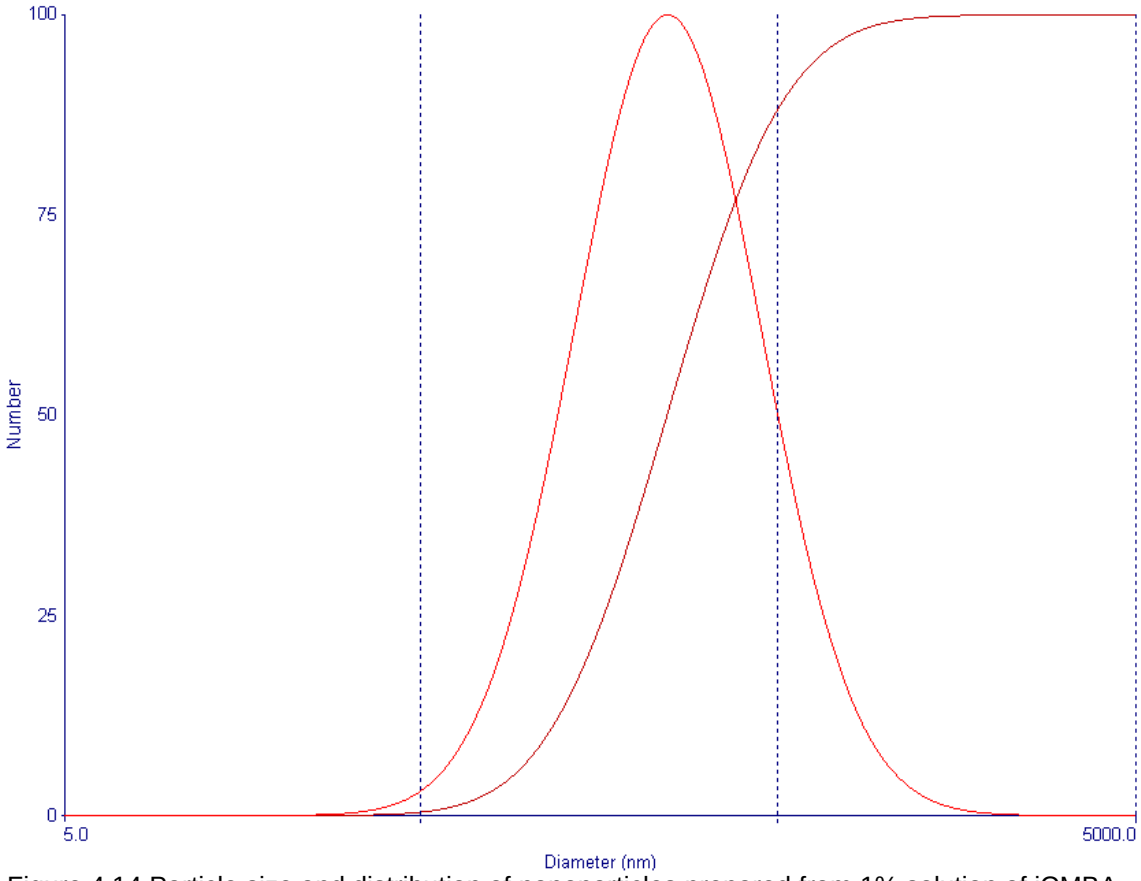

Figure 4.14 Particle size and distribution of nanoparticles prepared from 1% solution of iCMBA-P_{200} $D_{0.3}$, measured by dynamic light scattering.

4.4 Discussion

In the chapter 1 it was shown that water soluble iCMBA pre-polymers can be easily crosslinked in the presence of water, which resulted in formation of iCMBA hydrogel. The rate of crosslinking was dependent on multiple parameter, such as the amount of dopamine in the structure of polymer, length of PEG molecule, and the amount of crosslinking initiator, sodium periodate, which could be simply tuned based on requirements. The facile preparation of iCMBAs and their hydrogels from safe and non-hazardous constituent, and their remarkable capacity in maintaining high amount of water make iCMBA hydrogel attractive for many typical applications of hydrogels. Hydrogels maintain their original shapes in dehydrated and swollen states. In the dehydrated state the polymer chains are closely packed with little space for

diffusion of other molecules. After immersing hydrogel in a solvent, the polymer chains begin to separate and swell. The extent of swelling is determined by the properties of the solvent [180]. There are numerous factors that determine how much a hydrogel swells, including the degree of crosslinking of the hydrogel polymer, its chemical structure, and the existence of ionizable groups. Highly crosslinked polymers swell less than loosely crosslinked ones due to the tighter structure. The presence of more hydrophilic groups in the structure of polymer increases the swelling extent hydrogel. Another factor is the presence of pendant ionizable groups in the structure of hydrogel which can significantly affect its swelling in certain pH ranges depending on the type of ionizable group. The presence of pendent ionizable carboxylic groups makes iCMBA an ionic polymer and renders the resulted hydrogel pH sensitivity. The evaluation of swelling behavior of iCMBA-P_{200} $D_{0.3}$ PI:4% after incubation in PBS with different pH revealed a marked dependency of the swelling ratio on the pH of surrounding medium (Figure 4.3 and 4.4).

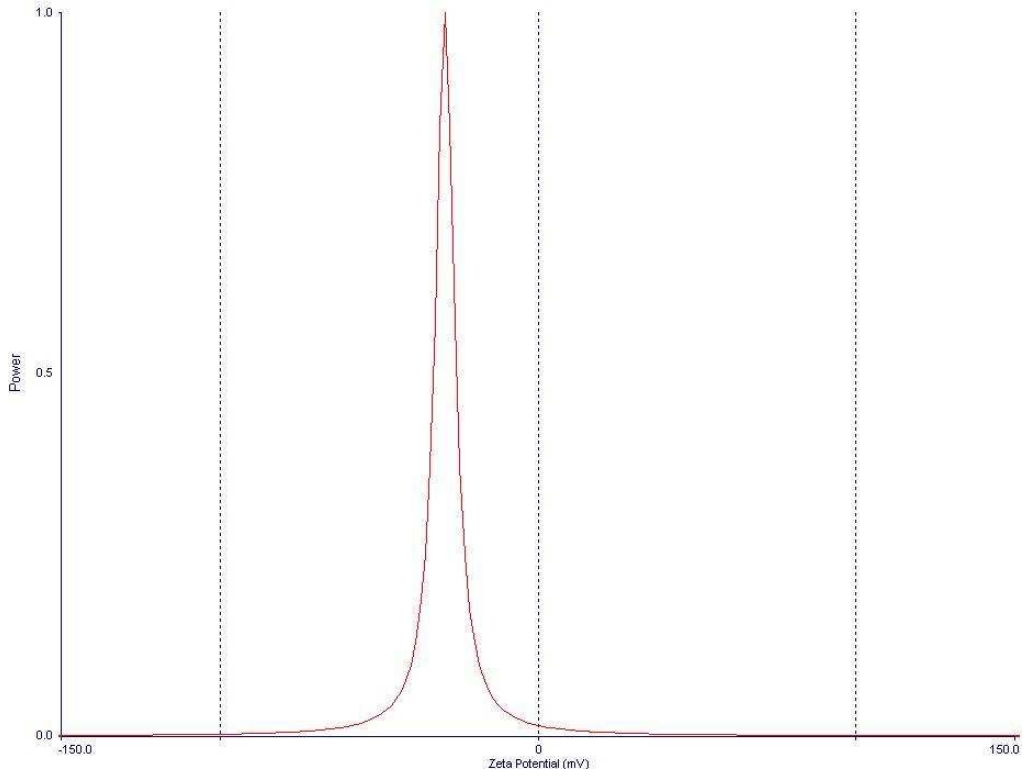

Figure 4.15 Zeta potential of iCMBA nanoparticles

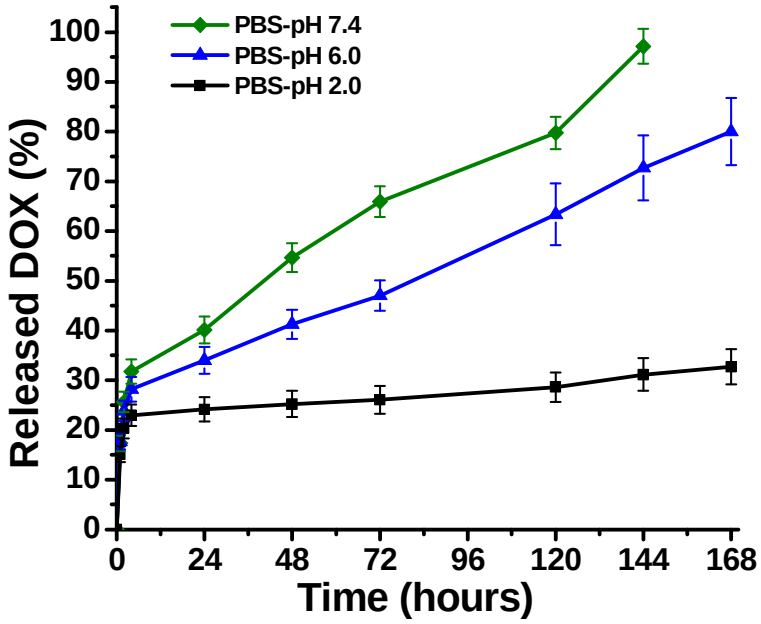

Figure 4.16 Release profile of doxorubicin from hydrogels prepared from iCMBA-P_{200} $D_{0.3}$ pre-polymer with pH 2.0 and incubated in PBS with three different pH at 37℃.

Although the amount of swelling ratio exhibited a slight increase with increasing the environmental pH from 2.0 to 5.0 and from 7.0 to 8.0, the biggest jumped occurred when the hydrogel was incubated in PBS with the pH in the neighborhood of 6.0, which is believed to be the apparent disassociation constant, pKa, of the utilized iCMBA [176]. The increase in swelling ratio at higher pH can be explained by presence of pendent anionic carboxylic groups in the structure of iCMBA hydrogel, which were exceedingly ionized when the pH of surrounding was brought closer to basic region causing an increase in the inward motion of ions into the hydrogel. The accumulation of water molecule and the electrostatic repulsion of ionized group inside the hydrogel network resulted in higher swelling [176, 180]. In addition, the ionization of carboxylic groups to anions, $-COO^-$, and subsequent repulsion forces between these anions, could also contribute to the expansion of the polymer network [176, 180]. In addition to carboxylic groups, amide groups also exist in the structure of the polymer, which were thought

to become ionized and form positively charged cations. If this was to happen, then the iCMBA hydrogel would have amphiphilic properties, i.e. it should have swollen at basic pH as well. But the lack of sudden swelling at basic environment suggested that these amid groups were not ionized. This could be explained by the fact that acidic or basic groups should be pendant from the backbone of a polymer to become ionized [176, 180]. Moreover, the nucleophilic properties of –NH– groups in the structure of iCMBA, which is essential to form cations, could be negatively impacted by the electrophilic nature of adjacent electronegative carbonyl and aromatic groups.

The amount of drug release from a hydrogel depends, among other factors, on the rate and mechanism of water diffusion in to the hydrogel network. Therefore, it is important to understand the mechanism of water transport into the network of polymer. Upon placing a dry polymer network into a solvent, such as water, the liquid begins to diffuse into the dry hydrogel network while polymer also diffuses into the fluid. Over time the polymer chains become relaxed and an equilibrium between the polymer network and the solvent is reached and an interface between the dry polymer and swollen hydrogel is formed. After reaching a chemical equilibrium between the hydrogel and the solvent, a single interface between the two is formed. The time and rate of complete swelling is dependent on the rate the fluid diffusion into the polymer network and the relaxation time of the polymer chains [178].

The degradation rate of iCMBA hydrogels was also a function of environmental pH. The increase in the pH of incubation medium, PBS, typically accelerated the degradation of iCMBA hydrogels. The degradation of iCMBA hydrogels was primarily due to the hydrolysis of existing ester and amide bonds in the structure of the polymer. Esters are susceptible to catalytic hydrolysis in both acidic and basic aqueous environment. Nevertheless, the degradation was much faster when the pH of saline was in the range neutral or slightly basic, i.e. 7.0 to 8.0 (Figures 4.5 to 4.7). This behavior can be attributed to the uptake of higher volume of water into the network of hydrogel (higher swelling) at elevated pH, which exposed the hydrolizable ester bonds of iCMBA to more water and faster bulk degradation. In addition, the enhanced swelling

of iCMBA hydrogel at higher pH might exert a stress on the polymer chains, which could accelerate hydrolytic cleavage of the ester bonds. The pH of pre-polymer, from which the hydrogel was synthesized, had also influenced the rate of degradation, in a manner that the higher pH of iCMBA pre-polymer accelerated the degradation rate of the resulted hydrogel (Figure 4.8). This could be related to the possible oxidation of some catechol hydroxyl groups, which are in fact the crosslinking sites for iCMBA, when iCMBA pre-polymer was exposed to higher pH, which, in turn, could decrease the density of crosslinking between polymer chains and, consequently, faster degradation of hydrogel. Nevertheless, the effect of pre-polymer pH was less pronounced than that of the environmental pH. The very initial rate of degradation for all samples and at different pH of PBS, was similar. This initial weight loss was related to the non-crosslinked portion of the iCMBA hydrogels, which was almost equal for all samples as all hydrogels were prepared from the same pre-polymer with identical initiator-to-prepolymer ratio.

Hydrogels are very similar to natural rubbers in their property to elastically respond to an applied stress [180]. The elastic behavior of hydrogels, particularly their full recovery to original dimension upon exposure to small deformation of less than 20%, was utilized to develop an equation (equation 4.1) based on rubber elasticity theory to study their structure and network properties, which was modified for hydrogels. The network properties of iCMBA hydrogel, such as molecular weight between two successive crosslink points, Mc, and crosslinking density, were a function of the amount of crosslinking initiator, sodium periodate. iCMBA-P_{200} $D_{0.3}$ crosslinked with 8% PI-to-prepolymer ratio had higher crosslinking density and lower Mc than 4%, as expected (Table 4.2). This could be explained by enhanced oxidation of catechol hydroxyl group to *o*-quinone, which, as explained in chapter 1, was believed to initiate crosslinking pathway of iCMBA. These results suggest that PI-to-prepolymer ratio can be used as a simple tool to control the iCMBA crosslinking rate and density, which, in turn influences the swelling and degradation rate of iCMBA hydrogel, hence the rate drug release.

iCMBAs nanoparticles were prepared using a facile technique without using any extra reagents, which was of significant advantage, because it eliminated the need for removing

surfactants and other toxic solvents, which are commonly used in typical NPs fabrication methods. The size of nanoparticles was a function of the concentration of the initial iCMBA solution, the higher the concentration the larger the size of resulted nanoparticles. Based on the zeta potential data (close to -30 mV), the iCMBA nanoparticles were shown to be moderately stable against agglomeration and aggregation of particles. Generally greater zeta potential, negative or positive means larger repulsive forces between particles. If these repulsive forces are large enough they can overcome attractive forces between the particles and prevent them from aggregating [195].

The kinetics of drug release from iCMBA hydrogels was shown to be affected by both swelling ratio and degradation rate of the hydrogel. If the degradation was exclusively hold accountable for the drug release, then the rate of drug release would match the degradation rate. However, in all samples the drug release occurred in a faster pace than hydrogel degradation. This suggests that in addition to degradation, swelling also acted as a force for driving the drug out of the hydrogel network through diffusion. This was particularly important at earlier stages of drug release when the degradation of the hydrogel was not yet begun. Therefore, the drug release can be attributed to both diffusion (due to swelling) and erosion (degradation) of the matrix [196]. It is also noteworthy to mention that there was an initial jump in the rate of drug release, which was observed even before the swelling extent of hydrogel reached the level of building osmotic pressure that was required to initiate the discharge of the drug out of hydrogel network. This phenomenon, which is called burst released and observed in most drug delivery systems, is due to release of drug molecules that are weakly bound or absorbed on the surface of hydrogel matrix rather than those inside the hydrogel network [196, 197]. The pH dependency of the rate of drug release from iCMBA hydrogels can be used to fabricate controlled drug delivery systems, which retain drug in lower pH or acidic environment and release their load in response to increase in external pH to more neutral and basic condition. This characteristic can be utilized to develop orally-administered drug delivery systems that preserve the drug from highly acidic and harsh environment of the stomach but

release their content into lower part GI tract, such as large intestine or colon, where the pH is in the neutral and slightly basic range. In comparison to injection-based drug delivery systems, the oral route of administration is advantageous because it increases patient compliance and comfort over injection, provides a simple, repeatable administration, and provides a large surface area of absorption in the GI tract [198]. In addition to various drugs, iCMBA pH-responsive hydrogels can be used to for oral delivery of oligonucleotides, such as small RNAs and DNAs, which need to be protected from degradation, particularly by nucleases, in order to be safely delivered to the area of interest in intestine [198]. The oligonucleotides, such as small interfering RNA (siRNA) and microRNA (miRNA), are increasingly utilized to improve treatment strategies for fighting variety of conditions including hypercholesterolemia, glaucoma, viruses, and cancer, through various mechanisms such as specific gene silencing [198].

Within the time period of drug release study of iCMBA nanoparticles, the rate and profile of drug release from iCMBA nanoparticles was found to be not significantly different from the drug release from bulk hydrogel under similar conditions and at similar time points. It can be concluded that the parameters that govern the release of drug from iCMBA bulk hydrogels, i.e. the external pH and the pH of pre-polymer, similarly influence the drug discharge from the nanoparticles. Smart micro and nanoparticles offer numerous advantages such as increasing the therapeutic efficacy of drugs in many ways trough detecting and sensing the environmental change and delivering their payload to a specified target or tissue [199]. Particles in nano scale may be designed to cross cell membrane and penetrate into cells and deliver their payload inside the cell, which can enhance therapeutic efficacy. Additionally, smaller particles have larger surface area-to-volume ratios, which increase their solubility and enhance the chance of interaction between particles with biological surfaces, which may be particularly important in the case of bioadhesion drug delivery system, such in mucoadhesive [200]. Nano-size iCMBA hydrogels (nanogels), offering the advantages of both pH-responsive hydrogels and nanoparticles, can be utilized for enhanced drug delivery through oral administration. In addition, nanoparticles loaded with drug and other therapeutic agents, such as siRNAs, can be

embedded into other stimuli-responsive matrices, such as iCMBA hydrogel, for better environmental protection of nanoparticles and their payload. Another plausible application of pH-responsive iCMBA nanoparticles could be in wound management. There are numerous studies on the environmental changes with different stages of wound. It was shown that the pH of a chronic wound was in the alkaline range, between 7.15 and 8.9 [201]. In contrast, the pH of the wound decrease toward neutral and eventually acidic range as the healing process of wound progresses [202]. This change in pH of topical wounds can be utilized to regulate the release rate of drugs, e.g. antibiotics, from the pH-sensitive iCMBA nanogels to accelerate healing process and prevent wound infections. A wound dressing containing drug-loaded iCMBA nanogels would have the capability of releasing more of its payload when the pH of the wound would increase due to worsening condition of the wound. As the wound would progress toward healing, the pH would decrease and the release of drug from the nanogels would be diminished. In addition, studies have shown that lowering the surface pH of a topical wound could also assist the process of wound healing. Considering the slightly acidic nature of iCMBAs, an iCMBA-nanogel-containing wound dressing could, therefore, augment the healing process of a topical wound.

4.5 Conclusion

In this chapter our goal was to prepare and investigate the properties of new pH-responsive hydrogel and nanoparticles based on our previously synthesized adhesive polymer, iCMBAs. iCMBA hydrogels swelling and degradation was dependent not only on the environmental pH but also on the pH of iCMBA pre-polymers. The swelling and degradation rate of the hydrogels increased in higher pH, particularly in neutral and alkaline range. On the other the lower pH of prepolymers caused a decrease in the rate of degradation, although this effect was less than that of environmental pH. The drug release from iCMBA hydrogels was found to be accelerated when incubated in solution with higher pH, confirming our initial hypothesis. The pH responsiveness of iCMBA was used to prepare drug-loaded matrix with potential applications in oral drug administration where the drug of interest should be protected from

acidic pH of stomach, but should be released in lower part of GI tract with higher pH. The nanoparticles of iCMBA, prepared through a facile technique, were also found to be an efficient nano-scale pH-sensitive drug delivery system. These nanogels can be potentially used as nano carries for drugs and other therapeutic agents for delivery to cells via mucus layer of large intestine, to treat various diseases. iCMBA nanogels may also have potential applications in enhancement of wound management by improving wound care and healing processes.

CHAPTER 5

FUTURE STUDIES

The present research demonstrate the importance of developing new biomaterials for applications such as tissue adhesives, hydrogels and injectable bone composites with novel properties to introduce new therapeutic approaches and tackle unmet clinical problems. To further improve upon iCMBA-based tissue adhesives and biomaterials, discussed in previous chapters, the following studies are suggested, which can help us better understand the structure-properties relationship of the iCMBAs and develop new applications for this new family of bioadhesives and hydrogels.

The hydrophilicity of iCMBAs can be tuned by partially replacing PEG with more hydrophobic monomers such as 1,8-octane diol. This change will allow more control on the iCMBAs swelling and degradation, which can result in preparing iCMBAs with lower water absorption capacity or slower degradation rate when there are such requirements. This change might also affect the adhesion properties of the iCMBAs, which needs to be investigated. In addition, our preliminary studies have shown that iCMBAs have photoluminescence property. Further investigation of this property may lead to preparation of adhesives hydrogels and nanoparticles, of which their location, degradation and drug release could be monitored using their fluorescence property. Further in vivo performance of iCMBAs, particularly in open surgeries and endoscopic treatment of internal bleeding and wounds, can also be a subject of study to better determine the efficacy of this family of tissue adhesives in bleeding control and wound management. iCMBAs might also be utilized in developing wound dressing materials with drug eluting property. iCMBA hydrogels and their composites with hydroxyapatite can be also used to develop cell-laden or growth-factor-containing hydrogels for both soft and hard tissue engineering and regeneration.

The injectable iCMBA-HA composites can also be designed to contain cells and/or growth factors (such as VEGF) to improve the formation of new bone tissue when injected to the site of defected bones.

The in-vivo performance of pH-responsive iCMBA hydrogels in drug delivery to lower GI tract can be another field of investigation. In addition, the possibility of encapsulation of various therapeutic agents such as oligonucleotides into iCMBA nanoparticles and their release behavior can also be investigated. This is particularly important for delivering these types of therapeutic agent through mucus layer of small or large intestine. In addition, the pH-dependency of drug release from iCMBA nanoparticles can be utilized to develop particles containing anti-infective to control the situation of open wounds where the pH of the wound is a function of the wound condition.

REFERENCES

1. Spotnitz WD. History of tissue dhesives. In: Sierra DH, Saltz R, editors. Surgical Adhesives and Sealants; Current Technology and Applications. Lancaster: Technomic Pub; 1996, p. 3-11.

2. Mathiowitz E, Chickering DE. Definitions, Mechanisms, and Theories of Bioadhesion. In: Mathiowitz E, Chickering DE, Lehr C, editors. Bioadhesive drug delivery systems : fundamentals, novel approaches and development. New York: Marcel Dekker; 1999, p. 1.

3. Mehdizadeh M, Yang J. Design Strategies and Applications of Tissue Bioadhesives. Macromol Biosci. 2012. DOI: 101002/mabi201200332.

4. Barnard J, Millner R. A review of topical hemostatic agents for use in cardiac surgery. Ann Thorac Surg. 2009;88:1377-83.

5. Otani Y, Tabata Y, Ikada Y. Hemostatic capability of rapidly curable glues from gelatin, poly(L-glutamic acid), and carbodiimide. Biomaterials. 1998;19:2091-8.

6. Spotnitz WD. Active and mechanical hemostatic agents. Surgery. 2007;142:S34-8.

7. Quinn JV. Overview of Tissue Adhesives. In: Quinn JV, editor. Tissue Adhesives in Clinical Medicine. 2nd ed. Hamilton: BC Decker Inc; 2005, p. 1.

8. Spotnitz WD, Burks S. Hemostats, sealants, and adhesives: components of the surgical toolbox. Transfusion. 2008;48:1502-16.

9. Wheat JC, Wolf JS, Jr. Advances in bioadhesives, tissue sealants, and hemostatic agents. Urol Clin North Am. 2009;36:265-75, x.

10. Traver MA, Assimos DG. New generation tissue sealants and hemostatic agents: innovative urologic applications. Rev Urol. 2006;8:104-11.

11. Kinloch AJ. Adhesion and Adhesives. London: Chapman and Hall; 1987.

12. Ebnesajjad S. Adhesives Technology Handbook. 2nd ed. Norwich: William Andrew Pub; 2008.

13. Mikos AG, Peppas NA. Scaling Concept and Molecular Theories of Adhesion of Synthetic Polymers to Glycoproteinic Networks. In: Lenaerts V, Gurny R, editors. Bioadhesive Drug Delivery Systems. Boca Raton, Fla.: CRC Press; 1990, p. 25-42.

14. Derjaguin BV, Toporov YP, Muller VM, Aleinikova IN. Relationship between Electrostatic and Molecular Component of Adhesion of Elastic Particles to a Solid-Surface. J Colloid Interf Sci. 1977;58:528-33.

15. Valbonesi M. Fibrin glues of human origin. Best Pract Res Clin Haematol. 2006;19:191-203.

16. Spotnitz WD, Prabhu R. Fibrin sealant tissue adhesive--review and update. J Long Term Eff Med Implants. 2005;15:245-70.

17. Brennan M. Fibrin glue. Blood Rev. 1991;5:240-4.

18. Quinn JV. Fibrin-based adhesives and hemostatic agents. In: Quinn JV, editor. Tissue Adhesives in Clinical Medicine. 2nd ed. Hamilton: BC Decker Inc; 2005, p. 77-112.

19. Sierra DH. Fibrin sealant adhesive systems: a review of their chemistry, material properties and clinical applications. J Biomater Appl. 1993;7:309-52.

20. Leggat PA, Kedjarune U, Smith DR. Toxicity of cyanoacrylate adhesives and their occupational impacts for dental staff. Ind Health. 2004;42:207-11.

21. Quinn JV. Clinical approches to the use of cyanoacrylate tissue adhesives In: Quinn JV, editor. Tissue Adhesives in Clinical Medicine. 2nd ed. Hamilton: BC Decker Inc; 2005, p. 27-76.

22. Ryan BM, Stockbrugger RW, Ryan JM. A pathophysiologic, gastroenterologic, and radiologic approach to the management of gastric varices. Gastroenterology. 2004;126:1175-89.

23. Shalaby SW, Shalaby WSW. Cyanoacrylate-based systems as tissue adhesives. In: Shalaby SW, Burg KJL, editors. Absorbable and Biodegradable Polymers. Boca Raton: CRC Press; 2004, p. 59-75.

24. Trott AT. Cyanoacrylate tissue adhesives. An advance in wound care. JAMA. 1997;277:1559-60.

25. Chafke N, Gasser B, Lindner V, Rouyer N, Rooke R, Kretz JG, Et al. Albumin as a sealant for a polyester vascular prosthesis: its impact on the healing sequence in humans. J Cardiovasc Surg (Torino). 1996;37:431-40.

26. Conrad K, Yoskovitch A. The use of fibrin glue in the correction of pollybeak deformity: a preliminary report. Arch Facial Plast Surg. 2003;5:522-7.

27. Laitakari K, Luotonen J. Autologous and homologous fibrinogen sealants: adhesive strength. Laryngoscope. 1989;99:974-6.

28. Radosevich M, Goubran HI, Burnouf T. Fibrin sealant: scientific rationale, production methods, properties, and current clinical use. Vox Sang. 1997;72:133-43.

29. Wallace DG, Cruise GM, Rhee WM, Schroeder JA, Prior JJ, Ju J, Et al. A tissue sealant based on reactive multifunctional polyethylene glycol. J Biomed Mater Res. 2001;58:545-55.

30. Wheat JC, Wolf JS, Jr. Advances in bioadhesives, tissue sealants, and hemostatic agents. Urol Clin North Am. 2009;36:265-75, x.

31. Albala DM. Fibrin sealants in clinical practice. Cardiovasc Surg. 2003;11 Suppl 1:5-11.

32. Sierra DH. Fibrin sealant adhesive systems: a review of their chemistry, material properties and clinical applications. J Biomater Appl. 1993;7:309-52.

33. Koveker G. Clinical application of fibrin glue in cardiovascular surgery. Thorac Cardiovasc Surg. 1982;30:228-9.

34. Spotnitz WD. Fibrin sealant in the United States: clinical use at the University of Virginia. Thromb Haemost. 1995;74:482-5.

35. Rousou J, Levitsky S, Gonzalez-Lavin L, Cosgrove D, Magilligan D, Weldon C, Et al. Randomized clinical trial of fibrin sealant in patients undergoing resternotomy or reoperation after cardiac operations. A multicenter study. J Thorac Cardiovasc Surg. 1989;97:194-203.

36. Stark J, de Leval M. Experience with fibrin seal (Tisseel) in operations for congenital heart defects. Ann Thorac Surg. 1984;38:411-3.

37. Schenk WG, 3rd, Goldthwaite CA, Jr., Burks S, Spotnitz WD. Fibrin sealant facilitates hemostasis in arteriovenous polytetrafluoroethylene grafts for renal dialysis access. Am Surg. 2002;68:728-32.

38. Shaffrey CI, Spotnitz WD, Shaffrey ME, Jane JA. Neurosurgical applications of fibrin glue: augmentation of dural closure in 134 patients. Neurosurgery. 1990;26:207-10.

39. Patel MR, Louie W, Rachlin J. Postoperative cerebrospinal fluid leaks of the lumbosacral spine: management with percutaneous fibrin glue. Am J Neuroradiol. 1996;17:495-500.

40. Currie LJ, Sharpe JR, Martin R. The use of fibrin glue in skin grafts and tissue-engineered skin replacements: a review. Plast Reconstr Surg. 2001;108:1713-26.

41. Staindl O. Tissue adhesion with highly concentrated human fibrinogen in otolaryngology. Ann Otol Rhinol Laryngol. 1979;88:413-8.

42. Ochsner MG. Fibrin solutions to control hemorrhage in the trauma patient. J Long Term Eff Med Implants. 1998;8:161-73.

43. Gauthier L, Lagoutte F. [Use of a fibrin glue (Tissucol) for treating perforated or pre-perforated corneal ulcer]. J Fr Ophtalmol. 1989;12:469-76.

44. Joch C. The safety of fibrin sealants. Cardiovasc Surg. 2003;11 Suppl 1:23-8.

45. Traver MA, Assimos DG. New generation tissue sealants and hemostatic agents: innovative urologic applications. Rev Urol. 2006;8:104-11.

46. Albes JM, Krettek C, Hausen B, Rohde R, Haverich A, Borst HG. Biophysical properties of the gelatin-resorcin-formaldehyde/glutaraldehyde adhesive. Ann Thorac Surg. 1993;56:910-5.

47. Braunwald NS, Gay W, Tatooles CJ. Evaluation of crosslinked gelatin as a tissue adhesive and hemostatic agent: an experimental study. Surgery. 1966;59:1024-30.

48. Elvin CM, Vuocolo T, Brownlee AG, Sando L, Huson MG, Liyou NE, Et al. A highly elastic tissue sealant based on photopolymerised gelatin. Biomaterials. 2010;31:8323-31.

49. Cooper CW, Falb RD. Surgical adhesives. Ann N Y Acad Sci. 1968;146:214-24.

50. Bachet J, Goudot B, Dreyfus G, Banfi C, Ayle NA, Aota M, Et al. The proper use of glue: a 20-year experience with the GRF glue in acute aortic dissection. J Card Surg. 1997;12:243-53; discussion 53-5.

51. Tatooles CJ, Braunwald NS. The use of crosslinked gelatin as a tissue adhesive to control hemorrhage from liver and kidney. Surgery. 1966;60:857-61.

52. Bonchek LI, Braunwald NS. Experimental evaluation of a cross-linked gelatin adhesive in gastrointestinal surgery. Ann Surg. 1967;165:420-4.

53. Bonchek LI, Fuchs JC, Braunwald NS. Use of a cross-linked gelatin tissue adhesive in surgery of the urinary tract. Surg Gynecol Obstet. 1967;125:1301-6.

54. Ennker J, Ennker IC, Schoon D, Schoon HA, Dorge S, Meissler M, Et al. The impact of gelatin-resorcinol glue on aortic tissue: a histomorphologic evaluation. J Vasc Surg. 1994;20:34-43.

55. Nakayama Y, Matsuda T. Newly designed hemostatic technology based on photocurable gelatin. ASAIO J. 1995;41:M374-8.

56. Peppas NA, Hilt JZ, Khademhosseini A, Langer R. Hydrogels in biology and medicine: From molecular principles to bionanotechnology. Adv Mater. 2006;18:1345-60.

57. Lamba NMK, Woodhouse KA, Cooper SL, Lelah MDPim. Polyurethanes in biomedical applications. Boca Raton: CRC; 1998.

58. Matsuda T, Nakajima N, Itoh T, Takakura T. Development of a compliant surgical adhesive derived from novel fluorinated hexamethylene diisocyanate. ASAIO Trans. 1989;35:381-3.

59. Matsuda T, Takakura T, Itoh T, inventors; Asahi Glass Co., Ltd., Sanyo Chemical Industries, Ltd., assignee. Surgical Adhesive1991.

60. Beckman EJ, Buckley M, Agarwal S, Zhang J, inventors; University of Pittsburgh, assignee. Medical Adhesive and Methods of Tissue Adhesion2007.

61. Benoit FM. Degradation of Polyurethane Foams Used in the Meme Breast Implant. J Biomed Mater Res. 1993;27:1341-8.

62. Nowick JS, Powell NA, Nguyen TM, Noronha G. An Improved Method for the Synthesis of Enantiomerically Pure Amino-Acid Ester Isocyanates. J Org Chem. 1992;57:7364-6.

63. Kobayashi H, Hyon SH, Ikada Y. Water-curable and biodegradable prepolymers. J Biomed Mater Res. 1991;25:1481-94.

64. Lee BP, Dalsin JL, Messersmith PB. Biomimetic adhesive polymers based on mussel adhesive proteins. In: Smith AM, Callow JA, editors. Biological Adhesives. Berlin Springer; 2006, p. 257.

65. Waite JH. Nature's underwater adhesive specialist. Int J Adhesion and Adhesives. 1987;7:9-14.

66. Waite JH, Tanzer ML. The bioadhesive of Mytilus byssus: a protein containing L-dopa. Biochem Biophys Res Commun. 1980;96:1554-61.

67. Strausberg RL, Link RP. Protein-based medical adhesives. Trends Biotechnol. 1990;8:53-7.

68. Waite JH, Qin X. Polyphosphoprotein from the adhesive pads of Mytilus edulis. Biochemistry. 2001;40:2887-93.

69. Deming TJ. Mussel byssus and biomolecular materials. Curr Opin Chem Biol. 1999;3:100-5.

70. Waite JH. The phylogeny and chemical diversity of quinone-tanned glues and varnishes. Comp Biochem Physiol B. 1990;97:19-29.

71. Monahan J, Wilker JJ. Specificity of metal ion cross-linking in marine mussel adhesives. Chem Commun (Camb). 2003:1672-3.

72. J.Herbert Waite SOA. <3,4-dihydroxyphenylalanine in an insoluble shell protein of Mytilus edulis.pdf>. Biochimica et Biophysica Acta. 1978;541:107-14.

73. Pardo J, Gutierrez E, Saez C, Brito M, Burzio LO. Purification of adhesive proteins from mussels. Protein Expr Purif. 1990;1:147-50.

74. Ninan L, Stroshine RL, Wilker JJ, Shi R. Adhesive strength and curing rate of marine mussel protein extracts on porcine small intestinal submucosa. Acta Biomater. 2007;3:687-94.

75. Wang J, Liu C, Lu X, Yin M. Co-polypeptides of 3,4-dihydroxyphenylalanine and L-lysine to mimic marine adhesive protein. Biomaterials. 2007;28:3456-68.

76. Yamamoto H, Asai M, Tatehata H, Ohkawa K. Structures, synthesis and surface characteristics of marine adhesive proteins. Peptide Chem 1996:349-52.

77. Yu ME, Deming TJ, Hwang J. Mechanistic studies of adhesion and crosslinking in marine adhesive protein analogs. Abstr Pap Am Chem Soc. 1999;217:U475-U.

78. Yamamoto H, Sakai Y, Ohkawa K. Synthesis and wettability characteristics of model adhesive protein sequences inspired by a marine mussel. Biomacromolecules. 2000;1:543-51.

79. Tatehata H, Mochizuki A, Kawashima T, Yamashita S, Yamamoto H. Model polypeptide of mussel adhesive protein. I. Synthesis and adhesive studies of sequential polypeptides (X-Tyr-Lys)(n) and (Y-Lys)(n). J Appl Polym Sci. 2000;76:929-37.

80. Tatehata H, Mochizuki A, Ohkawa K, Yamada M, Yamamoto H. Tissue adhesive using synthetic model adhesive proteins inspired by the marine mussel. J Adhes Sci Technol. 2001;15:1003-13.

81. Messersmith PB, Zeng XP, Westhaus E, Lee B, Eberle N. Synthesis and characterization of DOPA-PEG conjugates. Abstr Pap Am Chem Soc. 2000;219:U442-U.

82. Lee BP, Dalsin JL, Messersmith PB. Enzymatic and non-enzymatic pathways to formation of DOPA-modified PEG hydrogels. Abstr Pap Am Chem Soc. 2001;222:U319-U20.

83. Messersmith PB, Lee BP, Dalsin JL. Synthesis and gelation of DOPA-Modified poly(ethylene glycol) hydrogels. Biomacromolecules. 2002;3:1038-47.

84. Brubaker CE, Kissler H, Wang LJ, Kaufman DB, Messersmith PB. Biological performance of mussel-inspired adhesive in extrahepatic islet transplantation. Biomaterials. 2010;31:420-7.

85. Murphy JL, Vollenweider L, Xu F, Lee BP. Adhesive Performance of Biomimetic Adhesive-Coated Biologic Scaffolds. Biomacromolecules. 2010.

86. Brubaker CE, Messersmith PB. Enzymatically degradable mussel-inspired adhesive hydrogel. Biomacromolecules. 2011;12:4326-34.

87. Geim AK, Dubonos SV, Grigorieva IV, Novoselov KS, Zhukov AA, Shapoval SY. Microfabricated adhesive mimicking gecko foot-hair. Nat Mater. 2003;2:461-3.

88. Lee H, Lee BP, Messersmith PB. A reversible wet/dry adhesive inspired by mussels and geckos. Nature. 2007;448:338-U4.

89. Mahdavi A, Ferreira L, Sundback C, Nichol JW, Chan EP, Carter DJ, Et al. A biodegradable and biocompatible gecko-inspired tissue adhesive. Proc Natl Acad Sci U S A. 2008;105:2307-12.

90. Wang DA, Varghese S, Sharma B, Strehin I, Fermanian S, Gorham J, Et al. Multifunctional chondroitin sulphate for cartilage tissue-biomaterial integration. Nat Mater. 2007;6:385-92.

91. Christman KL, Fok HH, Sievers RE, Fang Q, Lee RJ. Fibrin glue alone and skeletal myoblasts in a fibrin scaffold preserve cardiac function after myocardial infarction. Tissue Eng. 2004;10:403-9.

92. Christman KL, Vardanian AJ, Fang Q, Sievers RE, Fok HH, Lee RJ. Injectable fibrin scaffold improves cell transplant survival, reduces infarct expansion, and induces neovasculature formation in ischemic myocardium. J Am Coll Cardiol. 2004;44:654-60.

93. Zhang X, Wang H, Ma X, Adila A, Wang B, Liu F, Et al. Preservation of the cardiac function in infarcted rat hearts by the transplantation of adipose-derived stem cells with injectable fibrin scaffolds. Exp Biol Med (Maywood). 2010;235:1505-15.

94. Zawaneh PN, Putnam D. Materials in surgery: a review of biomaterials in postsurgical tissue adhesion and seroma prevention. Tissue Eng Part B Rev. 2008;14:377-91.

95. Sajid MS, Hutson K, Kalra L, Bonomi R. The role of fibrin glue instillation under skin flaps in the prevention of seroma formation and related morbidities following breast and axillary surgery for breast cancer: A meta-analysis. J Surg Oncol. 2012.

96. Gupta PK, Leung SS, Robinson JR. Bioadhesives/Mucoadhesives in Drug Delivery to the Gastrointestinal Tract. In: Lenaerts V, Gurny R, editors. Bioadhesive Drug Delivery Systems. Boca Raton: CRC Press; 1990.

97. Waite JH. Adhesion a la moule. Integr Comp Biol. 2002;42:1172-80.

98. Lin Q, Gourdon D, Sun C, Holten-Andersen N, Anderson TH, Waite JH, Et al. Adhesion mechanisms of the mussel foot proteins mfp-1 and mfp-3. Proc Natl Acad Sci USA. 2007;104:3782-6.

99. Lee H, Scherer NF, Messersmith PB. Single-molecule mechanics of mussel adhesion. Proc Natl Acad Sci USA. 2006;103:12999-3003.

100. J.Herbert Waite SOA. <3,4-dihydroxyphenylalanine in an insoluble shell protein of Mytilus edulis.pdf>. Biochimica et Biophysica Acta. 1978;541:107-14.

101. Pardo J, Gutierrez E, Saez C, Brito M, Burzio LO. Purification of adhesive proteins from mussels. Protein Expr Purif. 1990;1:147-50.

102. Ninan L, Stroshine RL, Wilker JJ, Shi R. Adhesive strength and curing rate of marine mussel protein extracts on porcine small intestinal submucosa. Acta Biomater. 2007;3:687-94.

103. Yamamoto H, Asai M, Tatehata H, Ohkawa K. Structures, synthesis and surface characteristics of marine adhesive proteins. Peptide Chemistry 1995. 1996:349-52.

104. Yu ME, Deming TJ, Hwang J. Mechanistic studies of adhesion and crosslinking in marine adhesive protein analogs. Abstr Pap Am Chem S. 1999;217:U475-U.

105. Tatehata H, Mochizuki A, Kawashima T, Yamashita S, Yamamoto H. Model polypeptide of mussel adhesive protein. I. Synthesis and adhesive studies of sequential polypeptides (X-Tyr-Lys)(n) and (Y-Lys)(n). J Appl Polym Sci. 2000;76:929-37.

106. Tatehata H, Mochizuki A, Ohkawa K, Yamada M, Yamamoto H. Tissue adhesive using synthetic model adhesive proteins inspired by the marine mussel. J Adhes Sci Technol. 2001;15:1003-13.

107. Yu M, Deming TJ. Synthetic Polypeptide Mimics of Marine Adhesives. Macromolecules. 1998;31:4739-45.

108. Lee BP, Dalsin JL, Messersmith PB. Synthesis and gelation of DOPA-Modified poly(ethylene glycol) hydrogels. Biomacromolecules. 2002;3:1038-47.

109. Westwood G, Horton TN, Wilker JJ. Simplified polymer mimics of cross-linking adhesive proteins. Macromolecules. 2007;40:3960-4.

110. Messersmith PB, Zeng XP, Westhaus E, Lee B, Eberle N. Synthesis and characterization of DOPA-PEG conjugates. Abstr Pap Am Chem S. 2000;219:U442-U.

111. Lee BP, Dalsin JL, Messersmith PB. Enzymatic and non-enzymatic pathways to formation of DOPA-modified PEG hydrogels. Abstr Pap Am Chem S. 2001;222:U319-U20.

112. Lee H, Dellatore SM, Miller WM, Messersmith PB. Mussel-inspired surface chemistry for multifunctional coatings. Science. 2007;318:426-30.

113. Fan XW, Lin LJ, Dalsin JL, Messersmith PB. Biomimetic anchor for surface-initiated polymerization from metal substrates. J Am Chem Soc. 2005;127:15843-7.

114. Mahdavi A, Ferreira L, Sundback C, Nichol JW, Chan EP, Carter DJD, Et al. A biodegradable and biocompatible gecko-inspired tissue adhesive. Proc Natl Acad Sci USA. 2008;105:2307-12.

115. Mehdizadeh M, Weng H, Gyawali D, Tang L, Yang J. Injectable citrate-based mussel-inspired tissue bioadhesives with high wet strength for sutureless wound closure. Biomaterials. 2012;33:7972-83.

116. Yang J, Webb AR, Pickerill SJ, Hageman G, Ameer GA. Synthesis and evaluation of poly(diol citrate) biodegradable elastomers. Biomaterials. 2006;27:1889-98.

117. Yang J, Motlagh D, Allen JB, Webb AR, Kibbe MR, Aalami O, Et al. Modulating expanded polytetrafluoroethylene vascular graft host response via citric acid-based biodegradable elastomers. Adv Mater. 2006;18:1493-8.

118. Yang J, Webb AR, Ameer GA. Novel citric acid-based biodegradable elastomers for tissue engineering. Adv Mater. 2004;16:511-6.

119. Qiu HJ, Yang J, Kodali P, Koh J, Ameer GA. A citric acid-based hydroxyapatite composite for orthopedic implants. Biomaterials. 2006;27:5845-54.

120. Dey J, Xu H, Shen JH, Thevenot P, Gondi SR, Nguyen KT, Et al. Development of biodegradable crosslinked urethane-doped polyester elastomers. Biomaterials. 2008;29:4637-49.

121. Dey J, Xu H, Nguyen KT, Yang JA. Crosslinked urethane doped polyester biphasic scaffolds: Potential for in vivo vascular tissue engineering. J Biomed Mater Res A. 2010;95A:361-70.

122. Gyawali D, Nair P, Zhang Y, Tran RT, Zhang C, Samchukov M, Et al. Citric acid-derived in situ crosslinkable biodegradable polymers for cell delivery. Biomaterials. 2010;31:9092-105.

123. Tran RT, Thevenot P, Gyawali D, Chiao JC, Tang LP, Yang J. Synthesis and characterization of a biodegradable elastomer featuring a dual crosslinking mechanism. Soft Matter. 2010;6:2449-61.

124. Yang J, Gyawali D, Stark JM, Akcora P, Nair P, Tran RT, Et al. A rheological study of biodegradable injectable PEGMC/HA composite scaffolds. Soft Matter. 2012 DOI: 10.1039/c1sm05786c.

125. Yang J, Zhang Y, Gautam S, Liu L, Dey J, Chen W, Et al. Development of aliphatic biodegradable photoluminescent polymers. Proc Natl Acad Sci USA. 2009;106:10086-91.

126. Yang J, Zhang Y, Gautam S, Liu L, Dey J, Chen W, Et al. Development of aliphatic biodegradable photoluminescent polymers (vol 106, pg 10086, 2009). Proc Natl Acad Sci USA. 2009;106:11818-.

127. Graham DG, Jeffs PW. The role of 2,4,5-trihydroxyphenylalanine in melanin biosynthesis. J Biol Chem. 1977;252:5729-34.

128. Jorgensen PH, Jensen KH, Andreassen TT. Mechanical strength in rat skin incisional wounds treated with fibrin sealant. J Surg Res. 1987;42:237-41.

129. Abramoff MD, Magelhaes PJ, Ram SJ. Image Processing with ImageJ. Biophotonics Int. 2004;11:36-42.

130. Xie D, Chen D, Jiang B, Yang C. Synthesis of novel compatibilizers and their application in PP/nylon-66 blends. I. Synthesis and characterization. Polymer. 2000;41:3599-607.

131. Deming TJ, Yu ME, Hwang JY. Role of L-3,4-dihydroxyphenylalanine in mussel adhesive proteins. J Am Chem Soc. 1999;121:5825-6.

132. Barroso-Bujans F, Martinez R, Ortiz P. Stuctural characterization of oligomers from the polycondensation of citric acid with ethylene glycol and long-chain aliphatic alcohols. J Appl Polym Sci. 2003;88:302-6.

133. Matassi F, Nistri L, Chicon Paez D, Innocenti M. New biomaterials for bone regeneration. Clin Cases Miner Bone Metab. 2011;8:21-4.

134. Rezwan K, Chen QZ, Blaker JJ, Boccaccini AR. Biodegradable and bioactive porous polymer/inorganic composite scaffolds for bone tissue engineering. Biomaterials. 2006;27:3413-31.

135. Leung KS, Shen WY, Tsang HK, Chiu KH, Leung PC, Hung LK. An effective treatment of comminuted fractures of the distal radius. J Hand Surg Am. 1990;15:11-7.

136. Mears DC. External skeletal fixation. Baltimore ; London: Williams & Wilkins; 1983.

137. Mont MA, Hungerford DS. Non-traumatic avascular necrosis of the femoral head. J Bone Joint Surg Am. 1995;77:459-74.

138. Lai KA, Shen WJ, Yang CY, Shao CJ, Hsu JT, Lin RM. The use of alendronate to prevent early collapse of the femoral head in patients with nontraumatic osteonecrosis. A randomized clinical study. J Bone Joint Surg Am. 2005;87:2155-9.

139. Radke S, Kirschner S, Seipel V, Rader C, Eulert J. Magnetic resonance imaging criteria of successful core decompression in avascular necrosis of the hip. Skeletal Radiol. 2004;33:519-23.

140. Mont MA, Einhorn TA, Sponseller PD, Hungerford DS. The trapdoor procedure using autogenous cortical and cancellous bone grafts for osteonecrosis of the femoral head. J Bone Joint Surg Br. 1998;80:56-62.

141. Yaszemski MJ, Payne RG, Hayes WC, Langer R, Mikos AG. Evolution of bone transplantation: molecular, cellular and tissue strategies to engineer human bone. Biomaterials. 1996;17:175-85.

142. Iejima D, Saito T, Uemura T. A collagen-phosphophoryn sponge as a scaffold for bone tissue engineering. J Biomater Sci Polym Ed. 2003;14:1097-103.

143. Rodrigues CV, Serricella P, Linhares AB, Guerdes RM, Borojevic R, Rossi MA, Et al. Characterization of a bovine collagen-hydroxyapatite composite scaffold for bone tissue engineering. Biomaterials. 2003;24:4987-97.

144. Wiesmann HP, Nazer N, Klatt C, Szuwart T, Meyer U. Bone tissue engineering by primary osteoblast-like cells in a monolayer system and 3-dimensional collagen gel. J Oral Maxillofac Surg. 2003;61:1455-62.

145. Kolambkar YM, Dupont KM, Boerckel JD, Huebsch N, Mooney DJ, Hutmacher DW, Et al. An alginate-based hybrid system for growth factor delivery in the functional repair of large bone defects. Biomaterials.32:65-74.

146. Yang S, Wu X, Mei R, Yang C, Li J, Xu W, Et al. Biomaterial-loaded allograft threaded cage for the treatment of femoral head osteonecrosis in a goat model. Biotechnol Bioeng. 2008;100:560-6.

147. Yang S, Wu X, Xu W, Ye S, Liu X. Structural augmentation with biomaterial-loaded allograft threaded cage for the treatment of femoral head osteonecrosis. J Arthroplasty.25:1223-30.

148. Patterson J, Siew R, Herring SW, Lin AS, Guldberg R, Stayton PS. Hyaluronic acid hydrogels with controlled degradation properties for oriented bone regeneration. Biomaterials.31:6772-81.

149. Di Martino A, Sittinger M, Risbud MV. Chitosan: a versatile biopolymer for orthopaedic tissue-engineering. Biomaterials. 2005;26:5983-90.

150. Kim HJ, Kim UJ, Kim HS, Li C, Wada M, Leisk GG, Et al. Bone tissue engineering with premineralized silk scaffolds. Bone. 2008;42:1226-34.

151. Kim KH, Jeong L, Park HN, Shin SY, Park WH, Lee SC, Et al. Biological efficacy of silk fibroin nanofiber membranes for guided bone regeneration. J Biotechnol. 2005;120:327-39.

152. Xu HH, Quinn JB, Takagi S, Chow LC. Synergistic reinforcement of in situ hardening calcium phosphate composite scaffold for bone tissue engineering. Biomaterials. 2004;25:1029-37.

153. Zhang R, Ma PX. Poly(alpha-hydroxyl acids)/hydroxyapatite porous composites for bone-tissue engineering. I. Preparation and morphology. J Biomed Mater Res. 1999;44:446-55.

154. Lu HH, El-Amin SF, Scott KD, Laurencin CT. Three-dimensional, bioactive, biodegradable, polymer-bioactive glass composite scaffolds with improved mechanical properties support collagen synthesis and mineralization of human osteoblast-like cells in vitro. J Biomed Mater Res A. 2003;64:465-74.

155. Temenoff JS, Mikos AG. Injectable biodegradable materials for orthopedic tissue engineering. Biomaterials. 2000;21:2405-12.

156. Friedman CD, Costantino PD, Takagi S, Chow LC. BoneSource hydroxyapatite cement: a novel biomaterial for craniofacial skeletal tissue engineering and reconstruction. J Biomed Mater Res. 1998;43:428-32.

157. Chang CH, Liao TC, Hsu YM, Fang HW, Chen CC, Lin FH. A poly(propylene fumarate)--calcium phosphate based angiogenic injectable bone cement for femoral head osteonecrosis. Biomaterials. 2010;31:4048-55.

158. Anseth KS, Shastri VR, Langer R. Photopolymerizable degradable polyanhydrides with osteocompatibility. Nat Biotechnol. 1999;17:156-9.

159. Fisher JP, Vehof JW, Dean D, van der Waerden JP, Holland TA, Mikos AG, Et al. Soft and hard tissue response to photocrosslinked poly(propylene fumarate) scaffolds in a rabbit model. J Biomed Mater Res. 2002;59:547-56.

160. He S, Yaszemski MJ, Yasko AW, Engel PS, Mikos AG. Injectable biodegradable polymer composites based on poly(propylene fumarate) crosslinked with poly(ethylene glycol)-dimethacrylate. Biomaterials. 2000;21:2389-94.

161. Peter SJ, Lu L, Kim DJ, Mikos AG. Marrow stromal osteoblast function on a poly(propylene fumarate)/beta-tricalcium phosphate biodegradable orthopaedic composite. Biomaterials. 2000;21:1207-13.

162. Wang DA, Varghese S, Sharma B, Strehin I, Fermanian S, Gorham J, Et al. Multifunctional chondroitin sulphate for cartilage tissue-biomaterial integration. Nat Mater. 2007;6:385-92.

163. Gyawali D, Nair P, kim HKW, Yang J. Citrate-based biodegradable injectable hydrogel composites for orthopedic applications. Biomaterials Science DOI: 101039/c2bm00026a. 2013.

164. Hartles RL. Citrate in Mineralized Tissues. Adv Oral Biol. 1964;1:225-53.

165. Hu YY, Rawal A, Schmidt-Rohr K. Strongly bound citrate stabilizes the apatite nanocrystals in bone. Proc Natl Acad Sci U S A. 2010;107:22425-9.

166. Qiu H, Yang J, Kodali P, Koh J, Ameer GA. A citric acid-based hydroxyapatite composite for orthopedic implants. Biomaterials. 2006;27:5845-54.

167. Tas C. Synthesis of biomimetic Ca-hydroxyapatite powders at 37 C in synthetic body fluids. Biomaterials. 2000;21:1429-38.

168. Oyane A, Kim H, Furuya T, Kokubo T, Miyazaki T, Nakamura T. Preparation and assessment of revised simulated body fluids. Journal of Biomedical Materials Research Part A. 2003;65:188-95.

169. Ross FP. Osteoclast biology and bone resorption. In: Favus MJ, editor. Primer on the metabolic bone diseases and disorders of mineral metabolism. 6th ed. Washington, DC: American Society for Bone and Mineral Research; 2006.

170. Fracture [database on the Internet]. PubMed Health, NCBI, NLM, NIH. 2012. Available from: http://www.nlm.nih.gov/medlineplus/fractures.html.

171. Li P, Nakanishi K, Kokubo T, de Groot K. Induction and morphology of hydroxyapatite, precipitated from metastable simulated body fluids on sol-gel prepared silica. Biomaterials. 1993;14:963-8.

172. Kim SS, Sun Park M, Jeon O, Yong Choi C, Kim BS. Poly(lactide-co-glycolide)/hydroxyapatite composite scaffolds for bone tissue engineering. Biomaterials. 2006;27:1399-409.

173. Liu H, Li H, Cheng W, Yang Y, Zhu M, Zhou C. Novel injectable calcium phosphate/chitosan composites for bone substitute materials. Acta Biomater. 2006;2:557-65.

174. Quarles LD, Yohay DA, Lever LW, Caton R, Wenstrup RJ. Distinct proliferative and differentiated stages of murine MC3T3-E1 cells in culture: an in vitro model of osteoblast development. J Bone Miner Res. 1992;7:683-92.

175. Oh JK, Drumright R, Siegwart DJ, Matyjaszewski K. The development of microgels/nanogels for drug delivery applications. Prog Polym Sci. 2008;33:448-77.

176. Qiu Y, Park K. Environment-sensitive hydrogels for drug delivery. Adv Drug Deliv Rev. 2001;53:321-39.

177. Khandare J, Haag R. Pharmaceutically Used Polymers: principles, Structures, and Applications of Pharmaceutical delivery Systems. In: Schäfer-Korting M, editor. Drug delivery. Heidelberg ; London: Springer; 2010, p. 221-50.

178. Peppas NA, Keys KB, Torres-Lugo M, Lowman AM. Poly(ethylene glycol)-containing hydrogels in drug delivery. J Control Release. 1999;62:81-7.

179. Torres-Lugo M, Peppas NA. Novel pH-sensitive hydrogels with peg-tethered chains for oral delivery of calcitonin. Mater Res Soc Symp P. 1999;550:47-51.

180. Bajpai A. Stimuli responsive drug delivery systems : from introduction to application. Sharbury: iSmithers; 2010.

181. Li Q, Wang J, Shahani S, Sun DD, Sharma B, Elisseeff JH, Et al. Biodegradable and photocrosslinkable polyphosphoester hydrogel. Biomaterials. 2006;27:1027-34.

182. Jain RK. Delivery of molecular and cellular medicine to solid tumors. Adv Drug Deliv Rev. 1997;26:71-90.

183. Gabor F, Fillafer C, Neutsch L, Ratzinger G, Wirth M. Improving Oral Delivery. In: Schäfer-Korting M, editor. Drug delivery. Heidelberg ; London: Springer; 2010, p. 345-98.

184. Akala EO, Kopeckova P, Kopecek J. Novel pH-sensitive hydrogels with adjustable swelling kinetics. Biomaterials. 1998;19:1037-47.

185. Basak P, Adhikari B. Poly (vinyl alcohol) hydrogels for pH dependent colon targeted drug delivery. J Mater Sci Mater Med. 2009;20 Suppl 1:S137-46.

186. Brannon-Peppas L, Peppas NA. Dynamic and equilibrium swelling behaviour of pH-sensitive hydrogels containing 2-hydroxyethyl methacrylate. Biomaterials. 1990;11:635-44.

187. Chiu HC, Hsiue GH, Lee YP, Huang LW. Synthesis and characterization of pH-sensitive dextran hydrogels as a potential colon-specific drug delivery system. J Biomater Sci Polym Ed. 1999;10:591-608.

188. Markland P, Zhang Y, Amidon GL, Yang VC. A pH- and ionic strength-responsive polypeptide hydrogel: synthesis, characterization, and preliminary protein release studies. J Biomed Mater Res. 1999;47:595-602.

189. Peppas NA, Barrhowell BD. Characterization of the crosslinked structure of hydrogels. In: Peppas NA, editor. Hydrogels in Medicine and Pharmacy. Boca Raton, FL: CRC Press; 1986, p. 27-56.

190. Lowman AM, Dziubla TD, Bures P, Peppas NA. Structural and Dynamic Response of Neutral and Intelligent Networks in Biomedical Environments. In: Peppas A, Sefton MV, editors. Advances in chemical engineering: Elsevier Inc.; 2004, p. 75-130.

191. Peppas NA, Merrill EW. Crosslinked Polyvinyl-Alcohol) Hydrogels as Swollen Elastic Networks. J Appl Polym Sci. 1977;21:1763-70.

192. Doxorubicin [database on the Internet]. PubMed Health, NCBI, NLM, NIH. 2012. Available from: http://www.ncbi.nlm.nih.gov/pubmedhealth/PMH0000614/.

193. de Lange JH, Schipper NW, Schuurhuis GJ, ten Kate TK, van Heijningen TH, Pinedo HM, Et al. Quantification by laser scan microscopy of intracellular doxorubicin distribution. Cytometry. 1992;13:571-6.

194. Abraham SA, Edwards K, Karlsson G, MacIntosh S, Mayer LD, McKenzie C, Et al. Formation of transition metal-doxorubicin complexes inside liposomes. Biochim Biophys Acta. 2002;1565:41-54.

195. Ross S, Morrison I. Colloidal systems and interfaces. New York: Wiley; 1988.

196. Soppimath KS, Aminabhavi TM, Kulkarni AR, Rudzinski WE. Biodegradable polymeric nanoparticles as drug delivery devices. J Control Release. 2001;70:1-20.

197. Khan AA, Paul A, Abbasi S, Prakash S. Mitotic and antiapoptotic effects of nanoparticles coencapsulating human VEGF and human angiopoietin-1 on vascular endothelial cells. Int J Nanomedicine. 2011;6:1069-81.

198. Forbes DC, Peppas NA. Oral delivery of small RNA and DNA. J Control Release. 2012;162:438-45.

199. Caldorera-Moore M, Peppas NA. Micro- and nanotechnologies for intelligent and responsive biomaterial-based medical systems. Adv Drug Deliv Rev. 2009;61:1391-401.

200. Goldberg M, Langer R, Jia X. Nanostructured materials for applications in drug delivery and tissue engineering. J Biomater Sci Polym Ed. 2007;18:241-68.

201. Wilson IA, Henry M, Quill RD, Byrne PJ. The pH of varicose ulcer surfaces and its relationship to healing. Vasa. 1979;8:339-42.

202. Kaufman T, Eichenlaub EH, Angel MF, Levin M, Futrell JW. Topical acidification promotes healing of experimental deep partial thickness skin burns: a randomized double-blind preliminary study. Burns Incl Therm Inj. 1985;12:84-90.

BIOGRAPHICAL INFORMATION

Mohammadreza (Reza) Mehdizadeh received his Bachelors and Masters of Science degrees in Polymer Engineering from Amirkabir University of Technology and Iran Polymer and Petrochemical Institute, in Tehran, Iran. He then started working at Bayer AG, a globally-renowned German chemical and pharmaceutical company, where he obtained invaluable technical knowledge and working experiences in the field of polymer science and technology. In 2009, Reza was accepted into doctoral program in Materials Science and Engineering at the University of Texas at Arlington to pursue his education at doctoral level. He joined Dr. Jian Yang's research group, Biomaterials and Tissue Engineering lab in Bioengineering department, to work on his PhD dissertation. His research was focused on developing new biodegradable polymeric tissue adhesives and hydrogels for applications such as sutureless wound closure, tissue engineering and drug delivery systems. During his PhD program, Reza was also honored with various awards such as "Academic Excellent Award" and "Excellence in Abstract Writing" from the University of Texas at Arlington. He was also selected to "Tau Beta Pi", an engineering honor society and also served as an officer to the student chapter of ASM international, a society for materials scientists and engineers